Advances in the Synthesis of Organoborane Polymers for Optical, Electronic, and Sensory Applications

Frieder Jäkle*

Department of Chemistry, Rutgers University Newark, Newark, New Jersey 07102

Received January 26, 2010

Contents

* Fax: +1-973-353-1264. E-mail: fjaekle@rutgers.edu.

1. Introduction

The past decade has witnessed renewed interest and numerous unexpected discoveries in the area of main group organometallic chemistry. Unusual bonding modes have been uncovered,[1−4] new materials have been developed,[5,6] and new applications are being pursued.[7−12] With respect to new materials with unusual properties, an exciting field is the development of hybrid polymers that combine main group elements with typical organic structures in one framework.[13,14] Among main group organic−inorganic hybrid polymers, those involving Group 14 and Group 15 elements have received tremendous attention over the past several decades, with silicones, polysilanes, and polyphosphazenes among the most thoroughly studied materials.[15−17] A variety of other classes of new polymers containing not only silicon and phosphorus,[18−22] but also the heavier homologues, such as germanium, tin, arsenic, and antimony have been introduced more recently.[23−26]

In comparison, organometallic polymers that contain the Group 13 element boron[27−32] have until recently been far less well established, despite potentially intriguing properties associated with the electron-deficient nature of many boron compounds. The initially rather slow development of this field is primarily a result of synthetic difficulties encountered at the time: the hydrolytic and oxidative sensitivity of many boron-containing molecules was regarded as an obstacle in the pursuit of their incorporation into polymeric structures. However, more recent achievements over the past decade clearly demonstrate not only that boron-containing polymers of high molecular weight can be obtained readily, but also that many of the new materials are perfectly stable for extended periods of time under ambient or even forcing conditions. In addition, more complex polymer architectures including telechelic (end-group functionalized) polymers and block copolymers can now be realized through controlled/living polymerization techniques, providing an entry to boron-containing nanostructured materials. These remarkable advances were made possible for two specific reasons. (1) New synthetic procedures have been developed including mild hydroboration and transition-metal catalyzed coupling processes, controlled radical polymerization techniques, and highly selective polymer modification methods, just to name a few. (2) Equally important is that several approaches for stabilization of the resulting polymers were successfully introduced. For instance, the attachment of bulky mesityl

10.1021/cr100026f
Published on Web 06/10/2010

Frieder Jäkle is a Professor of Chemistry at the Newark Campus of Rutgers, The State University of New Jersey. He received his Diploma in 1994 and his Ph.D. in 1997 from the Technical University of Munich (TU München), where he pursued research in the field of organometallic chemistry with Prof. Matthias Wagner, who was at the time a Habilitand in the group of Prof. Wolfgang Herrmann. As a Deutsche Forschungsgemeinschaft (DFG) postdoctoral fellow, he then carried out work in the area of metal-containing polymers at the University of Toronto with Prof. Ian Manners. In 2000, he joined the Chemistry Department at Rutgers, where he was promoted to Associate Professor in 2006 and Full Professor in 2009. Currently he is a visiting professor at the Institut für Anorganische Chemie of the Johann Wolfgang Goethe Universität in Frankfurt (2009−2010). His research interests encompass polyfunctional Lewis acids, luminescent oligomers and polymers for optoelectronic and sensor applications, conjugated hybrid materials, stimuli-responsive polymers, and the self-assembly of block copolymers into supramolecular structures. He is the recipient of a National Science Foundation CAREER award (2004), an Alfred P. Sloan fellowship (2006), a Rutgers University Board of Trustees *Research Fellowship* (2006), a Rutgers University Newark *Hosford Lectureship* (2007), and a *Friedrich Wilhelm Bessel Award* of the Alexander von Humboldt Foundation (2009).

(2,4,6-trimethylphenyl) or tripyl (2,4,6-triisopropylphenyl) groups to boron turned otherwise highly air and moisture-sensitive organoborane polymers into materials that can be handled without any special precautions. In addition, incorporation of boron into cyclic or heterocyclic structures, such as diborazane, diazaborole, pyrazabole, 8-hydroxyquinolato borane, or BODIPY proved to have a remarkable stabilizing effect. The development of transition metal-catalyzed coupling of boron-containing monomers may serve to further illustrate this point: Not only has every major transition-metal catalyzed C−C bond forming reaction now been successfully utilized in the preparation of boron-containing polymers, it turns out that even Suzuki−Miyaura coupling reactions that are based on the cleavage of boronic acid groups can been applied in certain cases!

While the synthetic advances over the past decade have been tremendous, even more important is to emphasize that unusual and interesting properties can be realized that specifically rely on the presence of boron in the macromolecular structure. In the case of tricoordinate boron centers, overlap of the empty p-orbital with an adjacent organic π-system (e.g., aryl, vinyl, alkynyl) or heteroatom (e.g., O, N) has been demonstrated based on ^{11}B NMR, photophysical and electrochemical studies, and theoretical calculations to lead to a strong π-acceptor effect and to extension of π-conjugation. As a result, very desirable electronic and photophysical characteristics such as a strong photoluminescence, electroluminescence, nonlinear optical properties, *n*-type semiconductivity, etc. can be observed. Moreover, the ability of tricoordinate boron to bind Lewis basic substrates has been widely exploited for the development of sensory

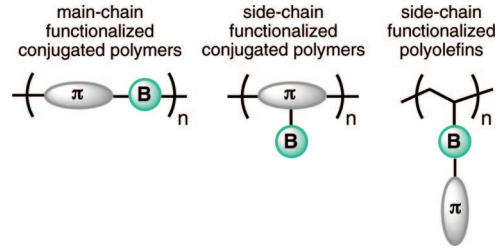

Figure 1.

materials for anions, neutral nucleophiles such as toxic amines, or biologically relevant species such as saccharides or dopamine. Polymers containing chromophores, in which boron is in a tetracoordinate state, on the other hand, have been studied for use as luminescent materials for biomedical imaging and in organic light emitting devices (OLEDs). These chromophores can not only be embedded into the polymer main chain or side chain of homopolymers, but also introduced at well-defined positions at the polymer chain end or as side groups of boron-containing block copolymers. Unusual luminescent supramolecular structures are realized, which have been, for example, investigated in tumor hypoxia imaging.

The objective of this review is to provide a comprehensive overview of these new developments. The primary focus will be on recently introduced synthetic methods for the preparation of organoborane polymers, their interesting optical and electronic properties, and applications as optoelectronic or sensory materials. The review is organized according to the chemical structure of the organoborane polymers: Chapter 2 focuses on polymers, which have boron embedded into the main chain of conjugated polymers, while Chapters 3 and 4 discuss the attachment of organoborane moieties as pendant groups to conjugated organic polymers and polyolefins, respectively (Figure 1). Applications of this diverse range of organoborane polymers as optical, electronic, and sensory materials are covered in detail in Chapter 5. Where appropriate in the context of the discussions, selected examples of related polymers, in which boron is not linked to the polymer framework via boron−carbon but rather via boron-heteroatom bonds are included. However, a comprehensive coverage of this class of polymers is beyond the scope of this review, as is the discussion of the equally interesting class of polymers containing borane and carborane clusters.

2. Main-Chain Functionalized Organoboron Polymers

The functionalization of organic polymers with boron in the main chain has been pioneered by Chujo and co-workers.[32,33] Early efforts in the 1990s focused on the incorporation of boron into nonconjugated polymeric systems. The first π-conjugated vinyl, alkynyl and arylborane polymers were reported in 1998 and this unusual class of conjugated polymers has received tremendous interest over the past decade due to the observation of unusual optical and electronic properties that are generally attributed to extended delocalization in polymers consisting of electron-deficient tricoordinate boron centers alternating with an organic π-system. Interesting optical and electronic properties have recently also been observed for main-chain type polymers with tetracoordinate boron. In that case, boron is typically incorporated into a heterocyclic structure, which generally leads to favorable stability under ambient conditions.

Hydroboration, haloboration and phenylboration polymerization techniques, first introduced by Chujo and coworkers, are among the most versatile synthetic methods for the incorporation of tricoordinate boron into the main chain of polymers.[33] Organometallic condensation reactions with Grignard reagents,[34] organolithium species,[35] and organotin precursors[36] are especially attractive for the preparation of conjugated organoborane polymers that contain alkynyl or arylene bridging units and are not accessible by hydroboration and related techniques. More recently, transition metal-catalyzed coupling procedures have been also utilized.[37−39] They have proven to be broadly applicable to the polymerization of boron monomers in which boron is stabilized by tetracoordination and incorporation into a cyclic system.[40−43] Alternatively, the formation of the B−N or B−O heterocycle itself may be used to achieve polymerization.[44−49] Synthetic routes that have so far proven useful in more specialized cases include the electropolymerization of oligothiophenes,[50] ring-opening polymerization of strained boron-bridged [1]ferrocenophanes[51] and the recently introduced spontaneous polycondensation of ditopic arylboranes (HXB)−Ar−(BXH) (X = H, Br; Ar = arylene) under borane elimination and formation of the polymeric species $(-Ar-B(X)-)_n$.[52,53]

Many of these main chain-type organoborane polymers are attractive for optoelectronic devices (OLEDs, FETs, photovoltaics, etc.),[54] as well as sensory applications, an aspect that will be further explored in section 5. In the following, the synthetic procedures and physical properties of specific examples of recently developed boron-containing polymers will be discussed. Moreover, where appropriate, details of the photophysical characterization and studies relating to possible extension of conjugation within the main chain will be pointed out. A summary of theoretical studies in this respect will be provided in section 2.1.4.

2.1. Polymers with Boron−Carbon Bonds in the Main Chain

2.1.1. Boron−Vinyl Linkages

In an early effort, Siebert, Corriu, and Douglas reported in 1998 the formation of conjugated main chain organoboron polymers **1**, which were obtained through hydroboration of 2,5-diethynylthiophene derivatives with BCl_3/Et_3SiH mixture (Scheme 1).[55] An interesting observation was that the polymers were differently colored depending on the substituents on the alkynyl groups and the boron center itself. However, quantification of the photophysical properties and molecular weight determinations were severely hampered by the high sensitivity to moisture and oxygen. Replacement of the chloro substituents in **1a** with 3-dimethylaminopropan-1-ol led to the formation of electronically stabilized boron chelates (**1d**), but further studies on this class of polymers were not reported.

Around the same time, Chujo and co-workers reported a breakthrough in the development of isolable and well-

Scheme 1

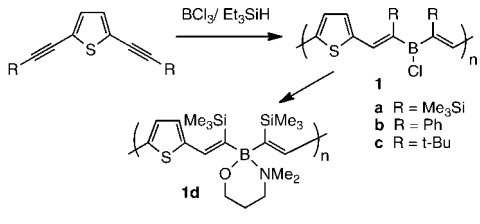

Scheme 2

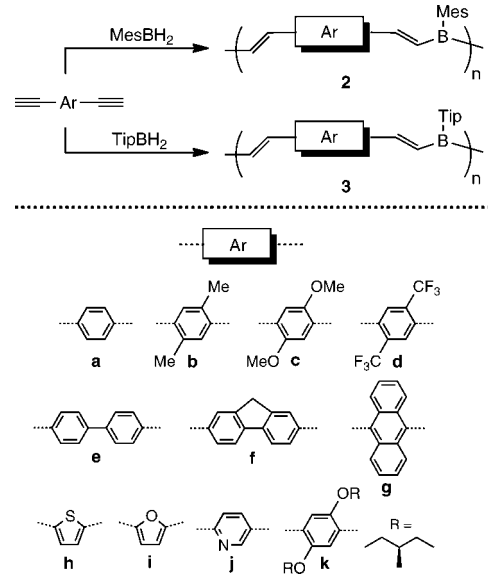

characterized conjugated organoborane polymers. They took advantage of the facile preparation and selective reactivity of sterically hindered arylboranes $ArBH_2$ (Ar = Mes (mesityl, 2,4,6-trimethylphenyl); Tip (tripyl, 2,4,6-triisopropylphenyl))[56,57] for the synthesis of far more stable conjugated organoboron polymers (**2**, **3**) via hydroboration polymerization (Scheme 2).[58,59] Importantly, the bulky aryl groups hinder attack of nucleophiles at boron and thus impart exceptionally high stability to oxygen and moisture. These polymers are well-soluble in common organic solvents, such that the molecular weights could be easily and reliably estimated by gel permeation chromatography (GPC) versus polystyrene (PS) standards. While the average number of repeating units (n) varied considerably depending on the exact structure of the dialkyne precursor,[58] optimization of the polymerization conditions and reprecipitation into hexane led to very respectable number-average molecular weights of up to M_n = 10500 Da for **2a**,[60] which corresponds to an average of 41 repeating units (Table 1).

For all of these polymers, ^{11}B NMR chemical shifts of ~31 ppm were recorded, which are to be compared to the chemical shift of related molecular species (e.g., 64.5 ppm for $(PhCH{=}CH)_2BTip$,[61] **3a-M** in Figure 2). The strong upfield shift for the polymers suggests effective p−π overlap leading to a certain degree of extended conjugation throughout the polymer main chain. Conjugation via the empty p-orbital on boron should be favorable when the boron atom and the two adjacent vinyl groups come to lie on the same plane. A look at the crystal structure of (**3a-M**), which mimics one repeat unit of polymer **3a**, confirms that such an arrangement is indeed favorable, even in the presence of a bulky Tip group on boron (Figure 2).

Extended conjugation is also reflected in the absorption and emission characteristics of the polymers. Depending on the specific electronic structure of the conjugated dialkyne, they absorb in the range of 317−450 nm in $CHCl_3$ solution, which is significantly red-shifted in comparison to the respective molecular bis(arylethenyl)mesitylboranes. Polymers **3** are generally strongly luminescent and emission quantum efficiencies in the range from 0.3 to 0.5 were reported for **3a**−**d**.[61] In most cases blue to green emission was observed, with the strong blue emission of **3a** being especially attractive for possible OLED applications. Com-

Table 1. Selected Data for Polymers with Tricoordinate Organoborane Moieties Embedded into a Conjugated Organic Backbone via Boron−Carbon Bonds

	δ (^{11}B)	M_n[a]	M_w[a]	PDI[a]	n[b]	solvent[c]	λ_{abs}/nm	λ_{em}/nm[d]	Φ_F[e]	ref
2a	31.4	6500[f]	16000[f]	2.5[f]	25	$CHCl_3$	399	441		58
2e		5100	10500	2.1	15	$CHCl_3$	390	440		58
2f		2800	4200	1.5	8	$CHCl_3$	350, 390, 407	455		58
2g		1300	1700	1.3	4	$CHCl_3$	364, 383, 405	412, 436, 462		58
2h	31.3	3000	4800	1.6	11	$CHCl_3$	350	488		59
2i		3000	5900	2.0	12	$CHCl_3$	356	495		59
2j		2900	4500	1.6	11	$CHCl_3$	450	416, 495, 593		59
3a	31.2	4100	6900	1.68	12	$CHCl_3$	400	437	0.4−0.5	61
3b	31.2	4700	9500	2.00	13	$CHCl_3$	400	452	0.4−0.5	61
3c	30.9	4200	7100	1.71	10	$CHCl_3$	438	505	0.4−0.5	61
3d	31.6	4200	5900	1.41	9	$CHCl_3$	317	470	0.3	61
5b	38					toluene	410	518	0.09	65
6a	29.2	3100	13200	4.3	8	$CHCl_3$	274			68
6b	46.4	2600	11200	4.3	6	$CHCl_3$	293	471		68
6c	45.7	7500	27000	3.7	16	$CHCl_3$	323	477		68
6d	30.1/46.4	3600	9400	2.6	10	$CHCl_3$	*g*			68
6e	10.1	1000	2300	2.3	3	$CHCl_3$	*g*			68
7b		2200	2500	1.1	4	$CHCl_3$	359	477		34
7c		2900	3500	1.2	5	$CHCl_3$	365	481		34
7d	31.6	3000	3400	1.2	4	$CHCl_3$	367	487		34
9a		1800	2000	1.1	4					35
9b	31.9	2700	3400	1.3	4	$CHCl_3$	397	456		35
10a	49	9400[h]	11200[h]	1.19	17	CH_2Cl_2	391	491	0.21	36
10b	46	5300[h]	7800[h]	1.48	9	CH_2Cl_2	413	529	0.15	36
11b	59	8800	14100	1.61	19	CH_2Cl_2	370, 391	401, 425	0.84	70
11c	57	10400	17400	1.68	19	CH_2Cl_2	371, 394	439, 423, 447	0.81	70
12a	13[i]				12[j]	thin film	362			66
12b	−4[k]	5100[l]	5800[l]	1.14[l]	13[l]	thin film	372 (sh)			66

[a] Molecular weights (Da) based on GPC analysis vs PS standards unless noted otherwise; PDI = M_w/M_n. [b] Number average of repeating units based on GPC measurements unless noted otherwise. [c] Solvent used for photophysical studies. [d] Emission maxima upon excitation at λ_{max}. [e] Fluorescence quantum efficiency. [f] A reprecipitated sample had M_n = 10500 Da, PDI = 2.25, n = 41; ref 60. [g] Not observed clearly. [h] GPC analysis of the pyridine-complexed polymers. [i] In DMF-d_7. [j] Estimated by ^{1}H NMR analysis. [k] In CD_3CN/THF-d_8. [l] GPC analysis after complexation with CH_3CN/THF.

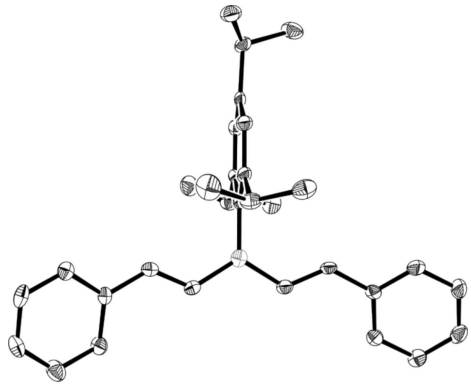

Figure 2. X-ray crystal structure of the monomeric model compound **3a-M**. Reproduced with permission from ref 61. Copyright 2009 American Chemical Society.

parison of a series of poly(vinylenearylenevinylene borane)s (**3a**−**d**) with different aromatic bridging groups revealed that electron donating alkoxy substituents lead to a bathochromic shift of the absorption and emission maxima, which is thought to be the result of an enhancement of charge transfer to boron (Figure 3).[61] Unusually large Stokes shifts were found for the heteroaromatic polymers containing thiophene (**2h**), furan (**2i**), and pyridine (**2j**) units in the main chain, which again is likely because of increasingly pronounced charge transfer character.[59] Intriguingly, white emission was observed for polymer **2j** derived from diethynylpyridine.[59] The latter is possibly a result of different regiochemistry in the hydroboration of the alkynylpyridine moiety, thus leading to a more complex polymer structure with multiple emitting chromophores. In related work, Marder and co-workers were able to demonstrate that attack at the pyridine ring can occur in the hydroboration of alkynylpyridines.[62] A chiral derivative

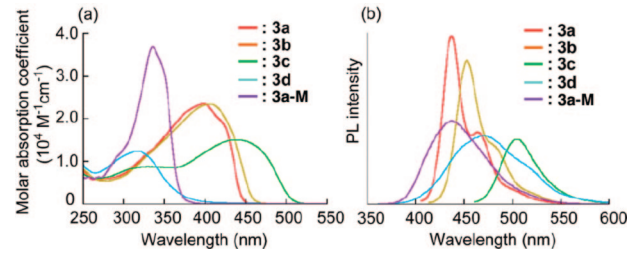

Figure 3. Effect of the substitution pattern of the phenylene ring on the absorption and emission spectra of polymers **3a**−**d** and comparison with the model system $(PhCH{=}CH)_2BTip$ (**3a-M**). Adapted with permission from ref 61. Copyright 2009 American Chemical Society.

(**3k**) was obtained by hydroboration polymerization of a chiral dialkyne with $TipBH_2$.[63] A solvent-dependent behavior was deduced from circular dichroism studies.

Luminescent polymer gels were prepared by hydroboration polymerization of $MesBH_2$ with a mixture of linear 1,4-diethynylbenzene and 1,3,5-triethynylbenzene as a cross-linker.[64] Partial gelation occurred when the reaction was performed in relatively concentrated THF solution. NMR and UV−vis spectroscopy were used to study the soluble parts of the reaction products. With increasing content of cross-linker a hypsochromic shift was observed in the UV−vis spectra (for 4:1 ratio, λ_{max} = 347 nm; cf., λ_{max} = 399 nm for the respective linear polymer **2a**), which might suggest that the meta-linkage at the cross-linker is less efficient in promoting extended conjugation. Thermogravimetric analysis of the gel showed slower thermal degradation and larger amounts of residue for the cross-linked material in comparison to the linear polymer.

Scheme 3

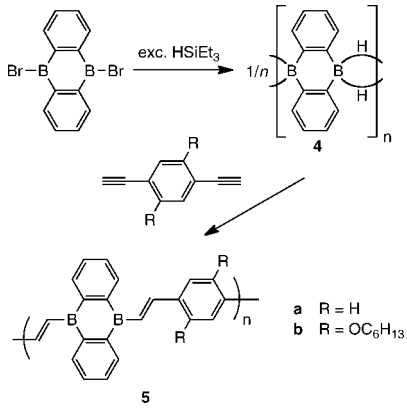

A ditopic organoborane species, 9,10-dihydro-9,10-diboraanthracene (**4**), was employed as a building block for conjugated polymers by Wagner, Holthausen, Jäkle, and co-workers[65] and related studies were reported almost simultaneously by Jia and co-workers[66] (Scheme 3). The rigid, planar diboraanthracene framework was chosen with the aim of maximizing π-overlap between boron and the aromatic substituents and to ensure good stability by incorporation of boron into a ring system. The diboraanthracene precursor is interesting in its own right because it adopts a polymeric structure in the solid state as a result of two-electron-three-center (2e3c) B−H−B bridges according to single-crystal X-ray diffraction studies by Wagner and co-workers.[65] Hydroboration with 1,4-diethynylbenzene furnished polymer **5a**, which was obtained as a bright yellow solid that proved to be only sparingly soluble in noncoordinating solvents. However, Wagner and co-workers[65] demonstrated that a polymeric material (**5b**) that is well-soluble in common organic solvents is obtained when using a hexyloxy-substituted dialkynylbenzene derivative. While the air sensitivity of polymers **5** prevented further analysis by GPC, the structure of **5b** was supported by matrix-assisted laser desorption ionization−time-of-flight (MALDI-TOF) mass spectrometric analysis, which revealed a peak pattern consistent with the expected repeating units of the polymer.

The longest wavelength absorption maxima of **5a** and **5b** are centered at 384[66] and 410[65] nm, respectively. For both polymers, the absorption spectra of thin films were similar to those in solution. Polymer **5b** shows a distinct green emission both in solution (λ_{em} = 518 nm in toluene) and in the form of a powder or thin film; the strongest luminescence intensity was observed for powdery materials (Figure 4). The bathochromic shift for the absorption maximum of **5b** relative to **5a** is likely because of the electron-donating effect of the alkoxy groups in **5b**, consistent with the results reported by Chujo and co-workers for poly(vinylenephenylenevinylene borane)s, **3**. Indeed, the green emission of **5b** is reminiscent of that of **3c** (λ_{em} = 505 nm[61]). The emission wavelength of **5b** undergoes a slight bathochomic shift with increasing solvent polarity, suggesting significant polarization of the excited state.[67]

As an alternative to the hydroboration route, Chujo and co-workers studied the halo-phenylboration of aromatic diynes with Ph_2BBr (Scheme 4).[68] Polymers **6a**−**d** exhibit characteristic ^{11}B NMR resonances at about δ = 46 ppm, which are significantly more downfield shifted than those measured for polymers **2** and **3** prepared by hydroboration polymerization. This would suggest less effective electronic

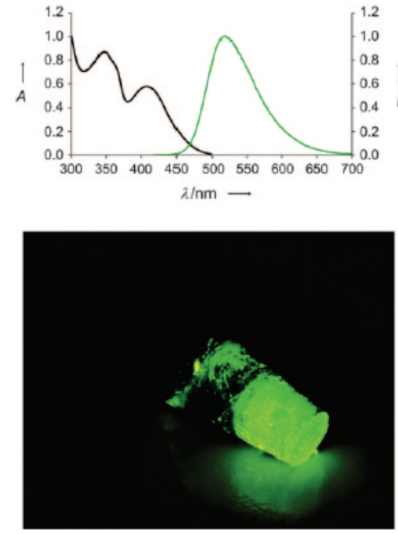

Figure 4. Absorption and emission spectra of **5b** and photograph illustrating the luminescence in the solid state. Reproduced with permission from ref 65. Copyright Wiley-VCH Verlag GmbH & Co. KGaA.

Scheme 4

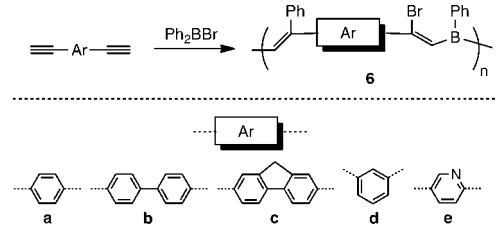

delocalization of the conjugated organic groups with the boron centers. An additional smaller peak at approximately δ = 29−30 ppm was attributed to possible formation of trivinylborane cross-links. For the pyridyl derivative **6e**, an unusual chemical shift of δ = 10 ppm was reported, which is in a region typically associated with tetracoordinate boron centers and therefore might suggest the presence of B−N donor−acceptor interactions.

Modest molecular weights in the range of M_n = 1000 up to 7500 Da were determined by GPC analysis. A distinct effect of the reaction temperature, time and concentration was evident, and gelation occurred at high temperatures and high concentration. The latter is indicative of cross-linking because of Ph_2BBr acting as a trifunctional monomer, in which the Br and both phenyl groups can add to different alkyne moieties. Given the absence of sterically demanding groups on boron, the polymers exhibited surprisingly good stability in air as deduced from comparison of the GPC results for freshly prepared samples with data acquired after exposure to air for one day. A possible explanation could be that the Ph and Br substituents on the vinylene moieties exert a remote steric protection effect at boron.

A comparison of the absorption and emission characteristics of polymers **6** with those of the related poly(vinylenephenylenevinylene borane)s (**2**) prepared by hydroboration polymerization is instructive. The absorption bands occur at much shorter wavelength (274−323 nm) for the halo-phenylboration products, which again suggests less effective conjugation between the aromatic π-systems and the empty p_π orbital on boron. This is consistent with the downfield shift of the ^{11}B NMR resonances discussed above and could be the result of cross-links or the steric and electronic effects

of the phenyl and bromo-substituents attached to the vinylene bridges. However, the emission spectra of **6b** and **6c** showed maxima at 471 and 477 nm, respectively, which are even slightly red-shifted relative to those of the respective hydroboration polymers **2e** and **2f**, suggesting more effective conjugation in the excited state.

2.1.2. Boron−Aryl and Boron−Alkynyl Linkages

Poly(arylene borane)s and poly(ethynylene boranes) are not accessible via hydroboration and related routes, hence organometallic polycondensation procedures are typically employed instead. A potential advantage of these classes of polymers is that higher thermal stability may be achieved, because β-elimination processes (the reverse process of the hydroboration polymerization) are precluded.

Organometallic polycondensation procedures for the preparation of conjugated organoborane polymers were first reported by Chujo and co-workers. The poly(*p*-phenylene borane)s (**7**) were obtained via polycondensation of aryldimethoxyboranes with difunctional Grignard reagents that were generated in situ from the respective dibromobenzene derivative (Scheme 5).[34] The best yields and highest molecular weights were achieved when using the sterically protected borane source $TipB(OMe)_2$ in combination with 1,4-dibromo-2,5-di-*n*-octyloxybenzene. The presence of the long alkyl side-chains was thought to improve the solubility of the growing polymer chains, thus having a beneficial effect on the molecular weight. An ^{11}B NMR signal of 31.6 ppm was reported for **7d**, which is in a similar range as for the vinylborane polymers **2** and **3**, but rather unusual for triarylborane moieties. This might indicate the presence of some residual methoxy groups attached to boron. The polymers showed absorption maxima in the range of 359−367 nm in $CHCl_3$ solution and emit blue-green light (477−496 nm) upon excitation at 350 nm.

In this context, it is also interesting to note that a series of multifunctional anthrylboranes (**8**) with up to six boron centers and divergently extended π-conjugation have been reported by Yamaguchi and Tamao and co-workers (Scheme 6).[69] The anthryl and mesityl groups serve to sterically protect the boron centers so that these dendritic compounds can be handled without special care under air. They are intensely red colored with $\lambda_{max} = 525$ nm (**8a**) and 534 nm (**8b**), which is in stark contrast to the bright orange color of trianthrylborane itself. As already discussed for the respective linear polymers, the bathochromic shift was attributed to a certain degree of extended delocalization via the boron centers.

The polycondensation of lithiated diacetylenes with aryldimethoxyboranes was used by Chujo to produce poly(ethynylenephenyleneethynylene borane)s (**9**) (Scheme 7).[35] Polymers **9** were obtained in 67−80% yield with moderate molecular weights in the range of $M_n = 1800-2700$ Da. The polymer structure was confirmed by ^{11}B NMR, which showed a single peak at 31.9 ppm. Protection of boron with bulky aryl groups (Ar = Mes, Tip) ensured good stability

Scheme 5

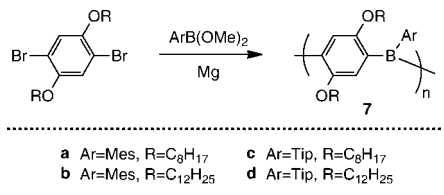

Scheme 6

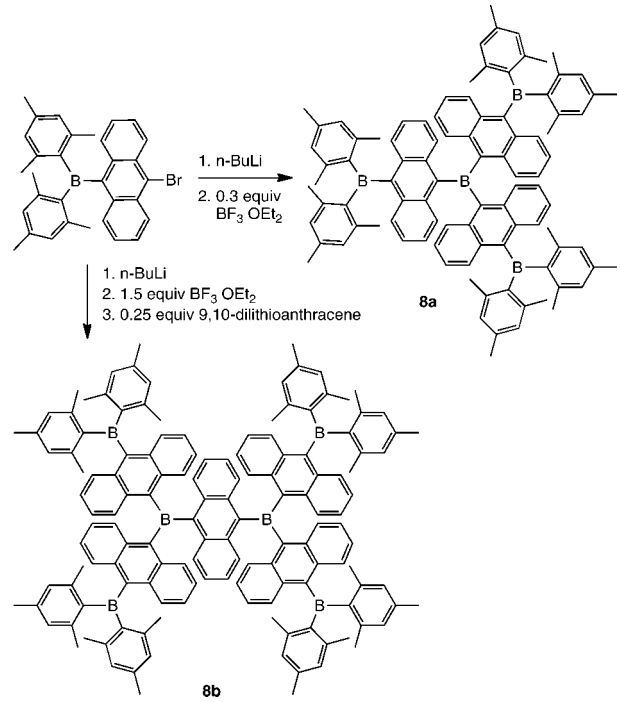

Scheme 7

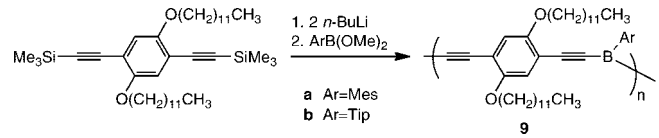

Scheme 8

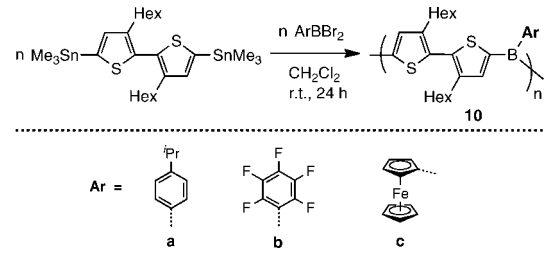

in air, and good solubility in organic solvents was achieved as a result of the pendant dodecyloxy substituents. Polymer **9b** exhibits an absorption maximum at $\lambda_{abs} = 397$ nm and emits blue light with $\lambda_{em} = 456$ nm in chloroform solution. This result can be compared with data for poly(vinylenephenylenevinylene borane) **3c**, which shows relatively longer wavelength absorption and emission maxima at 438 and 505 nm, respectively.

Tin−boron exchange reactions have been explored by Jäkle and co-workers as a potentially milder and more selective polymerization method (Scheme 8).[36] In this case, the polycondensation process occurs between a bifunctional haloborane and a ditin species with release of R_3SnX (R = Me, *n*-Bu; X = Br, Cl). The latter can be removed under high vacuum or by extraction with nonpolar solvents. Another important aspect is that the polymerizations can be conducted in noncoordinating solvents such as CH_2Cl_2 or toluene, avoiding the need for ether solvents, which are typically used for Grignard and organolithium reagents, but tend to react with highly Lewis acidic borane centers to elicit ether cleavage or Lewis acid−base complex formation.

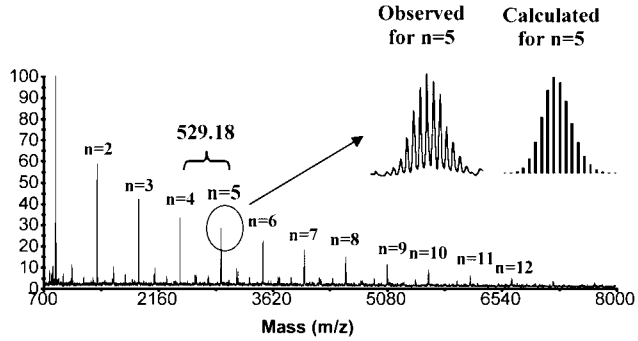

Figure 5. MALDI-TOF mass spectrum of **10c** (reflectron + ion mode with benzo[*a*]pyrene as the matrix). Reproduced with permission from ref 36. Copyright 2005 American Chemical Society.

Main chain organoborane polymers (**10**) contain highly Lewis acidic boron groups embedded into a polythiophene backbone (Scheme 8).[36] Because of the absence of bulky substituents on boron, these polymers are comparatively much more sensitive to air and moisture than the mesityl and tripylborane polymers discussed earlier. However, since the borane centers readily form Lewis acid−base complexes, the molecular weights could be estimated by GPC after complexation with pyridine. They range from $M_n = 5300$ to 9400 Da relative to PS standards. The polymer structures were further confirmed by ^{1}H NMR end-group analysis and high-resolution MALDI-TOF measurements. The mass spectra showed peak patterns that correlate well with those calculated for linear oligomers with $-Th_2B(Ar)-$ repeating units and bithiophene end groups as illustrated for **10c** in Figure 5.

An interesting feature is that the photophysical properties can be varied by appropriate choice of the pendant aryl substituents. The latter appear to control the electron-deficient character of the boron centers and thus the extent of π-overlap within the conjugated polymer chain. With phenyl groups on boron blue (thin film) to blue-green (solution) luminescence was observed, whereas the attachment of electron-withdrawing C_6F_5 substituents led to bright green emission. A derivative with a ferrocenyl group at boron (**10c**) was intensely red-colored, but the polymer emission was quenched by the ferrocene moieties. Clearly, variation of the pendant group on boron provides an additional means for tuning the photophysical characteristics of conjugated main chain organoboron polymers.

By taking advantage of the high selectivity of the tin−boron exchange protocol, a "universal" fluorescent conjugated organoborane polymer scaffold with dihexylfluorene groups alternating with bromoborane moieties was developed more recently (Scheme 9).[70] Polymer **11a** features reactive B−Br functionalities that can be exploited to tune the photophysical properties, stability toward air, and thermal stability by straightforward polymer modification reactions. A linear structure was established by multinuclear NMR and MALDI-TOF analyses that were performed on polymers **11b**,**c**, which were obtained by reaction with arylcopper reagents (Ar = Mes for **11b**, Ar = Tip for **11c**). Polymers **11b** and **11c** displayed broad ^{11}B NMR signals at $\delta = 59$ and 57 ppm, respectively, in the typical region for tricoordinate aryl boranes. The polymers are readily soluble in common organic solvents. GPC in THF gave number-average molecular weights of $M_n = 8800$ and 10400 Da for **11b** and **11c**, respectively, corresponding to an average number of

Scheme 9

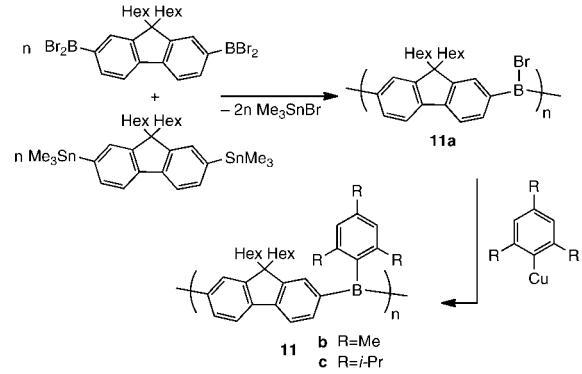

repeating units of $n = 19$. This number is predetermined by the number of repeating units for the precursor **11a**. Another interesting aspect of polymer **11a** is that different functional groups are readily incorporated, and the preparation of polymers with organoboron quinolate functionalities will be further discussed in section 2.3.

The absorption spectra of **11b** and **11c** in CH_2Cl_2 show bands with vibronic fine structure and maxima at approximately 390 nm that are red-shifted by approximately 20 nm in comparison with the related molecular species 2,7-bis(dimesitylboryl)-9,9-diethylfluorene (371 nm).[71] Both polymers are highly emissive in the blue-violet region (for **11b** $\lambda_{em} = 425$, 401 nm, $\Phi_F = 84\%$; for **11c** $\lambda_{em} = 423$, 399 nm, $\Phi_F = 81\%$ in CH_2Cl_2), and the emission bands almost perfectly mirror the absorptions with very small Stokes shifts, indicative of a highly rigid structure. Interesting to note is also that two reversible reduction waves were observed for **11c** by cyclic voltammetry, corresponding to successive reduction of alternating fluorenylborane moieties in the polymer chain. The first reduction occurs at −2.13 V vs Fc/Fc^+, which is considerably less anodic than that of polyfluorene itself.

Polycondensation via tin−boron exchange was also applied by Jia and co-workers for the preparation of polymers **12** (Scheme 10).[66] These polymers were designed to enhance the electron-deficient character by using the diboron building block 9,10-dibromo-9,10-dihydro-9,10-diboraanthracene in combination with phenylene or perfluorophenylene bridging moieties. For polymer **12a**, the reaction was performed with the tributylstannyl species 1,4-$C_6H_4(SnBu_3)_2$ in toluene at reflux, while for **12b** the more reactive trimethylstannyl derivative 1,4-$C_6F_4(SnMe_3)_2$ was employed under similarly forcing conditions. Polymers **12** were insoluble in noncoordinating solvents such as toluene and only weakly soluble in THF. In contrast, the solubility in DMF (**12a**), and acetonitrile/THF mixture (**12b**, 1:2 volume ratio) was high.

Scheme 10

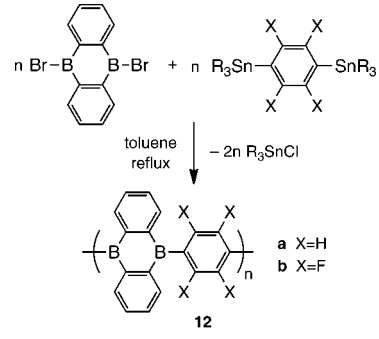

Scheme 11

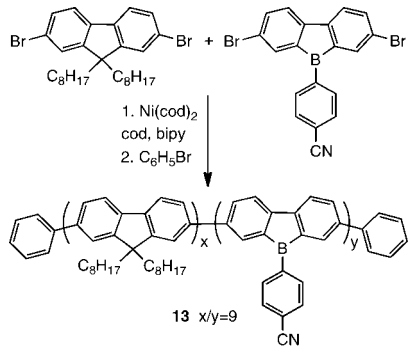

The latter is likely a result of coordination of the solvents to the Lewis acidic boron centers and this was further supported by ^{11}B NMR shifts in a region typical of tetracoordinate boron species (**12a**, $\delta = 13$ ppm in DMF-d_7; **12b**, $\delta = -4$ ppm in CD_3CN/THF-d_8).

Because of the lack of sterically demanding substituents on boron, especially **12a** and to a lesser extent **12b** are sensitive to air and moisture. Since **12b** forms relatively stable complexes with THF and CH_3CN, the molecular weight could be successfully determined for a preformed polymer complex by GPC analysis in $CHCl_3$, and M_n was estimated to be 5050 Da relative to PS standards. The average number of repeating units of **12a** ($n \approx 12$) and **12b** ($n \approx 14$) was also estimated by ^{1}H NMR integration and found to be in good agreement with the GPC results for **12b** ($n \approx 13$).

The absorption characteristics of polymers **12** were studied in coordinating solvents (THF, CH_3CN) and also for thin films that were deposited from those solutions. In thin films loss of the coordinated solvents occurs readily: the longest wavelength absorption maxima are observed at 362 nm for **12a** and as a shoulder at 372 nm for **12b**, which are significantly red-shifted with respect to solution data in THF. Moreover, unusually low-lying LUMO levels were derived from cyclic voltammetry measurements on thin films of polymers **12**. This aspect is of interest for use as *n*-type materials in optoelectronic applications as further elaborated in section 5.1.

A conceptually different synthetic approach was chosen by Bonifácio and co-workers.[38] They decided to first prepare the respective organoboron monomer, a dibrominated borafluorene species, which was then copolymerized with 2,7-dibromo-9,9-di-*n*-octylfluorene (Scheme 11). Yamamoto-type polycondensation was performed with Ni(cod)$_2$ as the catalyst and a molar ratio of 9:1 for fluorene to borafluorene. The copolymer **13** was analyzed by ^{1}H and ^{11}B NMR, which showed a peak at 43.2 ppm that was attributed to the borafluorene moiety. GPC analysis indicated relatively high molecular weight of $M_n = 22900$ Da relative to PS standards. The polymer was claimed to be stable under ambient conditions for at least 6 months, an aspect that was attributed to the electron-withdrawing effect of the cyano substituent.

2.1.3. Transition Metal-Containing Polymers

To incorporate transition metal complexes into conjugated organoborane polymers is an interesting objective because of the expected additional $d_\pi-p_\pi$ conjugation and the possibility for redox-tuning of the properties of the conjugated polymers. Moreover, interesting photophysical properties can be expected because of the presence of metal centers, for example, phosphorescence may accompany or replace the fluorescence typically observed for organoborane polymers. Thus, the functionalization of transition metal complexes with organoborane π-acceptor moieties has recently developed into a topical area of much interest.[72−78]

A number of conjugated organoboron polymers that contain transition metals in the main chain alternating with electron deficient boron centers have been reported over the past 10 years.[51−53,79−82] A polymer that contains a ruthenium−phosphine complex along with boron centers in the conjugated backbone (**14**) was prepared by Chujo and coworkers via hydroboration polymerization of a tetrayne type Ru complex with mesitylborane (Scheme 12).[80] Palladium and platinum acetylides (**15**) were incorporated into conjugated organoborane polymers using similar methods.[81] Hydroboration is believed to have taken place only at the terminal alkynyl groups due to the steric hindrance of the phosphine groups in combination with the bulkiness of the borane reagents. This was supported by ^{31}P NMR spectra for the polymers, which showed similar resonances to those of the monomeric precursors. Unusual ^{11}B NMR shifts of $\delta = 2.3$ (**14**), 8.0 (**15a**), and 8.5 ppm (**15b**) were reported; they are significantly upfield shifted in comparison to those of related metal-free dialkenylborane polymers (**3a**, $\delta = 31$ ppm).[61] The origin of this upfield shift is not entirely clear. The presence of both vinylene and acetylene groups was confirmed by IR spectroscopy. All polymers are well soluble in organic solvents and exhibit very respectable molecular weights of $M_n = 13000$ (**14**), 9000 (**15a**), 9100 Da (**15b**) according to GPC analyses relative to PS standards.

Polymer **14** showed very unusual photophysical properties. The UV−vis spectrum revealed two peaks, one at 359 nm that was attributed to a $\pi-\pi^*$ transition and another peak at 514 nm that was assigned to a $d_\pi-p_\pi^*$ transition of the ruthenium−phosphine complex. This implies that the $d_\pi-p_\pi^*$ transition is red-shifted by 141 nm compared to that of the ruthenium monomer. As a possible explanation, the push−pull

Scheme 12

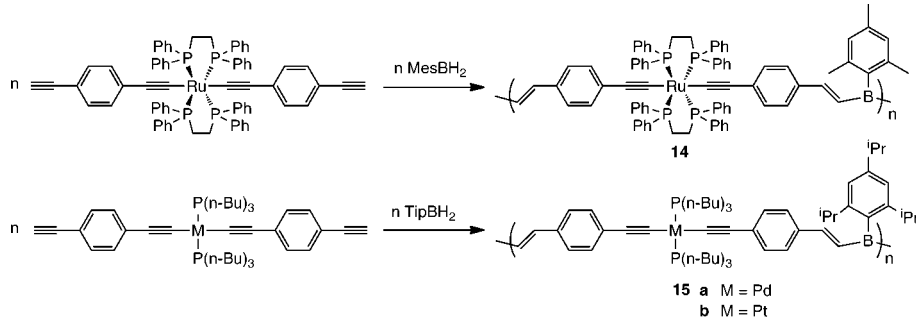

Scheme 13

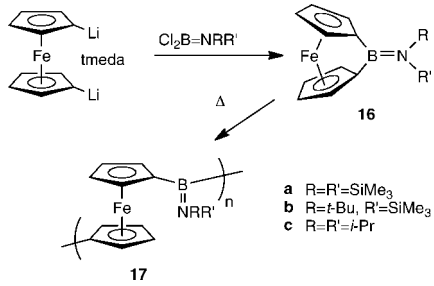

effect between the ruthenium center and the electron-deficient organoborane unit was invoked by the authors.[80] The palladium and platinum-containing polymers showed single absorption bands at ~390 nm and emitted green light with maxima at 481 nm (for **15a**) and 498 nm (for **15b**), respectively. A clear bathochromic shift relative to the monomeric transition metal complex was observed as a result of boron incorporation. When compared to related boron-containing polymers without transition metals, such as **3a**, the absorption maxima are in a similar range, but the emission is shifted from the blue to the green region.

The synthesis of ferrocenylborane polymers has been another fertile ground for exploration and this class of polymers was first pursued by Manners and Braunschweig via ring-opening polymerization of boron-bridged [1]ferrocenophanes **16** (Scheme 13).[51,79] These highly strained organoborane monomers show tilt-angles between the two Cp rings of up to 32.4°, which are among the largest reported for [1]ferrocenophanes. As a result of the high strain-energy, the boracycles readily undergo ring-opening reactions, a process that was monitored by differential scanning calorimetry (DSC). The DSC thermograms show melt endotherms in the range of 115 to 185 °C, which are followed by broad exotherms that are attributed to the ring-opening reaction (Figure 6). Preparative polymerization was performed by thermal treatment at 180−200 °C. However, the solubility of the resulting polymers (**17**) is moderate, and the soluble fraction consisted primarily of low molecular weight oligomers (n = 2,3).

Ferrocenylborane units were also incorporated into the main chain of the organometallic polymer poly(ferrocenylenesilane).[83] A diferrocenylborane with an Si−H functional group on each of the ferrocene moieties was generated by reaction of a strained Si-bridged ferrocenophane with $PhBCl_2$ in a 2:1 ratio and subsequent treatment with $Li[BEt_3H]$ (Scheme 14). The resulting disilane **18** was then used as a

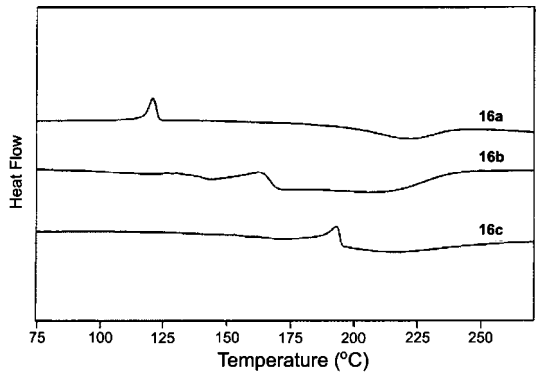

Figure 6. Differential scanning calorimetry (DSC) plots for compounds **16**. Reproduced with permission from ref 51. Copyright 2000 American Chemical Society.

Scheme 14

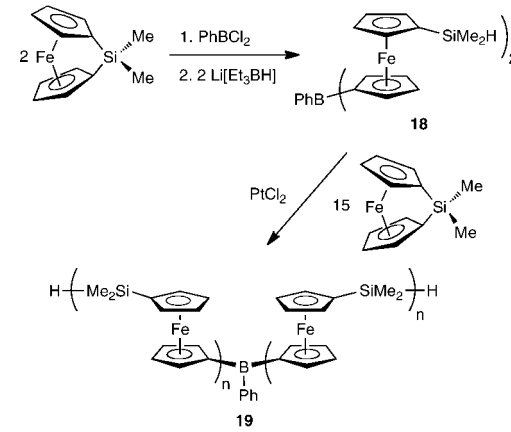

capping reagent in the $PtCl_2$-catalyzed polymerization of dimethylsila[1]ferrocenophane.

A new approach, which allows for placement of multiple highly electron-deficient borane moieties in the polymer chains has been discovered by Wagner, Holthausen, Jäkle, and co-workers (Scheme 15).[52,53,82] In an unusual redistribution/polycondensation reaction, the reactive bromine-substituted ferrocenylborane polymer (**20a**) was obtained upon treatment of 1,1′-fc$(BBr_2)_2$ (fc =1,1′-ferrocenediyl, Fe$(C_5H_4)_2$) with Et_3SiH. The intermediacy of a borane species 1,1′-fc$(BBrH)_2$ was postulated on the basis of density functional theory (DFT) calculations. The resulting polymer serves as a versatile precursor to other ferrocenylborane polymers by treatment with nucleophilic reagents. For instance, conversion with mesityl copper led to a dark red colored polymeric material (**20b**) that showed good stability in air, allowing for detailed investigation of the polymer structure and physical properties.[52] Reaction of **20a** with THF led to a ferrocenylborane polymer (**20c**) that features π-donating alkoxy groups on boron, consistent with an upfield shifted ^{11}B NMR resonance at 45 ppm.[82]

A related method makes use of condensation of a bifunctional ferrocenylhydridoborate species to build up the polymer chain (Scheme 15).[53] Treatment of Li_2[1,1′-fc$(BH_3)_2$] with Me_3SiCl was shown to lead to hydride abstraction and generation of the free borane 1,1′-fc$(BH_2)_2$, which can be trapped by complexation with Lewis bases such as amines or sulfides. However, in the absence of a Lewis base, 1,1′-fc$(BH_2)_2$ undergoes spontaneous polycondensation to polymer **20d**, most likely through a mechanism similar to that proposed for the formation of **20a**. Polymer **20d** is a rare polymeric analog of hydroborane species R_2BH, which are well-known for their versatile reactivity in hydroboration reactions. Treatment with phenylacetylene and *t*-butylacetylene, respectively, led to ferrocenylborane polymers [−fcB(CH=CHR)−]$_n$ (**20e**, R = Ph; **20f**, R = *t*Bu) with vinyl groups attached to boron.

Polymers **20b** and **20c** were further studied by GPC analysis coupled with multi-angle laser light scattering (GPC-MALLS). For **20b**, GPC-MALLS suggested a weight-average absolute molecular weight of M_w = 7500 Da, corresponding to an average of n = 24 repeating units, while batch-mode analysis of light scattering data using a Zimm plot for **20c** gave M_w = 7100 Da (n = 21). For all of these ferrocenylborane polymers, MALDI-TOF measurements revealed patterns consistent with the expected repeating units. Moreover, the polymer end groups could be determined and,

Scheme 15

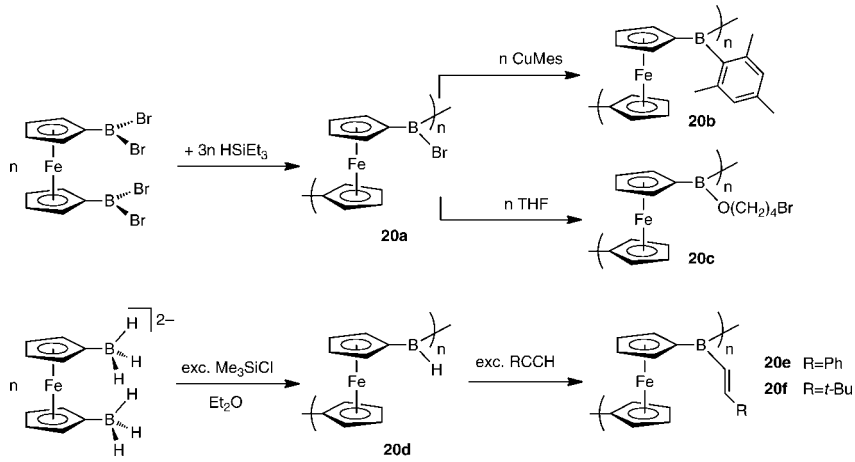

for example, for **20b**, the presence of both ferrocenyl and Mes_2B end groups was confirmed.

The question of how strongly the ferrocene moieties interact via the tricoordinate boron atoms is of particular interest.[75,84,85] One may expect that a highly electron-deficient borane center should very efficiently promote electronic delocalization via the empty p-orbital. Indeed, cyclic voltammetry measurements suggested that the iron atoms in **20b** strongly interact via the electron-deficient organoborane bridge. Two redox transitions with features of chemical reversibility were observed at $E^0 = 140$ and 845 mV (vs Fc/Fc^+, $Fc = Fe(C_5H_5)_2$) in CH_2Cl_2 containing $[NBu_4][B(C_6F_5)_4]$ as the supporting electrolyte (Figure 7). The exceptionally large potential difference of $\Delta E = 705$ mV between oxidation of the first and the second ferrocene moiety is consistent with significant electronic interaction via the tricoordinate boron centers. The extent of π-overlap between the p-orbital on boron and the ferrocene units is also expected to influence the UV−vis spectra. An absorption maximum of $\lambda_{max} = 506$ nm was found for **20b**, which is significantly red-shifted relative to the respective molecular ferrocenylborane model compound Fc_2BMes (490 nm). Bathochromic shifts, albeit less pronounced, were also found for **20e** ($\lambda_{max} = 495$ nm) and **20f** ($\lambda_{max} = 482$ nm) in comparison to dimeric model systems Fc_2BR (R = phenylvinyl 484 nm, *t*-butylvinyl 472 nm). In contrast, a comparatively higher energy absorption was observed for the alkoxyborane polymer **20c** with $\lambda_{max} = 475$ nm, presumably because of a diminished degree of electronic delocalization in the presence of the π-donating alkoxy groups.

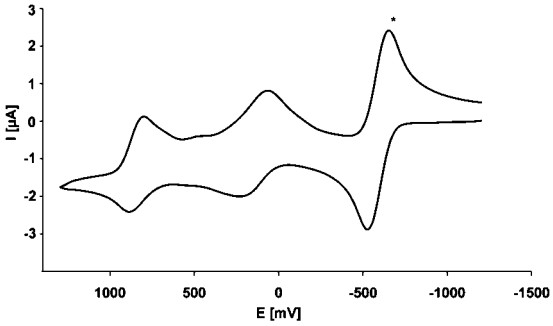

Figure 7. Cyclic voltammogram of **20b** (CH_2Cl_2, 0.1 M $[NBu_4][B(C_6F_5)_4]$, $v = 0.2$ V s^{-1} vs Fc/Fc^+; starred wave: $(C_5Me_5)_2Fe/(C_5Me_5)_2Fe^+$). Reproduced with permission from ref 52. Copyright 2006 Wiley-VCH Verlag GmbH & Co. KGaA.

2.1.4. Theoretical Studies

In triorganoboranes, the empty p-orbital typically overlaps strongly with π-substituents in the ground state LUMO, while p−π overlap is moderate in the HOMO. This is illustrated for a diborylated bithiophene derivative (**10b-M,** Figure 8) that mimics a part of the polymer chain in the poly(thiophene borane) **10b** (see Scheme 8).[86] A strong contribution of the p-orbitals is evident in the LUMO orbital. The resulting decrease in the LUMO orbital energy also affects the HOMO−LUMO separation, which in turn results in a bathochromic shift in the absorption and emission spectra.

As the conjugation pathway via the boron p-orbital increases from monomeric to dimeric, trimeric, and ultimately polymeric species, a further decrease in the HOMO−LUMO separation is anticipated. Chujo and co-workers carried out DFT calculations on oligomers that are structurally related to poly(vinylenephenylenevinylene borane) **3a** (Scheme 2).[61] A gradual decrease of the band gap with increasing chain length was deduced, as expected if conjugation is indeed extended via the empty p-orbital on boron (Figure 9). The effect leveled off at ∼4−5 repeating units, suggesting an effective conjugation length in that range.

Côté and co-workers performed DFT calculations on poly(2,7-borafluorene) (**13-P**), which contains the borafluorene moiety utilized by Bonifácio and Scherf as a building block in copolymer **13** (Scheme 11). When **13-P** was treated as a one-dimensional periodic system, a relatively small band gap was predicted, about 0.5 eV smaller than that for the respective fluorene and carbazole analogues.[87] Notably, steric effects disfavor a coplanar arrangement in **13-P** and an

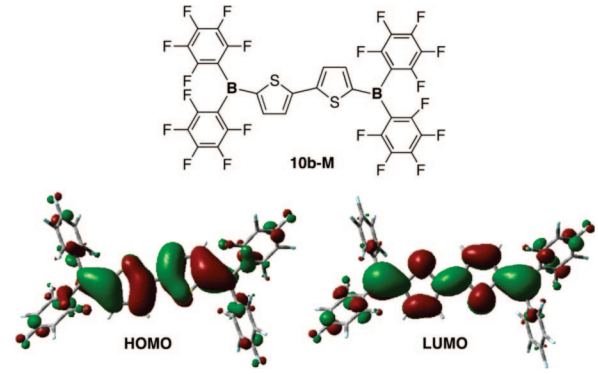

Figure 8. Frontier orbital plots for a diborylated bithiophene species that serves as a model for polymer **10b** (Scheme 8).

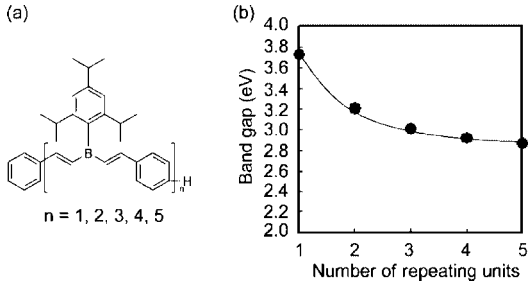

Figure 9. Dependency of HOMO−LUMO gap of oligomers **3a** (see Scheme 2) on chain length based on DFT calculations. Reproduced with permission from ref 61. Copyright 2009 American Chemical Society.

energy minimum was found for a torsion angle of 27° between monomer units. This likely limits the effective conjugation length to some extent.

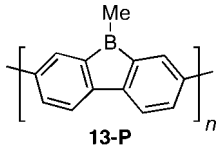

13-P

As we have seen, p−π interactions play an important role in defining the electronic structure and photophysical properties of conjugated organoborane polymers. An interesting question then arises: could incorporation of electron-deficient boron centers into suitably designed π-conjugated organic frameworks ultimately lead to intrinsic metallic properties? This has been a long-standing goal that has been tackled with various computational methods. In early studies, Tanaka and Yamanaka used self-consistent field−crystal orbital (SCF-CO) methods, which suggested that poly(boraacetylene) (**21a**) and poly(*p*-diboraphenylene)s (**21b**,**c**) could indeed be viable candidates (Chart 1).[88−90] More recently, small band gaps were also postulated by Lagowski and coworkers for oligomeric boroles **21d** based on DFT calculations using a modified B3P86 hybrid functional.[91] An interesting finding of this study is that oligomers with $n < 5$ should display an aromatic character with relatively large HOMO−LUMO gaps, but a quinoid structure with low-lying LUMO levels is predicted for the higher oligomers (n = 5−9). Ab-initio Hartree−Fock (3-21G) calculations on poly(borole) **21d** and related poly(heteroborole) copolymers **21e** and **21f** were reported by Narita and co-workers.[92] Ma

Chart 1

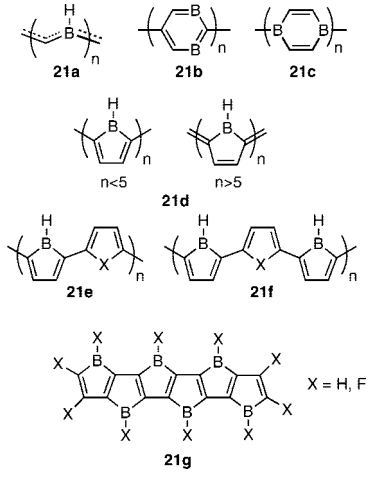

and co-workers used DFT methods to deduce a quinoid structure with diradical character for the thiophene-borole copolymer **21e** (X = S) with band gaps of ~2.0−2.2 eV, depending on whether a cyclic or linear model was used.[93] Most recently, oligoacenes containing borole building blocks **21g** were studied with DFT methods by Jiang and coworkers.[94] Their calculations specifically suggested that these types of conjugated systems should be useful ambipolar materials for field effect transistors.

While the electronic properties of polymers **21** are predicted to be highly intriguing, they are synthetically very challenging targets. One of the main obstacles will be that steric protection is almost certainly necessary for stabilization under ambient conditions. However, in the presence of highly bulky substituents, structural distortions may significantly diminish electronic delocalization. That interesting electronic properties can nonetheless be achieved is clear from the earlier discussion of the photophysical characteristics of the organoborane polymers successfully prepared to date. Further studies on their applications as device materials will be covered in section 5.1.

2.2. Polymers with Boron−Heteroatom Bonds in the Main Chain

Organoborane moieties have also been frequently embedded into polymeric materials via boron−oxygen and boron−nitrogen linkages. This can be achieved either via polycondensation routes, in which the boron−oxygen or boron−nitrogen bonds are formed during the polymerization process or via polymerization of preformed organoborane monomers. In the latter case, not only condensation polymerization but also addition and ring-opening polymerization methods have been employed.

Of particular interest is again the question, to what extent $p_\pi-p_\pi$ interactions between boron and the heteroatom are able to promote extended delocalization as already discussed for polymers featuring organic π-systems attached to boron. Another aspect that has received considerable attention for this particular class of polymers is the possibility for reversible formation of polymeric materials via dynamic covalent bonds.

2.2.1. Boron−Oxygen Linkages

Early studies on the formation of boronate polymers via condensation of phenylboronic acid with aliphatic diols by Gerwarth in the 1970s reflected a distinct feature of boronates $R-B(OR')_2$, which is the reversible formation and cleavage of the boron−oxygen bonds in the presence of trace amounts of water.[95] High molecular weight materials could not be obtained, but equilibria involving cyclic species were evident. Similar observations were later made by Wagener and coworkers when they studied the polymerization of boronate monomers by acyclic diene metathesis (ADMET).[96]

More recently, extensive studies have been performed on the dynamic covalent assembly of boronate polymer structures, ranging from macrocycles to linear polymers and 3-dimensional networks, including the preparation of covalent organic frameworks (COFs) for applications in gas storage and separation.[97−100] Of relevance with respect to optical materials is the work by Lavigne and co-workers.[47,101] They used 9,9-dihexylfluorene-2,7-diboronic acid as a building block for the preparation of polymers **22** by condensation with pentaerythritol and 1,2,4,5-tetrahydroxybenzene, re-

Scheme 16

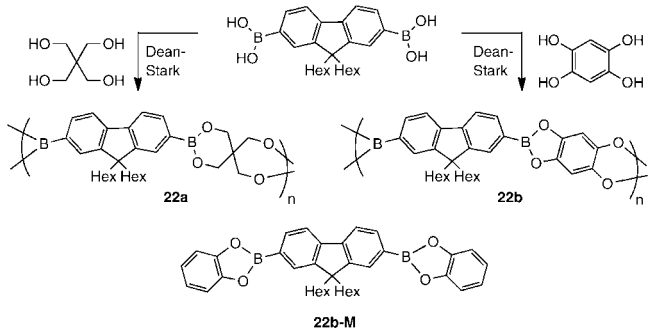

spectively, under Dean−Stark conditions (Scheme 16). Unlike the boronate polymers reported earlier by Gerwarth and Wagener, incorporation of the boronic ester functionality into a cyclic system leads to appreciable stability and only slow hydrolysis in the presence of water. Hence, **22** and related polymers could be analyzed by GPC without special precautions. Molecular weights of M_n = 10000−11000 Da (polydispersity index, PDI = 2.4 to 2.6) were readily achieved according to GPC analysis versus PS standards. Even higher molecular weights were realized after extended reaction times, but the solubility of those polymers was poor.

The possibility of extended delocalization in polymer **22b** was further probed.[47] As in other related molecular systems,[102] the trigonal planar boron environment in **22b-M** was found to be almost coplanar with the fluorene moiety according to a single crystal X-ray diffraction study, thereby providing for optimal overlap of the p-orbital on boron and the fluorene π-system.[47] Comparison of the absorption spectra revealed a significant red-shift (12 nm) for **22b** with its aromatic tetrahydroxobenzene linker in comparison to non-conjugated **22a**. Similarly, the fluorescence of blue emissive **22b** was shifted relative to that of **22a**. Most convincingly, a comparison of the absorption spectra of samples of **22b** of different molecular weight revealed a clear bathochromic shift with increasing molecular weight (Figure 10). This trend was also confirmed by computational methods. An effective conjugation length of about 3−5 bridging dioxaborole units was deduced.

A boronate transesterification approach was used by Trogler and co-workers to introduce a borylated fluorescein derivative into a dynamic covalent polymer framework (Scheme 17).[48] Reaction of 3′,6′-bis(pinacolatoboron)fluoran with pentaerythritol at 50 °C in a MeOH/water mixture gave

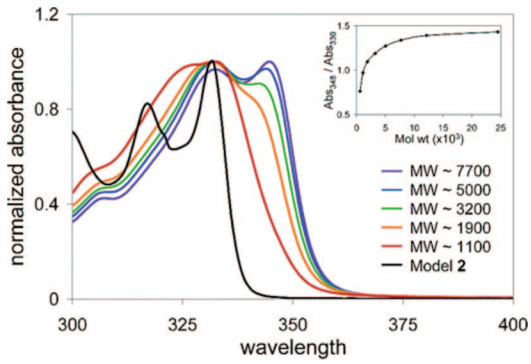

Figure 10. Normalized absorption spectra for **22b** of varying length and comparison with **22b-M** (model **2**). Inset: Change in the polymer absorption as a function of molecular weight. Reproduced with permission from ref 47. Copyright 2006 American Chemical Society.

Scheme 17

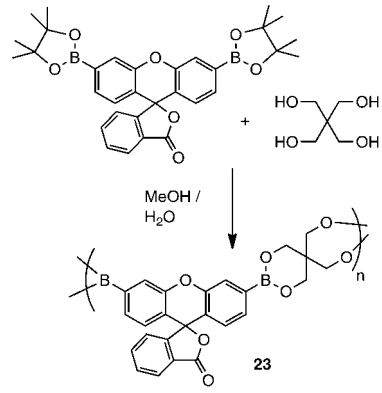

Scheme 18

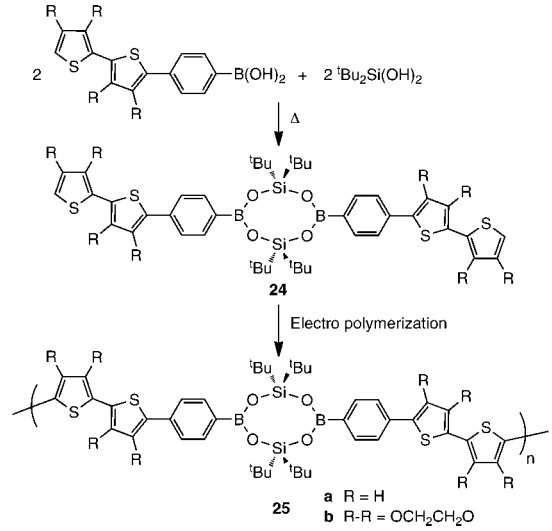

polymer **23** in 75% yield as a white powder. The molecular weight relative to PS standards was determined by GPC in THF to be M_n = 6700 Da, and the PDI was 1.5. While the polymer itself does not show any fluorescence, oxidative degradation leads to release of fluorescein, which can be exploited for sensory applications as further discussed in section 5.4.

Lee and co-workers used a borasiloxane cage to embed conjugated thiophene oligomers into polymeric structures.[50] Rather than linking the monomer units together through assembly of the borasiloxane ring system, Lee first prepared borasiloxane monomer **24** featuring two electro-polymerizable bithiophene substituents (Scheme 18). Thin films of **25** were deposited on polymer-coated indium tin oxide (ITO) electrodes. These films are initially green colored due to oxidative doping during the electropolymerization process. Upon electrochemical reduction, the color changes to orange. The presence of polaronic/bipolaronic states upon oxidative doping was inferred from cyclic voltammetry measurements.

2.2.2. Boron−Nitrogen Linkages

Polymers with aminoborane moieties in the main chain have been pursued by Chujo and co-workers.[103−105] One method that was successfully applied takes advantage of alkoxyboration of aliphatic or aromatic diisocyanate derivatives with dialkoxyborane species. For example, reaction of mesityldimethoxyborane with 1,6-hexamethylene diisocyanate in bulk at 140 °C resulted in a soluble polymeric material (**26**) in 43% yield with a molecular weight of M_n

Scheme 19

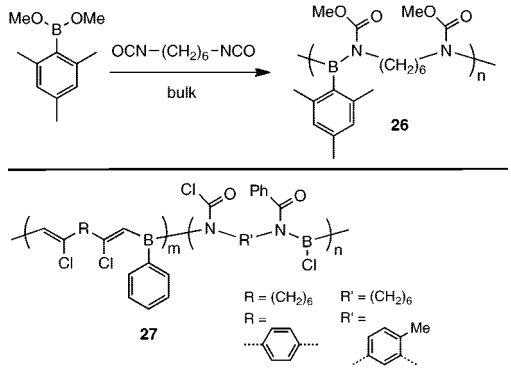

= 6700 Da (Scheme 19).[105] A significant B═N double bond character was deduced from the ^{1}H NMR data of **26** and an ^{11}B NMR shift of 31.7 ppm was reported, which is consistent with formation of diaminoborane functional groups. Both the pendant boron substituents and the bridging group between the diisocyanate moieties were varied, resulting in various poly(boronic carbamate)s with molecular weights ranging from M_n = 1200 to 10200 Da. The bulky mesityl group on boron proved critically important for the successful preparation of soluble polymeric materials and the hydrolytic stability was further improved when aromatic diisocyanates were employed.

Polymers with B−N linkages within the main chain were also prepared by boration copolymerization with diynes and diisocyanates.[103] Initial attempts by using a mixture of $PhBCl_2$, a dialkyne, and a diisocyanate gave copolymers **27**. However, the diyne component was incorporated to a much lesser extent than expected from the feed ratios, suggesting that the diyne monomer was reacting more slowly than the diisocyanate.

To achieve an alternating copolymer structure, a stepwise procedure was developed, in which the bifunctional phenylborane species **28** were first prepared by haloboration of the respective dialkyne precursor.[103,104] Treatment of **28** with the diisocyanate of choice in $CHCl_3$ at RT gave polymers **29** in moderate to good yields (Scheme 20). Molecular weights of up to M_n = 4300 Da (**29c**) were achieved. An alternating copolymer structure was proposed. Shifts of ca. 29−32 ppm were found for the major peak in the ^{11}B NMR spectra, but in several cases additional smaller peaks were observed, which might be a result of cross-linking points or polymer chain ends. Possible interaction of the carbonyl oxygen with boron was postulated based on the unusually large C═O stretching frequency observed in the IR spectra.

The combination of partial B═N double bonds with fully aromatic π-systems in polymers **29c**−**f** is of particular

Scheme 20

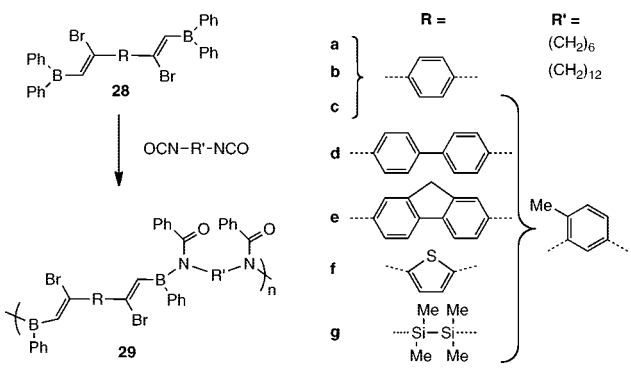

Scheme 21

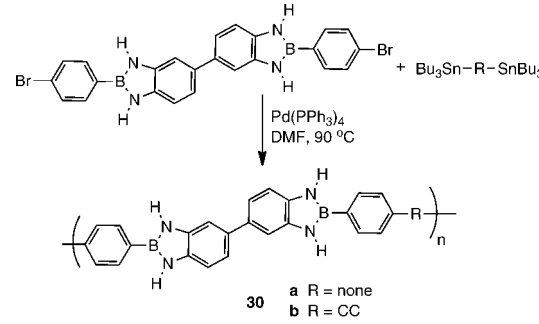

interest because of the potential for extended conjugation to occur. Moreover, for **29g** σ,π-electronic delocalization may occur via the disilane moieties. However, from the UV−vis spectra of **29g** no clear evidence could be obtained, possibly because of the presence of cross-links or due to the meta-linkage of the diisocyanate species. The thiophene derivative **29f** was found to emit green light and **29g** showed a strong emission in the violet region, which was tentatively attributed to the aminoborane-substituted disilane units.

Incorporation of the B−N linkage into a heterocyclic ring-system is attractive due to the expected stabilizing effect. Indeed, polymers that feature diazaborole units in the main chain are among the earliest examples of boron-containing polymers and were first reported by Marvel and co-workers in 1962.[106] They were obtained as soluble polymeric materials upon condensation of aromatic diboronic ester species (1,4-phenylene, 1,3-phenylene, and 1,1′-ferrocenylene diboronic esters) with 3,3′-diaminobenzidine in the melt. The high thermal stability of up to 500−600 °C for the phenylene derivative is remarkable. However, despite incorporation of boron into a cyclic structure, relatively facile hydrolytic degradation was observed and these materials were therefore not further investigated at the time. A new route to poly(benzdiazaborole)s that makes use of transition-metal catalyzed coupling reactions of a preformed bifunctional benzdiazaborole was recently developed by Yamaguchi and co-workers (Scheme 21).[43] Stille-type polycondensation, which is advantageous because it can be performed under anhydrous conditions, gave the desired polymers in high yields with molecular weights of M_n = 5560 (**30a**) and 3620 Da (**30b**), corresponding to an average number of repeating units of 14 and 9, respectively. Similar results were obtained by ^{1}H NMR end group analysis, assuming that the polymers are terminated by bromophenyl groups on both chain ends (no stannyl end groups were observed). The polymers proved to be stable to ca. 355 and 385 °C, respectively, according to TGA measurements under a nitrogen atmosphere.

The absorption maxima at 349 (**30a**) and 358 nm (**30b**) were slightly red-shifted in comparison to a molecular model system, which was attributed to extended delocalization along the polymer chains. Indeed, a certain B−N double bond character in the excited state of benzdiazaborole compounds has been proposed as early as 1960.[107] The larger shift for **30b** is consistent with the more delocalized structure of the diphenylalkyne linker. A further bathochromic shift to 395 nm was observed for a thin film of **30a** and attributed to an ordered π-stacked structure. Additional evidence for stacking interactions was gathered from powder X-ray diffraction (XRD) measurements, which suggested an ordered structure in an orthorhombic lattice, similar to that of poly(diphenylamine), $(PhNHPh)_n$. In DMSO solution, the polymers emit

in the green region at 513 and 529 nm, respectively. The unusually large Stokes shift was attributed to charge transfer processes.

2.3. Polymers with Tetracoordinate Boron in the Main Chain

The following section will introduce the synthesis and photophysical properties of polymers that feature boron heterocycles in which boron is tetracoordinate. This design can be advantageous for improved stability of the resulting materials, as a result of both incorporation of boron into a ring system (chelate effect) and electronic saturation because of Lewis acid−base interactions. However, it should be emphasized that in the case of the cyclodiborazane, pyrazabole, and organoboron quinolate-containing polymers discussed in the following, pronounced electronic delocalization should not be expected given that the boron centers are tetracoordinate, thereby largely interrupting the π-conjugation pathway. Nonetheless, as we will see, interesting photophysical properties are realized, especially when these chromophores are alternating with other organic π-systems in such a way that a donor−acceptor structure is formed.

In an early effort, a large variety of different poly(cyclodiborazane)s (**31**−**33**) were prepared by Chujo and co-workers using hydroboration of dicyano compounds with bifunctional boranes RBH_2 (R = *t*-Bu, Mes, Tip, isopinocampheyl) (Scheme 22).[108] The resulting materials displayed favorable stability and were readily isolated when the bulkier Mes and Tip groups were attached to the borane source.[46,109] The successful formation of the borazane heterocycle upon polymerization was evident from the ^{11}B NMR spectra, which showed a main signal close to 0 ppm, in the expected region of tetracoordinate boron. However, in most cases this large signal was accompanied by a smaller signal at ~30 ppm, which is attributed to aminoborane polymer end groups (Table 2).

The photophysical properties depend very strongly on the electronic structure of the aromatic dicyano compound. When electron-rich bridging groups (e.g., oligothiophenes, dialkoxybenzene) were used intramolecular charge transfer was apparent as the absorption and emission bands experienced a bathochromic shift.[110] Some color tuning was achieved by extension of the π-conjugation length of the linker with increasing number of thiophene rings.[111] Moreover, a polymer with dithiafulvene moieties (**32e**) showed semiconducting behavior (2×10^{-5} S cm^{-1}).[112] Incorporation of disilane moieties (**32k**) and transition metal alkynyl complexes (**32l**) as bridging groups was also studied.[113,114]

Chiral luminescent poly(cyclodiborazanes) (**33**, Chart 2) were prepared using the tmeda (N,N,N′,N′-tetramethylethylenediamine) adduct of enantiomerically pure isopinocampheylborane as a precursor.[115] Polymer **33c** shows a blue-green emission at 468 nm with a quantum efficiency of 18%, while polymers **33a** and **33b** emit only weakly in the UV. The different behavior of **33c** was again attributed to charge transfer involving the electron-rich dialkoxybenzene linker. Circular dichroism studies were performed, but a clear effect of the chiral pendant group on the main chain chirality could not be established, possibly because of cis-/trans-isomerism at the imine groups.

Polymerization via Sonogashira−Hagihara coupling was explored as an alternative route to poly(cyclodiborazanes) (Scheme 23).[40] Treatment of the cyclodiborazane monomer **34** with a dialkyne in the presence of $PdCl_2/Cu(OAc)_2$ as the catalyst led to formation of **35**, which exhibited slightly higher molecular weight than polymers **31** and **32**. While the polymer structure is generally similar, no aminoborane end groups (or defects due to borazine formation) were generated in this process: for **35** only one signal was observed at 0.9 ppm in the ^{11}B NMR spectrum. In conclusion, while the Sonogashira-Hagihara coupling is not as generally applicable as the hydroboration protocol, better control over end group coverage and ultimately the electronic structure of the polymer make this route very attractive.

Pyrazaboles, another important class of boron−nitrogen heterocycles, are touted for their exceptionally high stability. They have been explored, for example, as building blocks of supramolecular structures such as container molecules.[116−118] Chujo and co-workers studied the synthesis and properties of polymers that contain pyrazabole moieties in the main-chain using Sonogashira−Hagihara coupling polymerization. Coupling between iodo-functionalized pyrazabole and di-

Scheme 22

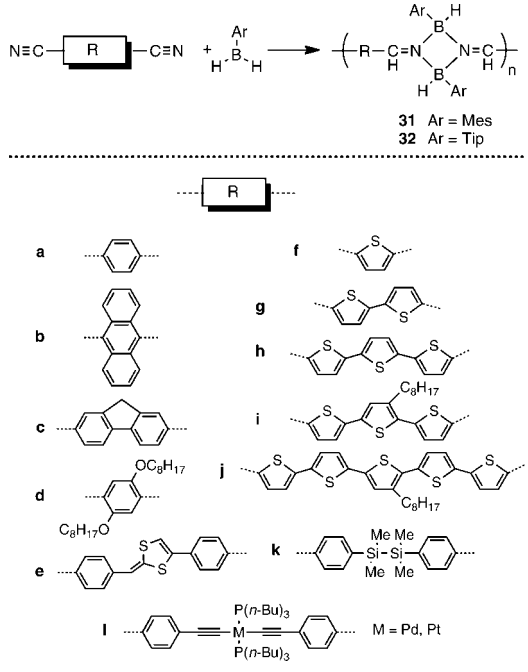

Chart 2

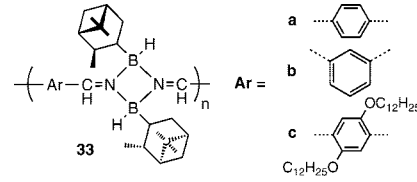

Scheme 23

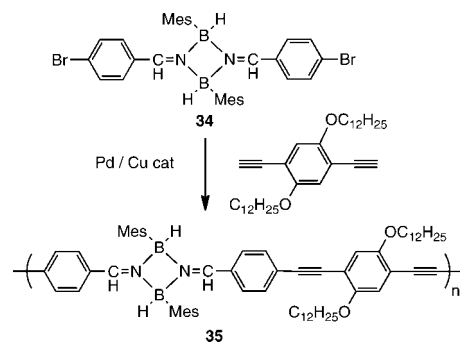

Table 2. Selected Data for Polymers with Tetracoordinate Organoborane Moieties Embedded into a Conjugated Organic Backbone

	δ (^{11}B)	M_n[a]	M_w[a]	PDI[a]	n[b]	solvent[c]	λ_{abs}/nm[d]	λ_{em}/nm[e]	Φ_F[f]	ref
31b	−3.0	4400	8800	2.0	9	$CHCl_3$	406	494		46
31d	0.9	5800	7900	1.4	9	$CHCl_3$	381	463		110
31f	0.9	4700	9400	2.0	12	$CHCl_3$	364	473		110
32e	4.8	3700	5700	1.5	5	$CHCl_3$	415	531		112
32g	−0.8	3200	8700	2.8	5	$CHCl_3$	391	453[g], 492, 518[g]	0.15	111
32h		2500	6100	2.4	4	$CHCl_3$	418	494, 525[g]	0.17	111
32i		2500	4700	1.9	4	$CHCl_3$	415	496, 526[g]	0.15	111
32j		2100	3100	1.5	3	$CHCl_3$	421	532	0.17	111
32k	4.3	9400	13900	1.5	12	$CHCl_3$	301	380, 403		113
36a	−0.9	34000	42000	1.2	55	$CHCl_3$	320	383[h]	0.43	41
36b	2.2	9000	19700	2.2	13	$CHCl_3$	350	406[h]	0.56	41
36c	0.7	33000	61000	1.8	40	$CHCl_3$	308, 360	430[h]	0.67	41
36d	−3.6	11400	41300	3.62	17	$CHCl_3$	295, 313, 342	350, 371	0.23	119
36e	−1.9	11400	21300	1.87	17	$CHCl_3$	332	350	0.11	119
36f	−2.6	6400	12000	1.92	10	$CHCl_3$	277, 317	*i*	*i*	119
36g	−3.7	8600	23500	2.73	12	$CHCl_3$	320	353, 384	0.63	119
36h	−1.7	9000	18000	2.0	13	$CHCl_3$	430	470	0.53	41
38a	7.2	3200	5300	1.7	5	$CHCl_3$	376	486	0.26	126
38b	7.1	8800	20700	2.4	11	$CHCl_3$	380	489	0.27	126
38c	7.4	6600	15100	2.3	7	CH_2Cl_2	376	484	0.20	127
38d	7.3	6600	15400	2.3	7	CH_2Cl_2	375	478	0.20	127
38e	7.5	5200	10500	2.0	6	CH_2Cl_2	375	472	0.29	127
39a	8.9	3200	6100	1.9	4	$CHCl_3$	313, 374	421, 502	0.54	128
39b	6.5	11200	24500	2.2	12	$CHCl_3$	287, 316, 374	433, 564	0.10	128
39c	5.2	7800	10900	1.4	8	$CHCl_3$	297, 314, 377	427, 598	0.01	128
39d	4.9	3400	4900	1.4	6	$CHCl_3$	264, 356, 372	414, 501	0.58	128
39e	3.9	3100	5500	1.8	5	$CHCl_3$	279, 359, 375	420, 561	0.14	128
39f	4.9	2200	6600	3.0	4	$CHCl_3$	287, 360, 377	415, 601	0.00	128
40a	2.4	2100	5100	2.5	4	CH_2Cl_2	333	500	0.14	129
40b	3.0	11200	32600	2.9	15	CH_2Cl_2	361	502	0.17	129
40c	2.7	18100	39700	2.2	19	CH_2Cl_2	376	503	0.23	129
41a	10.3	7900	14100	1.78	16	CH_2Cl_2	394	504	0.21	70
41b	9.3	10800	18200	1.69	18	CH_2Cl_2	444	639	0.001	70
42a	11	10900	20700	1.90	9	CH_2Cl_2	443	611[h]	0.01	49
42b	12	17400	27200	1.56	16	CH_2Cl_2	411	536	0.19	49
43a		1680	2130	1.27	5	$CHCl_3$	640	661	0.24	132
43b		4390	7230	1.65	5	$CHCl_3$	633	664	0.08	132
43c		5980	9610	1.61	11	$CHCl_3$	571	615	0.24	132
43d		3430	5560	1.62	3	$CHCl_3$	575	637	0.25	132
44a		21600	45400	2.1	18	CH_2Cl_2	606	641	0.25	133
44b		19200	36500	1.9	19	CH_2Cl_2	635	657	0.24	133
44c		15700	31400	2.0	18	CH_2Cl_2	628	664	0.06	133
45a		16500	29700	1.8	35	CH_2Cl_2	659	678	0.21	133
45b		23800	45200	1.9	39	CH_2Cl_2	665	683	0.23	133
45c		14400	34600	2.4	28	CH_2Cl_2	650	680	0.14	134
45d		20600	51500	2.5	29	CH_2Cl_2	662	684	0.15	134
45e		26700	64100	2.4	30	CH_2Cl_2	669	690	0.13	134
46a		22500	39400	1.75	30	CH_2Cl_2	557	587	0.64	135
46b		19100	31500	1.65	28	CH_2Cl_2	547	585	0.56	135
46c		18400	33100	1.80	27	CH_2Cl_2	549	588	0.85	135
47a	−13.8	24200[j]	*j*	*j*	33	$CHCl_3$	348, 519	532	0.80	42
47b	−14.2	20500[j]	*j*	*j*	24	$CHCl_3$	370, 519	532	0.71	42
47c	−13.8	11300	22100	1.96	14	$CHCl_3$	372, 519	532	0.85	42

[a] Molecular weights (Da) based on GPC analysis vs PS standards; PDI = M_w/M_n. [b] Number average of repeating units based on GPC analysis. [c] Solvent used for photophysical studies. [d] Bands corresponding to transitions centered on the boron heterocycle and/or $\pi-\pi^*$ transitions of organic linker. [e] Emission maxima upon excitation at λ_{max}. [f] Fluorescence quantum efficiency. [g] Shoulder. [h] Only the most intense of multiple emission bands is given. [i] Polymer was nonemissive. [j] Polymodal profiles were observed due to formation of aggregates.

alkyne monomers or between diethynylpyrazabole and dibromoarene compounds gave polymers **36** (Scheme 24).[41,119] Relatively high molecular weights were achieved with M_n up to 34000 Da (average of 55 repeating units) for **36a**. However, no significant red-shift in the UV−vis absorption was observed compared to the monomer units, consistent with a lack of significant extension of π-conjugation via the pyrazabole moiety with its tetracoordinate boron centers. Notwithstanding, most of these polymers showed intense fluorescence in the near-UV, which was attributed to emission from the pyrazabole moieties. For those polymers containing an alkyne linker with extended delocalization (e.g., **36h**), the fluorescence maximum shifted to longer wavelengths, while π-acceptor groups (e.g., **36g**) led to shorter wavelengths. Hence it was possible, to some extent, to tune the emission by incorporating different groups into the polymer. Emission was also stimulated by exposure to neutrons or alpha particles, suggesting potential use as scintillating materials for neutron detection.[120]

Related transition metal-containing pyrazabole polymers were prepared by dehydro-halogenation reactions (Scheme 25). Red-shifted absorption bands attributed to MLCT absorption bands were observed for the Ni- and Pt-containing polymers **37a** and **37c**, but not for the respective polymer containing Pd (**37b**), which showed structured high energy bands attributed to the pyrazabole moiety itself.[121] However,

Scheme 24

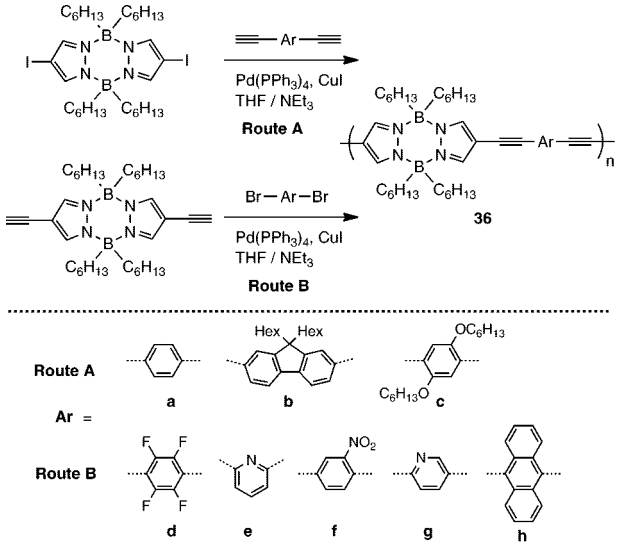

Scheme 25

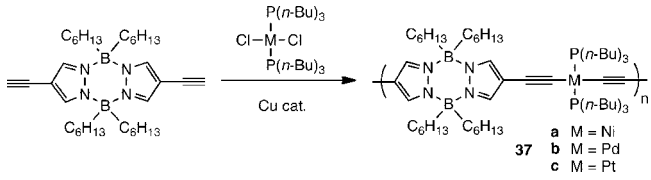

these polymers proved to be very weakly emissive with only low emission quantum yields of less than 1%.

Organoboron quinolato (R_2Bq; q = 8-hydroxyquinolate) moieties have attracted considerable attention as chromophores following the discovery by Wang and co-workers that they can be advantageously employed in OLEDs as electron conduction and emission layer, serving as an alternative to the widely used aluminum tris(8-hydroxyquinolate) (Alq_3) and its derivatives.[122] In regard to incorporation of this chromophore into polymers, early work focused on polyolefins and is further discussed in Section 4.[123−125] Several approaches to the incorporation of this and related chromophores into the main chain of polymers have since been reported. Further discussed here is the design where the boron quinolate chromophore is alternating with organic π-systems.

Chujo and co-workers reported the first examples of main chain organoboron quinolate polymers in 2007.[126,127] Polymerization was perfomed via Sonogashira−Hagihara coupling of preformed diiodo-functionalized organoboron quinolate monomers with different dialkynes (Scheme 26). The latter contained long alkyl side chains to promote good solubility of polymers **38** in organic solvents. The molecular weights relative to PS standards ranged from M_n = 3200−8800 Da with PDIs from 1.7 to 2.4.

For those polymers featuring the parent 8-hydroquinoline ligand, absorptions at 376−380 nm were observed and excitation at the absorption maxima led to strong blue-green emission at 484−489 nm with emission quantum efficiencies in the range of 20−27%.[126] Methyl substitution in 2- or 4-position of the quinolate group led to a shift of the emission to high energy (e.g., from 484 nm for **38c** to 472 nm for **38e**) and an increase in the emission quantum efficiency from 20% to 29%.[127] Thus, polymer **38e** displayed a desirable blue emission both in solution and after casting into a thin film. A slight red-shift of the emission wavelength was observed

Scheme 26

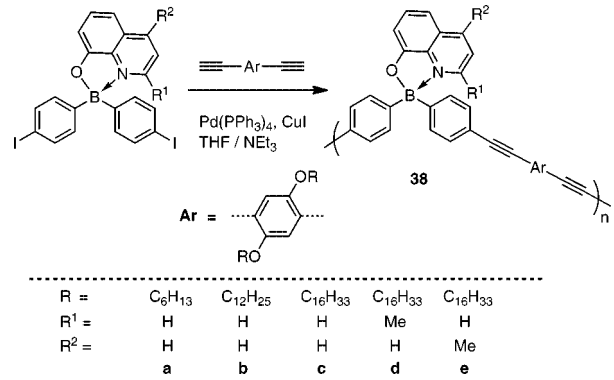

R =	C_6H_{13}	$C_{12}H_{25}$	$C_{16}H_{33}$	$C_{16}H_{33}$	$C_{16}H_{33}$
R^1 =	H	H	H	Me	H
R^2 =	H	H	H	H	Me
	a	b	c	d	e

Chart 3

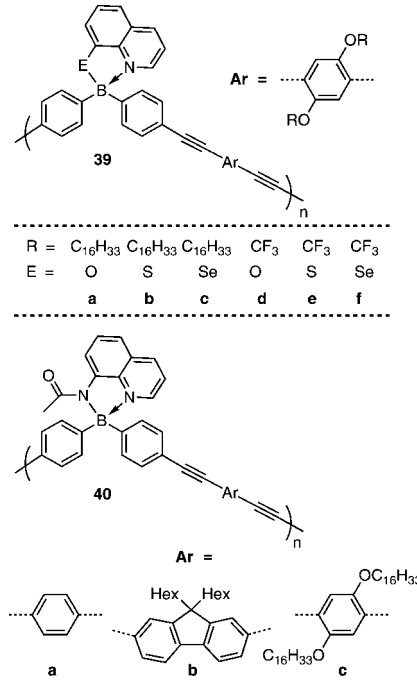

R =	$C_{16}H_{33}$	$C_{16}H_{33}$	$C_{16}H_{33}$	CF_3	CF_3	CF_3
E =	O	S	Se	O	S	Se
	a	b	c	d	e	f

for thin films of some of these polymers in comparison to $CHCl_3$ solutions. A very interesting feature is that the strong absorbance of the dialkyne chromophore leads to an antenna effect, where energy transfer occurs from this chromophore to the organoboron quinolate moiety, leading to very intense emission colors.

Chujo and co-workers also investigated the effect of changing the heteroatom in the hydroxyquinolate derivatives from oxygen to sulfur and selenium.[128] Polymers (**39**, Chart 3) were prepared through similar synthetic methods as those described for **38**. Strong bathochromic shifts in the emission spectra were observed with increasing atomic number of the Group 16 element, consistent with decreasing HOMO−LUMO gaps as confirmed by DFT calculations on molecular model systems. At the same time, the emission quantum efficiencies decreased dramatically, which was attributed to enhanced intersystem crossing because of the heavy atom effect of the Group 16 element. Dual emissions were observed for all these compounds but were most pronounced for the heavier analog **39c**. This peculiarity was attributed to competing pathways of emission from the dialkyne (emission at 427 nm) and the quinolato moiety (emission at 598 nm) of **39c** and less efficient energy transfer to the quinolate moieties with increasing atomic number.

Scheme 27

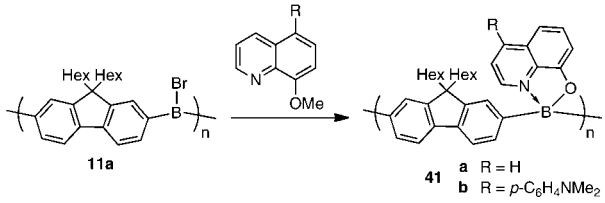

Aminoquinolate polymers (**40**, Chart 3) were similarly prepared using an acetylaminoquinoline-functionalized borane in the Sonogashira-Hagihara coupling reactions.[129] An advantage of such a system is that the additional attachment point at the amino group can facilitate further functionalization of the ligands architecture. Moreover, DFT calculations show a lower LUMO level for the molecular species $Ph_2B(aq)$ (aq = acetylaminoquinolate) in comparison to the respective hydroxyquinolate derivative Ph_2Bq, suggesting the potential for improved electron transport properties. The HOMO−LUMO gap is slightly smaller, and this is also reflected in the absorption and emission characteristics of polymers **40**. Specifically, the emission maxima are red-shifted by about 10−15 nm relative to those of the respective hydroxyquinolate polymer **38c**. Energy transfer from the dialkyne linker to the aminoquinolate moiety was found to be highly efficient, resulting in intense green emission of these polymers.

According to studies by Jäkle and co-workers, polymer modification can also be utilized to incorporate the organoboron quinolate moiety into the polymer main chain. Treatment of the bromoborane precursor polymer **11a** (see Scheme 9) with methyl-protected quinolato ligands gave polymers **41** under mild conditions with MeBr as the only byproduct of the reaction (Scheme 27).[70] The molecular weights are predetermined by the number of repeating units of the precursor polymer and were measured to be M_n = 7900 and 10800 Da for **41a** and **41b**, respectively, corresponding to ∼16−18 repeating units. The structures were further confirmed by MALDI-TOF mass spectrometry, which showed two main series that correspond to polymer chains with fluorene or quinolato end groups, that is, H-[FlBQ]$_n$ and QB-[FlBQ]$_n$ (Fl = 9,9-dihexylfluorenylene, Q = 8-hydroxyquinolato). The photophysical properties mirror those described by Chujo and co-workers for polymers **38**, except for that the 4-dimethylaminophenyl pendant group in **41b** leads to a strong bathochromic shift resulting in a very weak red emission.

Jäkle and co-workers introduced a method for the preparation of polymers, which contain both the boron and quinolato moieties embedded in the main chain.[49] Organoboron quinolate polymers **42** were prepared under mild conditions via a polycondensation reaction involving boron-induced ether cleavage between methyl-protected bifunctional hydroxyquinolate ligands[130] and a bifunctional bromoborane (Scheme 28). This polymerization proceeds without the need for any catalyst, and the byproduct MeBr is again readily removed under high vacuum. The photophysical properties of polymers **42** are strongly dependent on the nature of the conjugated bridge connecting the quinolato groups: with a highly delocalized Th−C_6H_4−Th linker, the lowest energy absorption corresponds to intramolecular charge transfer (ICT) from this conjugated linker to the pyridyl moiety. In contrast, with a less delocalized biphenyl linker, ICT occurs from the fluorene moiety of the diboron monomer to the

Scheme 28

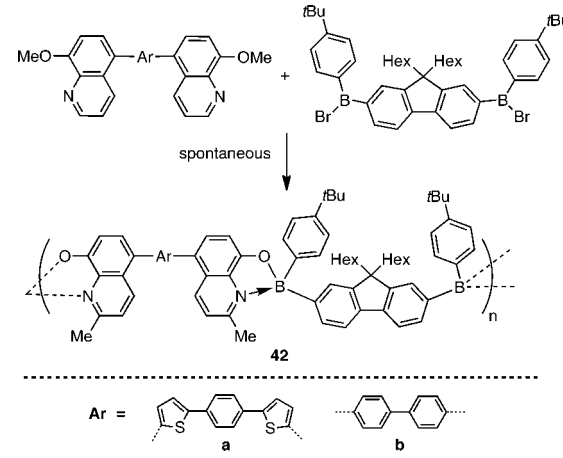

Scheme 29

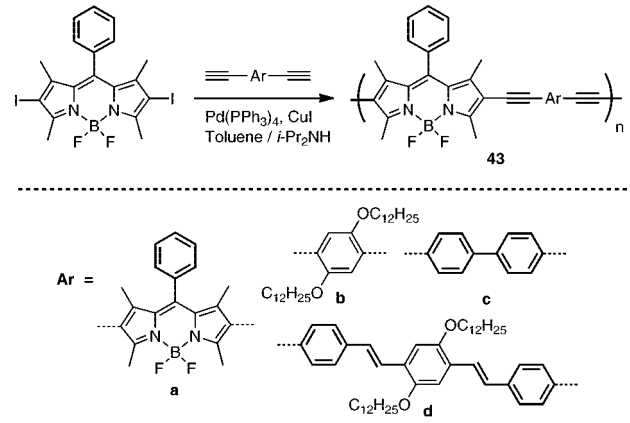

pyridyl rings based on time-dependent DFT calculations on molecular model systems. The polymer with the biphenyl linker displays a strong yellow-green emission while the Th−C_6H_4−Th linker shows a concentration dependent dual emission, presumably as a result of excimer formation.

4,4-Difluoro-4-bora-3*a*,4*a*-diaza-*s*-indacene (BODIPY) is another boron chromophore that is enjoying widespread use due to a combination of high stability under ambient conditions, strong luminescence, and the possibility for effective tuning of the emission color through the substitution pattern on either boron or the pyrrolic ring systems.[131]

Li and co-workers reported on the incorporation of BODIPY into a phenyleneethynylene conjugated polymer framework via Sonogashira-Hagihara coupling.[132] The THF-soluble fraction of polymers **43** consisted of moderate molecular weight material (M_n = 1700−6000 Da) according to GPC measurements (Scheme 29). The lowest energy absorptions with maxima in the range from 570 to 640 nm and corresponding red emissions (615−664 nm) are attributed to BODIPY-centered $\pi-\pi^*$ transitions that are strongly red-shifted due to extension of π-conjugation at the pyrrolic 2,6-positions. Consequently, the exact emission color depends to some extent on the electronic structure of the conjugated dialkyne precursor. Emission quantum efficiencies of up to 25% were realized, which is rather high for red-emissive organic materials. An investigation into the nonlinear optical properties of these polymers revealed a critical role of the BODIPY chromophore.

Similar methods were used by Liu and co-workers for the preparation of the related polymers **44** and **45** (Chart 4).[133,134]

Chart 4

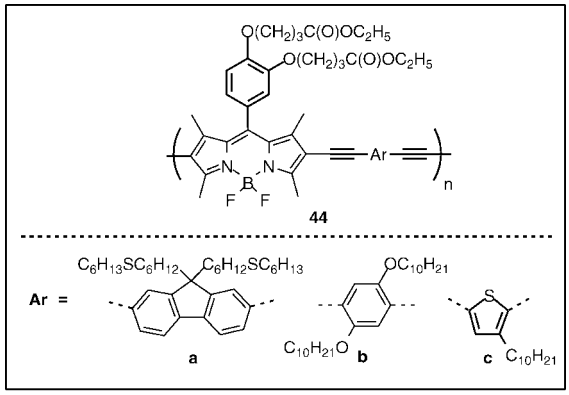

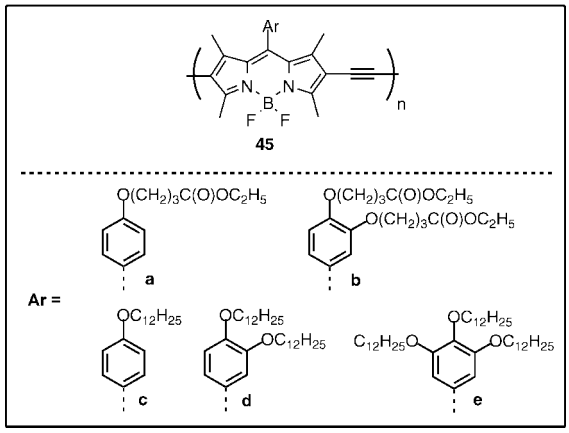

Scheme 30

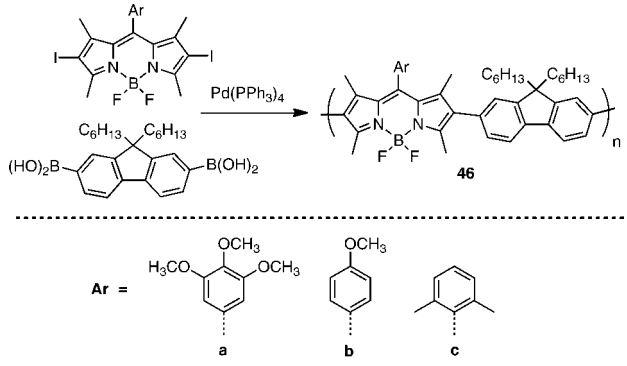

These polymers display comparatively higher solubility due to functionalization of the aryl group with long alkoxy side chains. Consequently much higher molecular weights in the range from M_n = 14400−26700 Da could be realized. As in the case of polymers **43**, the emission maxima are in the red region, as far as 690 nm (**45e**), with emission quantum efficiencies up to 25% (**44a**). A further red-shift was observed for thin films cast from polymer solutions in CH_2Cl_2, which resulted in near-infrared emission.[134]

The dependence of the emission wavelength on the exact nature of the conjugated spacer is also evident in copolymers with fluorene (**46**), which were prepared by Suzuki coupling procedures (Scheme 30).[135] The emission maxima fall into a narrow range from 585−588 nm with high emission quantum yields of 56−85%.

Chujo and co-workers prepared highly fluorescent polymers that contain derivatives of BODIPY embedded into the main chain via B-alkynyl linkages (Scheme 31).[42] Sonogashira coupling of a suitably functionalized BODIPY

Scheme 31

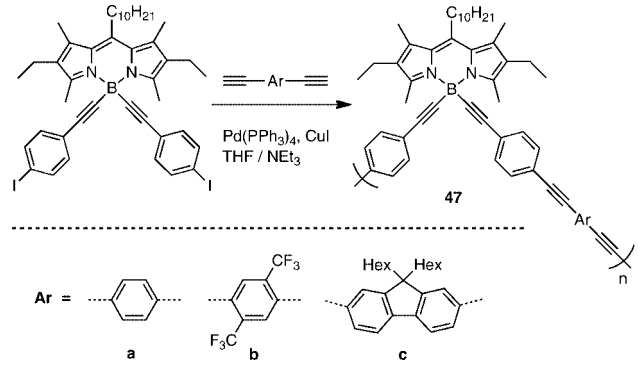

building block was applied to give polymers **47** in high yields. GPC analysis indicated the presence of larger aggregates for polymers **47a** and **47b**, which was subsequently confirmed by scanning electron microscopy (SEM) and transmission electron microscopy (TEM) analyses. Aggregation was attributed to π-stacking due to a rod−coil structure, in which the alkynyl main chain serves as a rigid rod that is decorated with flexible decyl pendant groups as the coil. In chloroform as the solvent, gelation occurred over a period of 24 h. The resulting gel with its network structure, which is depicted in Figure 11, could be redissolved in benzene at 50 °C or upon sonication.

In solution, all three polymers showed absorption bands at ca. 519 nm that are assigned to the BODIPY fragment, while higher energy absorptions in the range of 348−372 nm are attributed to the alkynyl linker. Excitation at either the lower energy or higher energy band resulted in strong emission at 532 nm with emission quantum efficiencies Φ_F ranging from 70−85%.

In the context of polymers bearing boron−nitrogen heterocycles in the main chain, it is worth noting that Wagner and co-workers prepared a series of redox-active ferrocene-containing B−N macrocycles. Reaction of 1,1′-fc[B(Me)Br]$_2$ with 2,2′:4′,4″:2″,2‴-quaterpyridine resulted in the redox-active macrocycle **48a**[136] and treatment of 2,5-di(pyrazol-1-yl)hydroquinone with 1,1′-fc[B(Me)NMe$_2$]$_2$ gave macrocycle **48b** (Chart 5).[137] The structures were confirmed by multinuclear NMR and ESI mass spectrometry, as well as GPC. Moreover, the solid-state structure of **48b** was solved from high-resolution X-ray powder diffraction patterns.

Wagner and co-workers also demonstrated that donor−acceptor interactions can be used for the formation of dynamic organoborane polymers.[118,136,138−140] Equimolar reaction of 1,1′-bis(dimethylboryl)ferrocene with aromatic diamines, such as pyrazine or 4,4′-bipyridine, led to spontaneous and reversible formation of one-dimensional coordination polymers (Scheme 32). Polymers **49** display inter-

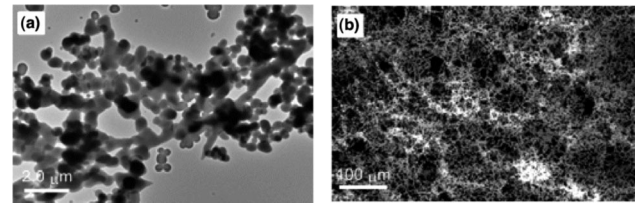

Figure 11. (a) TEM micrograph of a THF solution of **47a**, dried at RT for 5 h on a carbon-coated copper grid and (b) SEM micrograph of a dried gel of **47a** deposited from $CHCl_3$. Adapted with permission from ref 42. Copyright 2008 American Chemical Society.

Chart 5

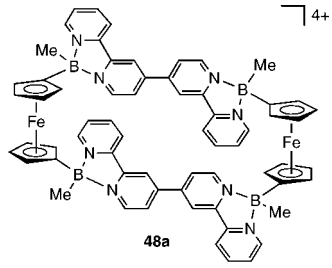

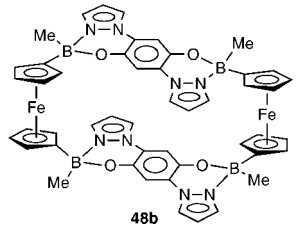

Scheme 32

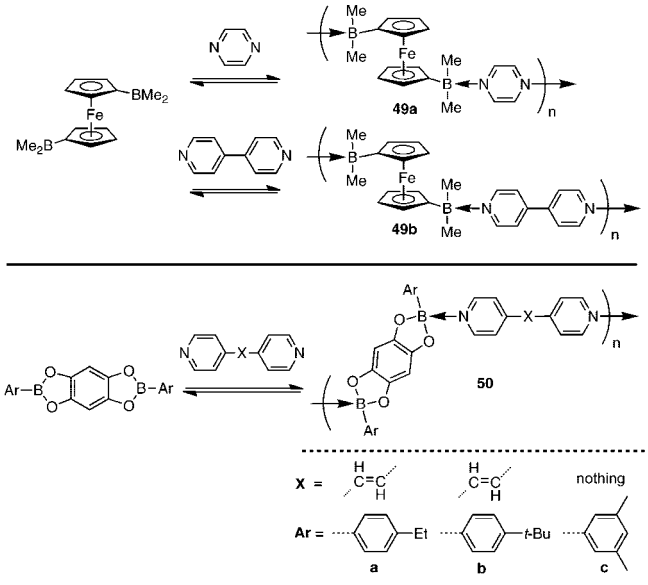

esting electronic structures as evidenced by intense colors in the visible region that are attributed to charge transfer processes from the electron-rich ferrocene to the electron-deficient boron-bound heterocycles. The polymeric nature of these materials in the solid state was confirmed by single-crystal X-ray crystallography and powder diffraction studies.[139,140] According to DSC and TGA studies, polymer **49a** is thermally stable in the solid state to ~140 °C and polymer **49b** to ~240 °C. However, in solution equilibration takes place and complete dissociation occurs at temperatures above 85 °C in toluene, based on multinuclear NMR studies.

Severin and co-workers demonstrated that bifunctional organoboronates form coordination polymers with similar donor−acceptor structures upon reaction with 4,4′-bipyridine.[141] An interesting aspect is that these coordination polymers were prepared through 3-component self-assembly from 1,2,4,5-tetrahydroxybenzene, an aromatic boronic acid, and the aromatic diamine. X-ray crystal structures of **50a** and **50c** were recorded and confirmed the polymeric nature of the products in the solid state. However, relatively long B−N bond lengths indicated rather weak B−N bond strengths. Indeed, NMR spectroscopy in $CDCl_3$ revealed almost complete dissociation in solution as reflected in an ^{11}B NMR shift of 28.8 ppm for **50a**, which is close to the chemical shift of typical uncomplexed arylboronates. Solid-state NMR spectra further confirmed this conclusion, as the signals were strongly upfield shifted relative to those in solution. Similar to the ferrocene-containing coordination polymers described above, a striking feature of these polymers is their deep purple color in the solid state, which stands in contrast to the formation of colorless solutions. The intense color in the solid state was attributed to charge transfer from the tetrahydroxybenzene ring to the 1,2-bis(4-pyridyl)ethylene linker based on coupled cluster calculations on model systems.

3. Side-Chain Functionalized Conjugated Organoboron Polymers

In recent years, the side-chain functionalization of conjugated polymers has been explored as an alternative to the incorporation of boron into the backbone of conjugated polymers. There are several fundamental differences between these two polymer architectures, and the side-chain approach comes with some significant potential benefits: (i) the fully π-conjugated organic backbone remains intact thereby retaining the excellent electronic characteristics that are a hallmark of typical organic π-conjugated polymers such as polythiophenes, poly(phenylene ethynylene)s, polyaniline, etc. Moreover, if the organoborane group is directly attached and therefore electronically coupled with the conjugated backbone, it can strongly influence the electronic structure of the conjugated polymer itself. This aspect in particular could prove beneficial with respect to the design of new conjugated polymers with unusual optical or electronic characteristics. Their use in plastic electronics and as sensory materials that function based on a change of the electronic structure of the polymer backbone as a result of analyte binding to the pendant borane groups is anticiptated. (ii) In contrast to main-chain-type organoboron polymers in which two of the three valencies at boron are tied up in the polymer backbone, the side chain functionalization approach only uses one valency to connect the active organoborane site to the polymer backbone leaving the remaining two for tuning of the polymer properties. For instance, in the case of triorganoborane-functionalized conjugated polymers, the electronic characteristics, optical properties, as well as thermal and air stability can be optimized by choice of suitable pendant groups on boron. Moreover, other classes of organoborane polymers become accessible, the most important example being boronic acid (-$B(OH)_2$) functionalized materials, which have received tremendous interest as sensory materials.

A number of different tools for the side-chain modification of conjugated polymers have been successfully implemented over the past several years. Generally, these involve (a) polymer modification via recently developed C−H activation[142] and silicon−boron exchange[143] procedures or (b) direct polymerization of boron-containing monomers via electrochemical, oxidative, and transition metal-catalyzed[37] C−C bond forming reactions.

3.1. Conjugated Polymers with Triorganoborane Groups

Modification of conjugated polymers with highly electron-deficient triorganoborane groups has been studied with the goal of generating new conjugated materials, in which boron acts as a strong π-acceptor because of effective overlap of

Scheme 33

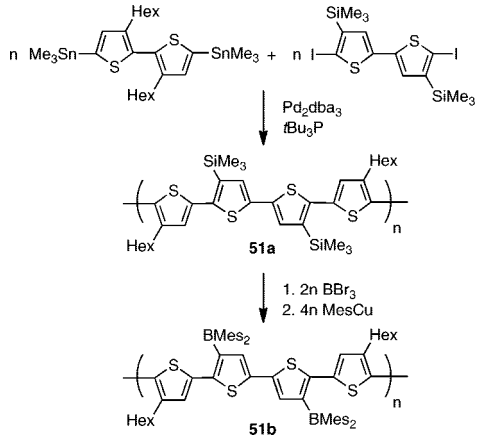

its empty p-orbital with the conjugated organic π-system.[144] As a result of this mutual interaction, unusual optical and electronic properties can be expected. Generally, bulky aryl groups are used as the additional substituents on boron to ensure high stability while maintaining the electron-deficient character of boron.

The functionalization of polythiophene with electron-deficient tricoordinate organoborane moieties was accomplished by Jäkle and co-workers (Scheme 33).[143] A postpolymerization modification approach was chosen. First, a silylated polythiophene (**51a**) was prepared in 60% yield by Stille-type polycondensation, resulting in a polymer with an average of ~45 thiophene units (n = 11) based on GPC-MALLS analysis (Table 3). Reaction of **51a** with a slight excess of BBr_3 in CH_2Cl_2 at room temperature led to essentially quantitative cleavage of the Si−C(sp^2) bonds and subsequent treatment of the resulting dibromoborylated polymer with mesityl copper $(MesCu)_n$ (n = 4, 5) gave the triarylborane polymer **51b** as an air-stable red solid in ~50% yield. GPC-MALLS analysis in THF revealed a molecular weight of M_n = 11000 Da (n = 11), which is in good agreement with the results for the silylated precursor polymer. The polymer structure was further confirmed by MALDI-TOF mass spectrometry, which also indicated the presence of different polymer end groups as a result of different termination modes in the Stille-type polycondensation procedure.

A strong bathochromic shift of ~60 nm of the longest wavelength absorption maximum of **51b** relative to the precursor **51a** was attributed to the electron withdrawing effect of the boryl side groups that leads to narrowing of the optical gap from ca. 2.70 to 2.36 eV. Likewise, the red emission of **51b** (617 nm) is strongly shifted relative to that of **51a** (554 nm), thereby further confirming a significantly lower HOMO−LUMO gap upon boryl substitution. The absence of a shift in the absorption and emission of thin films of **51b** suggests that the bulky side groups prevent interchain aggregation.

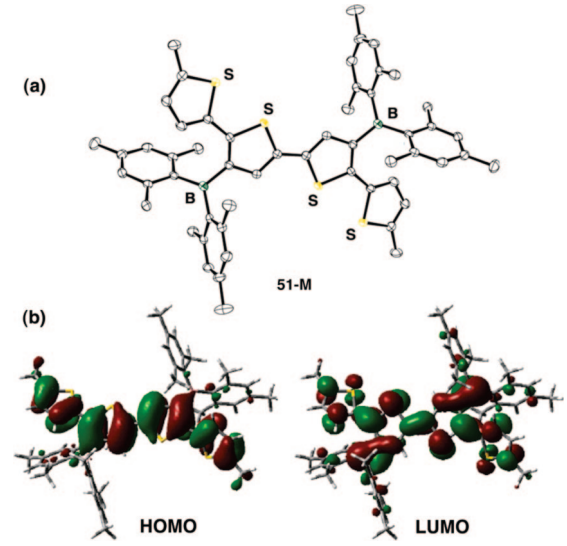

Figure 12. (a) X-ray crystal structure of quarterthiophene **51-M** and (b) frontier orbital plots.

A quaterthiophene model system (**51-M**) was used to further examine the conformation of the thiophene groups, the orientation of the boryl groups with respect to the conjugated π-system, and the resulting electronic structure. From the X-ray crystal structure of **51-M** it is evident that despite the bulky boryl groups a coplanar conformation of the thiophene rings in the polymer chain is feasible (Figure 12a). However, the boryl group is somewhat twisted relative to the plane of the thiophene ring it is attached to, thereby limiting the overlap of the p-orbital with the organic π-system. It should be kept in mind, however, that the conformation in the solid state is not necessarily representing the most favorable conformation in solution. Indeed, a related bithiophene derivative with a Mes_2B group attached to the 3-position was reported by Yamaguchi to show a more favorable orientation of the boryl group relative to the thiophene ring, albeit at the expense of the two thiophene rings being more strongly twisted relative to each other.[145] DFT calculations revealed effective overlap of the empty p-orbital on boron with the quaterthiophene π-system in the LUMO (Figure 12b).

According to cyclic voltammetry studies, **51b** ($E_{1/2}$ = −2.18 V vs Fc/Fc^+) more readily accepts electrons than the silylated precursor polymer (**51a**; $E_{1/2}$ = −2.35 V). The first

Table 3. Selected Data for Triarylborane-Modified Conjugated Polymers

	M_n[a]	M_w[a]	PDI[a]	n[b]	solvent[c]	λ_{abs}/nm	λ_{em}/nm[d]	Φ_F[e]	ref
51a	6700	9100	1.35	11	CH_2Cl_2	382	554	0.10	143
51b	11000	20700	1.88	11	CH_2Cl_2	344, 441	617	0.03	143
53a	57700	173100	3.0	59	C_6H_6	432	487	0.85	37
53b	41400	111800	2.7	32	C_6H_6	436	499	0.87	37
53c	52100	114600	2.2	42	C_6H_6	468	525	0.95	37
53d	12600	22700	1.8	10	C_6H_6	432	523	0.98	37
53e	16100	19300	1.2	13	C_6H_6	452	567	0.96	37
55	2300	4000	1.8	4	CH_2Cl_2	353	407	0.80	39
56	4900	6000	1.2	12	CH_2Cl_2	310, 365	484	0.54	39

[a] Molecular weights (Da) based on GPC analysis vs PS standards; for **51a** and **51b** absolute molecular weights from GPC-MALLS analysis; PDI = M_w/M_n. [b] Number average of repeating units from GPC analysis. [c] Solvent used for photophysical studies. [d] Emission maxima upon excitation at λ_{max}. [e] Fluorescence quantum efficiency.

Scheme 34

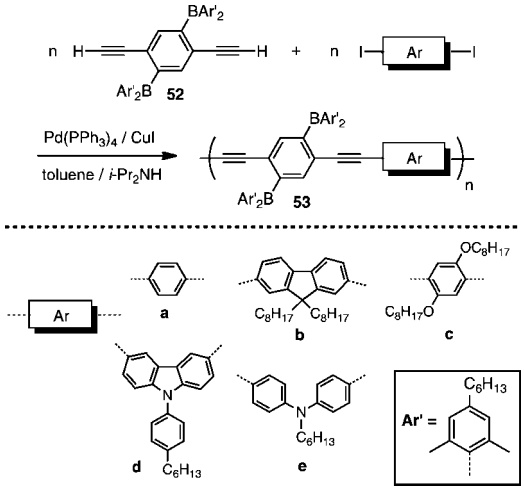

reduction potential is similar to that reported by Shirota and co-workers for the molecular electron transport material 5,5′-bis(dimesitylboryl)-2,2′-bithiophene[146] ($E_{1/2} = -1.76$ V vs Ag/Ag^+ corresponding to approximately -2.26 V vs Fc/Fc^+).

Yamaguchi and co-workers pursued the functionalization of poly(aryleneethynylene)s (PAEs) with electron-deficient organoborane moieties.[37] Their approach involves the organoborane monomer (**52**) as a key building block. The Mes' (2,6-dimethyl-4-*n*-hexylphenyl) ligand is employed instead of the more commonly used Mes groups to ensure good solubility of the targeted polymeric materials. Pd(0)-catalyzed Sonogashira-Hagihara coupling of **52** with a variety of diiodoarenes produced boryl-substituted polymers **53** in moderate (arylamine species) to high (other arenes) yields (Scheme 34). Remarkably high molecular weights ranging from $M_n = 12600$ to 57700 Da were achieved based on GPC analysis relative to PS standards.

In the absorption spectra, the lowest energy band was observed at 432 to 468 nm. This band was assigned to an intramolecular charge transfer (ICT) transition from the π-conjugated backbone to the diborylphenylene moiety, based on studies on related molecular species.[147] In comparison to molecular compounds the absorption bands are red-shifted, reflecting the extension of π-conjugation along the conjugated polymer backbone. The fluorescence of the polymers strongly depends on the electronic nature of the comonomer units. With an increase in the electron-donating ability of the comonomer, the emission maxima gradually shift to longer wavelength, from 487 nm for the phenylene derivative **53a** to 567 nm for the 4,4′-disubstituted *N*-octyldiphenylamine derivative **53e**.

The quantum yields are very high, in the range from $\Phi_F = 0.87$ to 0.98 in benzene solution. Moreover, the emission quantum efficiency of thin films is almost equally high ($\Phi_F = 0.36-0.62$), and the absorption and emission maxima are essentially unchanged relative to those in benzene solution. The exceptionally bright emission is attributed to (i) the presence of the bulky groups on boron, which suppress aggregation phenomena, and (ii) enhancement of the oscillator strength of the radiative decay upon extension of the π-conjugation ($\Phi_F = 0.14$ for **53a-M**: vs $\Phi_F = 0.85$ for **53a**).

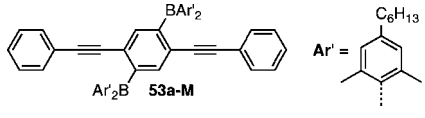

Chart 6. Structures of Triarylamine and Carbazole Functionalized Organoboranes Studied for Electropolymerization[a]

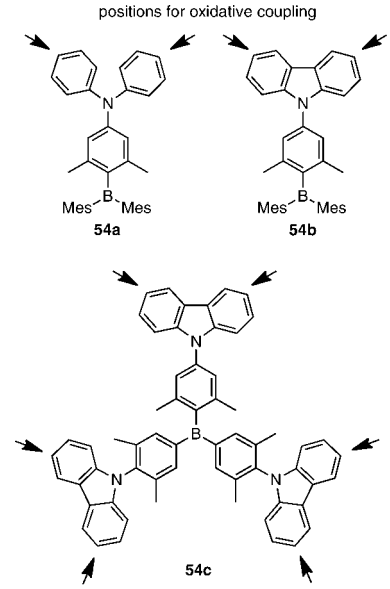

[a] The positions prone to oxidative coupling are indicated with arrows.

Finally, it should be noted that polymers **53d** and **53e** are ambipolar in that they contain both electron-deficient organoborane and electron-rich arylamine groups in the same polymeric material. The combination of the hole transport properties of arylamines with the electron-transport characteristics of arylboranes in a single ambipolar material has been successfully employed by Wang and others for the development of highly efficient small molecule organic light emitting devices.[78] To prepare polymeric materials with ambipolar characteristics resulting form the combination of an arylamine main chain with an arylborane motif as side chain is therefore an intriguing goal. Hence, further studies of polymers **53d** and **53e** in this regard might prove very interesting.

Lambert and co-workers investigated the functionalization of polycarbazoles with pendant organoborane moieties as a means of preparing ambipolar materials. Polycarbazoles are known for their excellent hole transporting properties, which are combined with high thermal stability and good glass forming properties.[148] Initial studies focused on the electropolymerization of borylated triarylamine and carbazole species **54**.[149] While oxidative cycling of **54a** and **54b** led to the formation of dimeric species, polymeric films with 3,3′-carbazolyl linkages (in para position to the amino groups) were formed from **54c** based on cyclic voltammetry (Chart 6).

More recently, Lambert and co-workers investigated the preparation of borylated polycarbazoles via metal-catalyzed coupling reactions (Scheme 35). Two different systems were examined, one with a 3,6-linkage and the other with a 2,7-linkage between the carbazole moieties.[39] The conjugation pathway for these two systems is very different, because the 2,7-linkage as in **55** leads to a poly(*para*-phenylene)-type structure with extended conjugation over several repeating units, while poly-3,6-carbazoles as in **56** are better described as nitrogen-connected benzidines. The extended conjugation of poly(2,7-carbazoles) is especially attractive because it commonly leads to high fluorescence quantum yields in solution.

Scheme 35

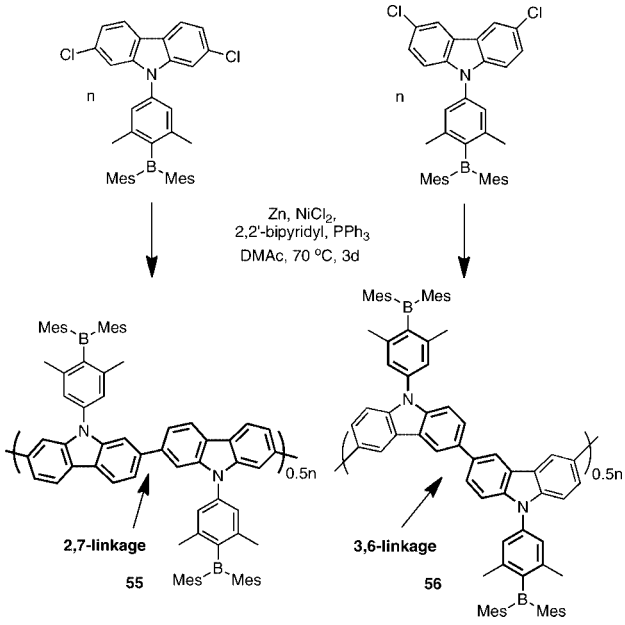

As in the case of Yamaguchi's PAEs described above, organoborane monomers were used with sterically protected tricoordinate organoborane moieties attached via a phenylene linker to the carbazole nitrogen. Polymerization was performed by nickel-catalyzed Yamamoto coupling in the presence of Zn (Scheme 35). The molecular weights of the polymers based on GPC in THF were moderate with M_n = 2300 Da (ca. 4 repeating units; *PDI* = 1.1) for **55** and M_n = 4900 Da (ca. 12 repeating units) for **56**, respectively. However, the actual molecular weights may be underestimated due to the poor solubility of the polymers. The polymer chains are for most part terminated by hydrogen atoms according to MALDI-TOF measurements.

The two polymers display vastly different photophysical properties. The organoborane acceptor substituents do not seem to influence the optical properties of **55**. The absorption maximum of **55** at 353 nm is similar to that of other nonborylated carbazole polymers and overlaps with the absorption band expected for the triarylborane moiety. Similarly, a strong emission at 407 nm is typical of poly(2,7-carbazoles). Moreover, only very weak solvatochromic effects were detected for the absorption and emission of **55**. These observations clearly suggest that the boryl substituent only weakly interacts with the polymer backbone and that the optical properties are primarily governed by the conjugated carbazole backbone.

In contrast, the presence of the triarylborane acceptor has a strong impact on the optical properties of the 3,6-linked carbazole main chain in **56**. The absorption spectrum of **56** displays a less intense red-shifted maximum at 367 nm in addition to a stronger band at 310 nm. The weaker low energy band shows a distinct negative solvatochromism (Figure 13a) and is consequently assigned to a charge transfer (CT) transition from the carbazole to the borane units. A positive solvatochromic effect was found for the emission (Figure 13b), suggesting a reversal in the dipole moment in the excited state relative to the ground state. This behavior is similar to that of related monomeric species, suggesting that the CT state is localized on one of the repeating units of the polymer. Compared to other 3,6-linked polycarbazoles the quantum yield of 54% is surprisingly high, which was attributed to the presence of the low-lying fluorescent CT state. It is also interesting to note that the observation of two absorption bands, one originating from the polycarbazole backbone and another one from an intramolecular CT process resembles the situation in the polythiophene **51b** reported by Jäkle and co-workers, except for that in the case of the borylated polythiophenes the higher energy band was attributed to an ICT process and the lower energy band to a $\pi-\pi^*$ transition of the conjugated polymer backbone. This is also believed to be the case for the 2,7-linked polycarbazole **55**.

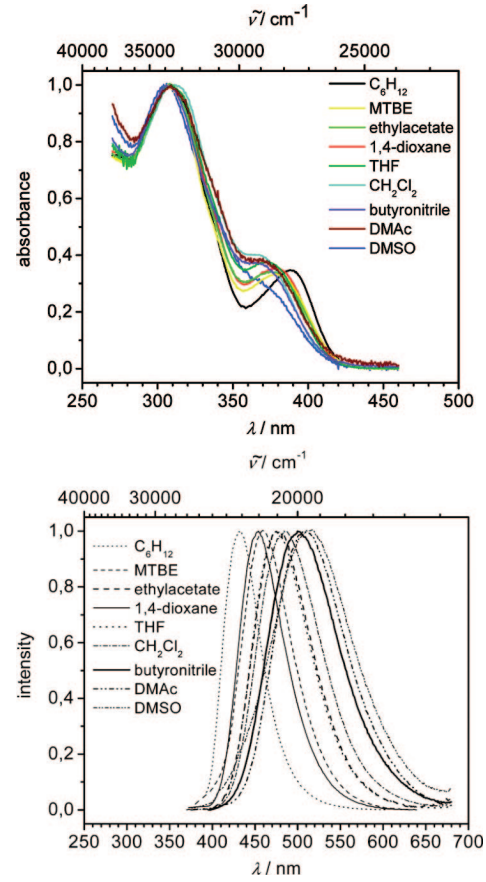

Figure 13. Solvatochromic effects for polymer **56** in the (top) absorption and (bottom) emission spectra. Adapted with permission from ref 39. Copyright 2009 American Chemical Society.

Table 4. Electrochemical Data for Triarylborane-Modified Polycarbazoles. Data taken from ref.[39]

	$E_{1/2}$ (ox) (V)	$E_{1/2}$ (red) (V)	HOMO[a] (eV)	LUMO[a] (eV)	E_g[a] (eV)
55	+0.58, +0.83, +1.02	−2.53	−5.43	−2.42	3.01
55x[b]		−2.51	−5.15	−2.52	2.63
56	+0.53/+0.83	−2.49	−5.04	−2.54	2.50

[a] Based on onset of the reversible reduction (LUMO) and oxidation (HOMO) process; Fc/Fc^+ is taken as 4.8 eV below the vacuum level. [b] After cross-linking by anodic oxidation.

Cyclic voltammetry measurements on **56** revealed two oxidation waves at +0.53 and +0.83 V and a reversible reduction at −2.49 V vs Fc/Fc^+ that is likely localized on the borane moieties (Table 4). A similar reduction potential of −2.53 V was found for **55**. An electrochemical bandgap of 2.50 eV was determined for **56**, which is significantly lower than that of **55** before (3.01 eV) and after (2.63 eV) cross-linking via anodic electrochemical oxidation.

3.2. Conjugated Polymers with Organoborane Groups Linked by Heteroatoms

3.2.1. Systems with Tricoordinate Boron

The preparation of phenylene-fluorene copolymers with diazaborole moieties attached to the phenylene groups was pursued by Yamamoto and co-workers.[150] They explored two different methods, direct polymerization under Suzuki coupling conditions and a postmodification procedure in which they reacted a preformed amino functionalized polymer with arylboronic acid derivatives under formation of the diazaborole moieties (Scheme 36). The direct polymerization approach led to deborylated **57** rather than the desired boron-containing polymers. The postmodification approach proved more successful with formation of several new polymers (**58**) containing different aryl groups on boron. On the basis of ^{1}H NMR analysis and ICP (inductively coupled plasma) spectroscopy degrees of functionalization of 73−85% were achieved, depending on the particular aryl group attached to boron. GPC data suggested molecular weights in the range of M_n = 5700−9800 Da, whereas light scattering indicated much higher molecular weights (>180000 Da). This apparent discrepancy was attributed to the formation of larger aggregates because of hydrogen bonding interactions between the uncomplexed amino groups of different polymer strands.

The polymers absorbed strongly with maxima at 354−360 nm in $CHCl_3$ and emitted in the blue-violet region with maxima at 407−420 nm. While the absorptions and emissions were not significantly red-shifted in comparison to the amino-functionalized precursor polymer **57**, the emission quantum efficiencies increased from 11% for **57** to 48% for the diazaborole polymer **58b**. Electrochemical oxidation of polymers **58** occurred at slightly higher potential (0.54−0.71 V vs Ag^+/Ag) than for the amino-precursor **57** (0.47 V).

3.2.2. Systems with Tetracoordinate Boron

A conjugated poly(phenylene ethynylene) with 8-hydroxyquinolato binding groups incorporated into the conjugated main chain (**60**) was developed by Chujo using Sonogashira−Hagihara coupling (Scheme 37).[151] 5,7-Dibromo-8-hydroxyquinoline was first protected with a Boc (*t*-butyloxycarbonyl) group and then reacted with 1,4-diethynyl-2,5-bis(hexadecyloxy)benzene in the presence of $Pd(PPh_3)_4$/CuI as the catalyst system to give polymer **59** with M_n = 5600 Da based on GPC analysis. The Boc group was then removed with piperidine and the resulting 8-hydroxyquinoline moities were reacted with a large excess of Ph_3B to ensure quantitative functionalization with borane groups.

Scheme 37

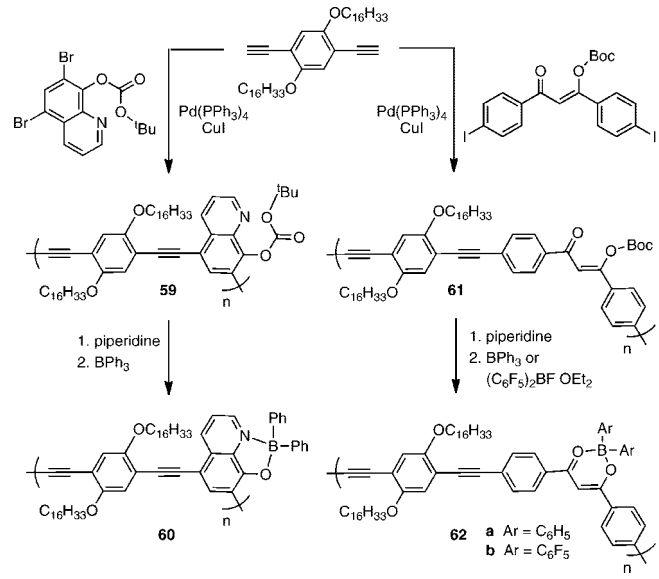

The reaction sequence was followed by IR spectroscopy after each step to confirm successful conversion, and the product (**60**) was further characterized by NMR and elemental analysis. An ^{11}B NMR signal at 9.0 ppm is consistent with data on related molecular species; moreover, elemental analysis data were in agreement with the expected structure and degree of polymerization based on the precursor polymer **59**. Both **59** and **60** showed strong absorptions at ∼400 nm that are likely the result of $\pi-\pi^*$ transitions related to the conjugated polymer backbone. An additional bathochromic shoulder was observed for the borylated polymer **60** at ∼470 nm. This band was attributed to formation of the organoboron quinolato complex and is in good agreement with results for molecular complexes with extended π-systems attached to the quinoline moiety.[152−154] As shown in Figure 14, boron modification resulted in an orange emission of the polymer **60**, whereas the precursor polymers emit in the blue to blue-green region. The absolute emission quantum yield of Φ_F = 0.003 for **60** is low in comparison to that of most of the main chain-functionalized quinolate polymers (e.g., **38**, Scheme 26), but the large molar absorptivity of the poly(phenylene ethynylene) (PPE) backbone makes these materials brightly luminescent. Based on these observations, the phenylene-ethynylene units appear to act as an antenna that facilitates efficient charge transfer to the boron quinolato chromophores.

As an alternative chromophore, Chujo and co-workers also studied the incorporation of β-diketonate moieties into the

Scheme 36

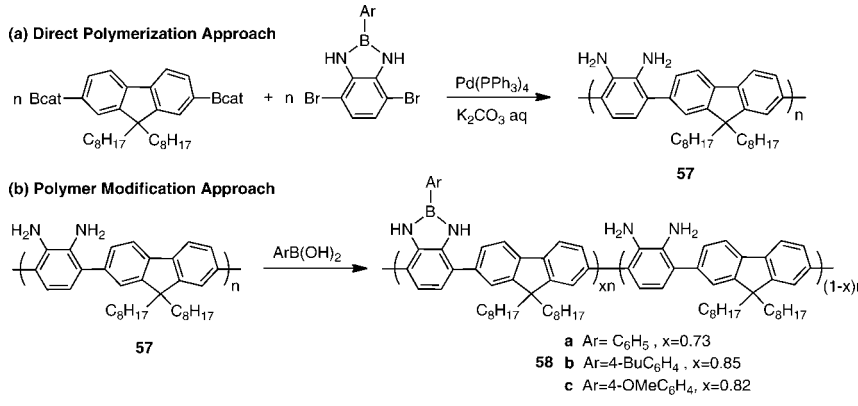

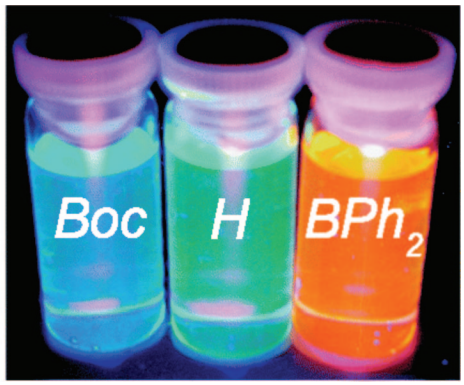

Figure 14. Comparison of the emission color of **59** before (left) and after (middle) Boc deprotection with that of **60** (right). Adapted with permission from ref 151. Copyright 2008 American Chemical Society.

conjugated backbone of PPE.[155] Again, a Boc-protected dihalogenated precursor was chosen and reacted with 1,4-diethynyl-2,5-bis(hexadecyloxy)benzene under Sonogashira-Hagihara coupling conditions (Scheme 37). Polymer **61** was obtained as a yellow solid in 84% yield with M_n = 5100 Da. Deprotection was accomplished by treatment with piperidine, and the product was directly converted to the desired organoboron chelates **62a** and **62b** by treatment with Ph_3B or $(C_6F_5)_2BF{\bullet}OEt_2$, respectively. IR, NMR, and elemental analysis data confirmed successful borylation. Moreover, the molecular weights of the boron polymers measured by GPC were consistent with that of the precursor **61**. The absorptions of polymers **62** in $CHCl_3$ solution were significantly broadened toward longer wavelengths as a result of boron complexation. And especially the emission of **62b** (**62a**, λ_{em} = 535 nm; **62b**, λ_{em} = 652 nm) was distinctly red-shifted from that of the ligand precursor **61** (λ_{em} = 515 nm). The relatively low emission quantum efficiencies were attributed to the very large Stokes shift, but due to the antenna effect of the conjugated organic segments relatively intense emission colors were observed. Thin films of **62a** showed a clear red-shift in the emission.

3.3. Boronic Acid-Functionalized Conjugated Polymers

3.3.1. Electrochemical Polymerization

Boronic acid- and boronate-functionalized conjugated polymers (**63**−**68**, Chart 7) are accessible by electropolymerization of boron-functionalized thiophene, pyrrole, and aniline derivatives as demonstrated by the research groups of Fabre, Freund, and He.[156−159] For example, a redox-active film of polypyrrole (**66**) was electrodeposited onto a platinum electrode from acetonitrile solution.[160,161] Similarly, electrochemical polymerization of 3-aminophenylboronic acid in aqueous medium was used to produce thin films of poly(anilineboronic acid) (**67**) on electrodes.[156,162] For effective electrochemical polymerization of 3-aminophenylboronic acid to occur, the presence of fluoride ions proved necessary. The latter is attributed to the binding of fluoride to boron, which transforms the boryl groups into an electron-donating substituent.[156] Fluoride binding in acidic aqueous solution was confirmed by a distinct upfield shift in the ^{11}B NMR spectrum of the respective monomer. High fluoride concentrations led to better stability, better adhesion properties, and increased sensitivity of the polymer-coated electrodes. Nafion is also commonly added as a polyanion that is beneficial in these electrochemical polymerizations.[162,163]

Chart 7

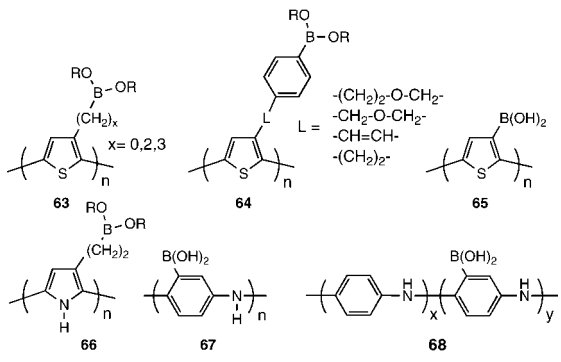

3.3.2. Chemical and Enzymatic Polymerization

Wolfbeis and co-workers demonstrated that aniline boronic acid can be copolymerized with aniline through chemical oxidation with ammonium persulfate in acidic aqueous solution leading to deposition of the respective copolymer film (**68**).[164] More recently, Freund and co-workers found that oxidative polymerization of the fructose complex of aniline boronic acid with ammonium persulfate in the presence of fluoride leads to a self-doped water-soluble form of poly(aniline boronic acid) (**69a**, Chart 8). Conversion to **69b** was achieved by precipitation into distilled water followed by washing with 0.5 M HCl to remove the fructose.[165,166] This is a reversible process, as addition of fructose and fluoride regenerates **69a**. An exceptionally high molecular weight of M_n = 1676000 Da and a PDI of 1.05 were reported for **69b** based on GPC analysis.[167] Freund and co-workers also further investigated the materials properties of self-doped poly(anilineboronic acid) (**69b**): This polymer exhibits unusually high thermal stability according to TGA measurements, while dehydration by vacuum treatment at 100 °C for 24 leads to anionic cross-links between a boronic acid-imine and a boronic acid moiety of another polymer chain. The resulting cross-linked material (**70**) maintains high conductivity of 0.09 S cm^{-1}, which is attributed to the presence of ∼21% tetracoordinate boron moieties that act as doping sites.[168]

As an alternative to chemical oxidants, Kumar, Samuelson, Lee, and co-workers used horseradish peroxidase in combination with poly(styrene sulfonate) (PSS) to copolymerize aniline with aniline boronic acid.[169] This method was also successfully applied by He for the preparation of composites with DNA and carbon nanotubes (vide infra).[170]

Senkal and co-workers reported the preparation of poly(thiophene boronic acid) (**65**) by oxidative coupling of 3-thiopheneboronic acid in the presence of $K_2Cr_2O_7$ (Chart 7).[171] Liu and co-workers recently introduced a polymer modification approach for the functionalization of polythiophene with boronic acid groups (Scheme 38). A Grignard metathesis polymerization (GRIM) protocol was used to

Chart 8

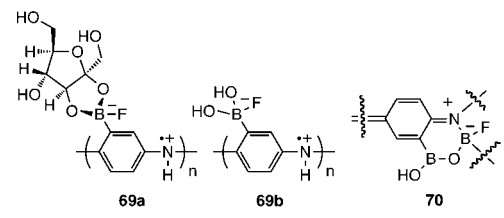

Scheme 38

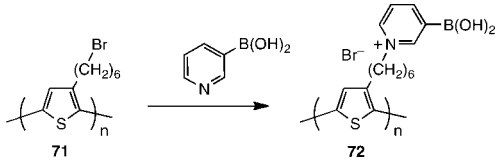

prepare the regioregular polymer **71**, which has a relatively high molecular weight of M_n = 25900 Da (PDI = 1.75). **71** was then treated with 3-pyridylboronic acid to give the ionic, water-soluble polymer **72**.[172] Structurally this polymer is distinct from the ones described above in that the boronic acid groups are not in conjugation with the polymer main chain. However, a beneficial aspect of this methodology is that better control over the molecular weight and structural integrity of the conjugated polymer chain can be achieved. Polymer **72** exhibits similar photophysical properties as the precursor polymer **71**; it absorbs at 410 nm and emits at 560 nm in aqueous solution with a quantum efficiency of 2.1%.

3.3.3. Composites and Higher-Order Structures

The observation of very favorable electrical properties for self-doped forms of **69** triggered a series of studies aimed at the development of conductive composites. Freund and co-workers used layer-by-layer deposition of **69** and ribonucleic acid (RNA) to prepare composite films at neutral pH.[173] RNA served as both a dopant and a polyelectrolyte that balances the positive charges of **69** in the absence of fluoride. UV−vis spectroscopy confirmed the layer-by-layer deposition process, which results in an increase in the absorbance with each layer. The interactions between **69** and RNA are believed to be multifold, involving boronic ester formation, B−N donor−acceptor bonding, and an electrostatic component. Because of the redox-active nature of **69**, potential-induced release of RNA could be triggered.

When 3-aminophenylboronic acid was oxidatively polymerized in 0.5 M HCl solution in the presence of fluoride and different alchohols, nanostructured materials were isolated upon precipitation of the products into 0.1 M HCl solution.[174] As shown in Figure 15, different alcohols give different morphologies, ranging from nanoparticles to globular networks and nanofibers. UV−vis kinetic measurements, XPS, and ^{11}B NMR results suggest that the formation of these nanostructures is influenced by the polymerization rate, the degree of self-doping, and the polarity of the solvents used.[174] Oxidative polymerization of 3-aminophenylboronic acid was carried out in a similar manner in 0.1 M phosphoric acid in the presence of fluoride to give dispersions consisting of 25−50 nm size particles.[175]

He and co-workers prepared composites of **69** with carbon nanotubes that had been modified with single-stranded DNA.[159,176−180] In situ polymerization, as schematically illustrated in Figure 16, proceeded faster than without the nanotubes, and the presence of a thin skin of the conducting polymer led to strongly enhanced conductivity of the resulting carbon nanotube networks.[159,176,180] UV−vis measurements suggest that **69** exists to a greater extent in the conductive and stable emeraldine salt state in comparison to other samples of **69** prepared in the absence of the nanotube composites. Consequently, the conductance of the network-like composite after the percolation threshold is 2 orders of magnitude higher than that of a network of carbon nanotubes alone. Apparently, the conducting polymer acts as glue that is bridging the individual, highly conductive carbon nanotubes.

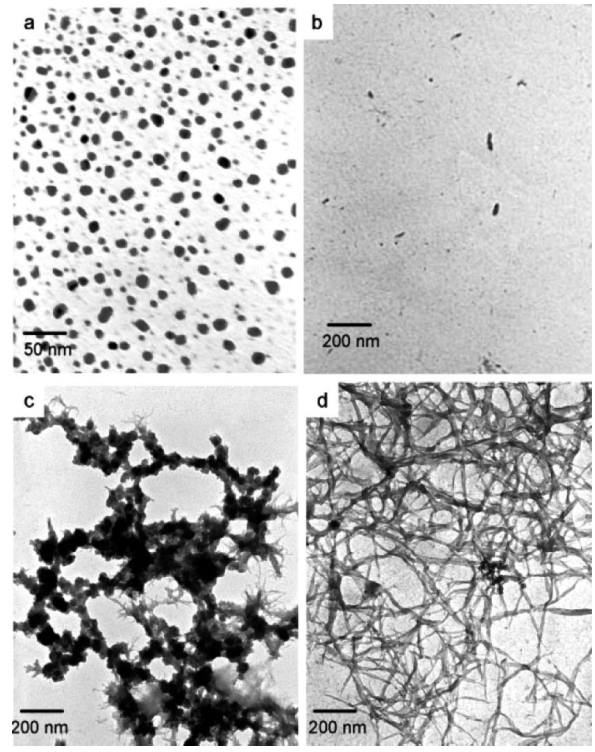

Figure 15. TEM images of nanostructures of **69b** prepared in 0.1 M HCl (a), methanol (b), ethanol (c) and 1-propanol (d). Reproduced with permission from ref 174. Copyright 2008 American Chemical Society.

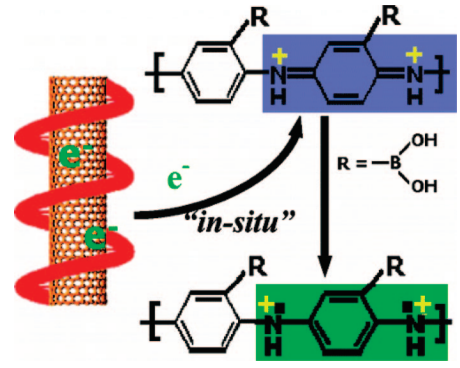

Figure 16. Schematic illustration of the polymerization of 3-aminophenylboronic acid in the presence of DNA-wrapped carbon nanotubes. Reproduced with permission from ref 159. Copyright 2008 American Chemical Society.

4. Nonconjugated Polymers Functionalized with Organoborane Chromophores

As discussed in the preceding sections, a diverse range of synthetic routes for the incorporation of boron into the polymer main chain have been developed. However, most of these methods lack control over molecular weight and polymer architecture, which at times can limit the versatility of the products, especially in applications that benefit from properties associated with chain entanglement of high molecular weight polymers and from the ability of block copolymers and other more sophisticated polymer architectures to assemble into nanostructured materials. Functionalization of polyolefins and other chain growth polymers can therefore offer advantages, including (i) the facile realization

of soluble organoboron polymers with high molecular weights, controlled architecture, and variable degree of functionalization, (ii) the possibility of chain extension for the synthesis of copolymers with different functionalities, and (iii) if boron is placed as a pendant or terminal group, two different substituents can be attached to the boron center thereby potentially allowing for further tuning of the optical and electronic properties, as well as their thermal characteristics and stability.

Organoborane-functionalized polyolefins can generally be synthesized either by polymerization of boron-functionalized monomers or via postpolymerization modification reactions. Both methods have been applied successfully for the attachment of boron substituents to the side chains of polyolefins.[28,29] For direct polymerization of boron-containing monomers standard free radical polymerization[28] and controlled free radical polymerization[181−189] methods have proven especially useful because of the availability of straightforward synthetic procedures and the reasonably good compatibility with B−C bonds. Ziegler−Natta polymerization on the other hand has been utilized for highly reactive and strongly Lewis acidic monomers which tend to be not very well suited for other polymerization techniques.[190,191]

The alternative route of postpolymerization modification is particularly interesting for the synthesis of polymers that cannot easily be obtained by polymerization of borane-functionalized monomers because of incompatibilities of the functional monomers with a given polymerization method (side reactions with catalysts, thermal instability, etc). However, the challenging aspect in this case is to find methods that allow for selective and quantitative installment of the desired boryl moieties to the polymeric material. Recently developed synthetic techniques that have proven very successful for the preparation of organoboron polymers include transition metal catalyzed C−H activation procedures,[192,193] the hydroboration of polyolefins that contain vinyl groups in the backbone or side-chain,[194,195] and organometallic transformations involving metalated polystyrenes and related polyolefins.[28]

4.1. Polymers with Tricoordinate Organoborane Pendant Groups

In some early work, Lequan and co-workers reported a polyurethane that features a chromophoric triarylborane moiety as the side chain.[196,197] They pursued the attachment of triarylborane donor-π-acceptor moieties for applications as nonlinear optical (NLO) materials. The chromophore, which consists of an arylamine donor linked by a diazo group to a Mes_2B acceptor, was functionalized with a dihydroxyethylamine group that allowed for its use as a bifunctional monomer (**73**) in polyaddition reactions with diisocyanates (Scheme 39). While no molecular weight data were provided, the resulting polymers (**74**) were found to be thermally stable

Scheme 39

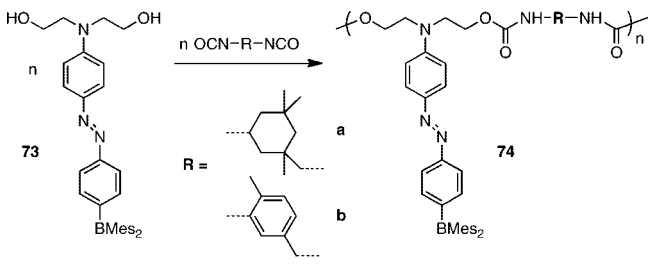

Scheme 40

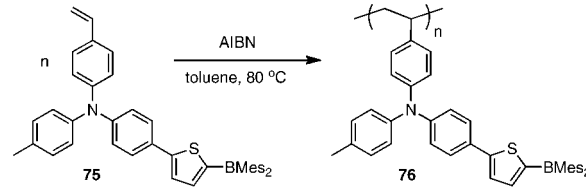

Scheme 41

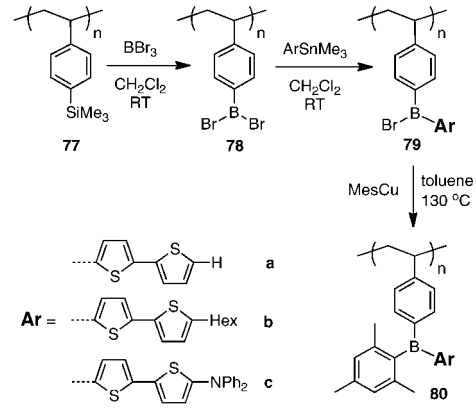

well beyond the glass transition temperature of 146 °C and 159 °C, respectively. Moreover, they were stable in air and showed high photostability.

Shirota and co-workers used the ambipolar organoborane monomer **75** that is functionalized with a vinyl group for incorporation into polyolefins. They reported that standard free radical polymerization of **75** gives a polymeric material (**76**) that exhibits high thermal stability, a high glass transition temperature of 194 °C, and good film forming capability (Scheme 40).[198] This polymer again contains both electron-rich amine and electron-deficient borane moieties in the side-chains and, due to its ambipolar character, undergoes reversible anodic oxidation at 0.58 V and cathodic reduction at −2.25 V versus Ag/Ag^+. In THF solution, a strong green emission at $\lambda_{em} = 521$ nm ($\Phi_F = 0.58$) was observed upon excitation at the absorption maximum of $\lambda_{abs} = 425$ nm.

A versatile polymer modification approach was developed by Jäkle and co-workers to introduce different luminescent triarylborane moieties as side groups to polystyrene (Scheme 41).[199] One boron substituent is used for steric stabilization, while the second pendent group represents an extended organic π-system that can effectively overlap with the empty *p*-orbital on boron. The synthetic method involves initial decoration of polystyrene with silyl groups (**77**) that can then be quantitatively replaced with boron tribromide to give the reactive polymer poly(4-dibromoborylstyrene) (**78**). This process provides an exceptionally high level of control over molecular weight, polymer architecture, and degree of borane functionalization.[181,200−205] By taking advantage of the high selectivity of tin−boron exchange reactions, one of the bromine substituents of each BBr_2 group was replaced with a bithiophene derivative to give the substituted polymers **79**, which were treated in situ with mesityl copper (MesCu)[206] to attach bulky Mes groups for steric protection.

The final polymers **80** were of high molecular weight, in the range expected based on that of the poly(4-trimethylsilylstyrene) precursor **77** ($M_n = 29200$ Da, *PDI* = 1.10), which allowed for facile isolation and processing into thin films. Polymers **80a** and **80b** contain bithiopheneborane side groups which are strongly emissive in the blue region with

Scheme 42

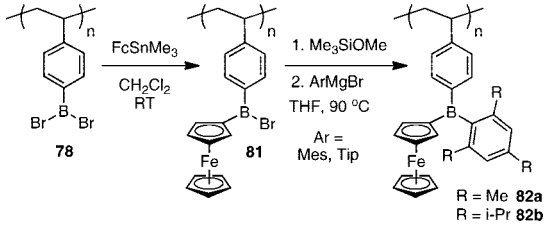

a maximum at ca. 460 nm, while the amino-functionalized derivative **80c** emits in the green at $\lambda_{em} = 537$ nm, consistent with a bathochromic shift due to the donor-π-acceptor structure generated upon attachment of the aminobithiophene substituents.

Using a similar polymer modification strategy, redox-active ferrocene-containing triarylborane polymers (**82**) were prepared from dibromoboryl-substituted polystyrene (Scheme 42).[207] Again, **78** was treated with an organotin species, $FcSnMe_3$, as a mild aryl transfer reagent to selectively install one of the functional groups on each boron center. The monosubstituted intermediate **81** was then reacted with MesMgBr or TipMgBr. The resulting dark-red colored polymers feature pendant organoborane moieties that are substituted with a redox-active ferrocene moiety along with a Mes (**82a**) or a Tip (**82b**) group for steric protection. While both polymers exhibit high thermal stability (>275 °C) and good stability in air, the polymer with the bulkier Tip group is relatively more stable than that with the Mes group attached to boron.

The photophysical and electrochemical properties of the polymers were investigated and compared with molecular model compounds based on one repeating unit of the polymer. The deep red color that is characteristic of both polymers can be traced back to a relatively intense ferrocene-based d−d transition at ∼485 nm. According to cyclic voltammetry studies both polymers undergo oxidation at a potential close to but slightly higher than that of ferrocene itself, while reduction of the boron centers occurs at highly negative potentials of approximately −2.8 V relative to the Fc/Fc^+ couple.

4.2. Polymers with Tetracoordinate Organoborane Pendant Groups

Organoboron chelates have also been attached as pendant groups to polyolefins. As discussed already in the context of main-chain organoboron polymers, polymer functionalization with these chromophores is attractive, because a diverse range of tetracoordinate complexes of boron have been identified as possible candidates for new electroluminescent device materials.[122]

Polymer substitution reactions provide a straightforward route to organoboron quinolate polymers as shown in Scheme 43.[123,124] In 2004, Jäkle and co-workers reported the preparation of polymeric organoboron quinolates (**84**) via alcoholysis of one of the B-aryl substituents in polymers (**83**) with 8-hydroxyquinoline.[123] This transformation occurs with high selectivity at the thienyl-boron over the phenyl-boron bond as confirmed by studies on molecular model compounds. The resulting high molecular weight organoboron quinolate polymers are close to being fully functionalized (>95% based on NMR and elemental analysis), highly soluble in common organic solvents, and solution processing yields smooth thin films that efficiently emit green light upon excitation at the absorption maxima.

Jäkle and co-workers more recently prepared a second generation of organoboron quinolate polymers (**86**) through a more efficient procedure that takes advantage of the high selectivity of Sn/B exchange reactions of aryldibromoboranes ($ArBBr_2$) with phenyl trimethyltin derivatives.[124] The selective formation of the diarylbromoborane species (**85**) allows for direct attachment of the quinolato group without the need to go through the triarylborane derivative (Scheme 43).

Again, polymers **86** are highly soluble, and luminescent thin films can readily be cast from solution. Importantly the emission characteristics of these materials are tunable by simple variation of the substituent R (R = Bpin, C_6F_5, Cl, p-C_6H_4OMe, p-$C_6H_4NMe_2$) on the quinoline moiety, covering almost the entire visible spectrum from blue to red emission (Figure 17, Table 5).[154] In addition the phenyl-substituted products exhibit superior stability characteristics in comparison to the thiophene-substituted polymers **84**.

A different synthetic approach to side-chain functionalized organoboron quinolate polymers was chosen by Weck and co-workers.[125] The hydroxyquinoline-functionalized polymers **87** and **88** of different degree of functionalization were prepared from poly(styrene-*ran*-chloromethylstyrene) copolymers (GPC for precursor polymer with $n/m = 2/1$, $M_n = 6100$ Da, PDI = 1.90; for precursor polymer with $n/m = 9/1$, $M_n = 6400$ Da, PDI = 1.50) by polymer modification reactions (Scheme 44). The ligand-functionalized polymers were then treated with triphenylborane at RT for 24 h, resulting in formation of the target polymers **89** and **90** in essentially quantitative yields.

Scheme 43

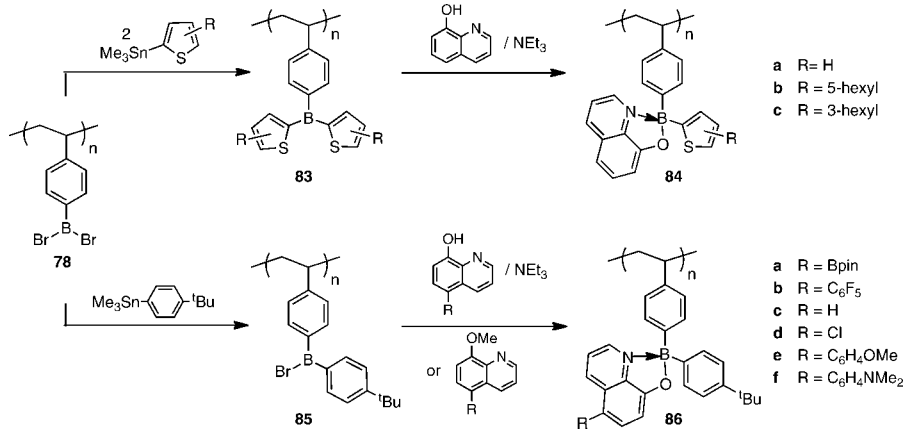

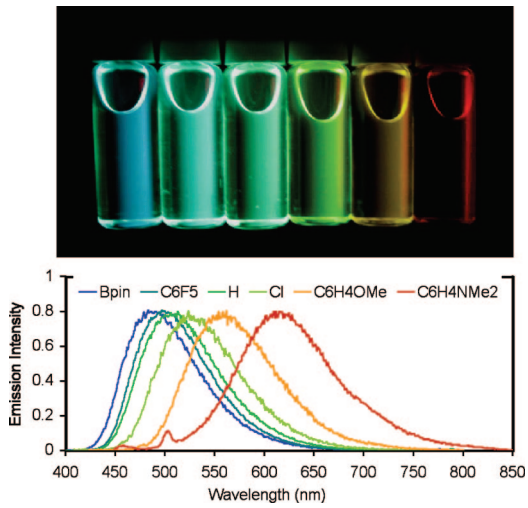

Figure 17. Photographs and emission spectra for solutions of the organoboron quinolate polymers **86** (from left to right: R = Bpin, C_6F_5, H, Cl, C_6H_4OMe, $C_6H_4NMe_2$). Adapted with permission from ref 124. Copyright 2006 American Chemical Society.

Scheme 44

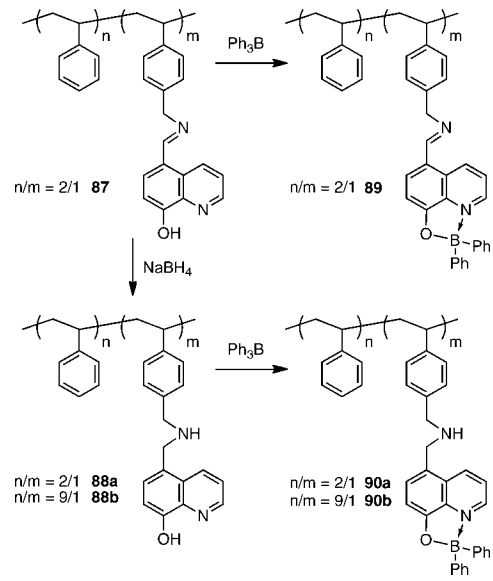

The photophysical properties of these polymers were examined in solution and in the form of thin films. The absorption and emission data were similar to those of Ph_2Bq with a strong green emission at ~500 nm as the dominant feature. Lifetime measurements indicated slightly shorter lifetimes for polymers **90** (4 ns for **90a**; 17 ns for **90b**), which correlated well with slightly lower emission quantum efficiencies ($\Phi_F = 0.16$ for **89**; 0.10 for **90a**; 0.20 for **90b**) in comparison to that of the molecular species (32 ns/Φ_F = 0.23). This effect was attributed to the possible presence of randomly distributed impurities that act as exciton traps.

BODIPY dyes have been incorporated into polyolefins by attachment to methacrylate groups and subsequent copolymerization with unfunctionalized methyl methacrylate. For instance, García-Moreno and Arbeloa and co-workers compared the lasing properties of materials in which BODIPY dyes were physically dissolved in methacrylate polymers with those derived from free radical copolymerization of polymerizable derivatives.[208−211] Chujo and co-workers prepared luminescent homo- and block copolymers using a methacrylate monomer that was derivatized with a luminescent difluoro or dialkynyl-BODIPY derivative (**91**).[186] Reversible addition−fragmentation chain transfer (RAFT) polymerization was performed as a means to control the molecular weight of the resulting functionalized poly(methyl methacrylate) (PMMA) and to ultimately prepare block copolymers with polystyrene as a second block (**93**) as shown in Scheme 45.

Controlled/living polymerization of monomers **91** was supported by kinetic analysis. The final polymers showed low PDIs; for example, **92b** had a molecular weight of M_n = 11800 Da with a PDI = 1.12. Chain extension with styrene in a bulk polymerization gave block copolymer **93b** with M_n = 59300 Da and a somewhat larger PDI of 1.41. For homopolymers **92**, scanning electron microscopy (SEM) of THF solutions that were allowed to dry up on glass slides showed the presence of chain-like structures formed by aggregation of individual micrometer-sized particles. The

Table 5. Selected Data for Polyolefins with Pendant Organoborane Moieties

	δ (^{11}B)	M_n[a]	M_w[a]	PDI[a]	n[b]	solvent[c]	λ_{abs}/nm	λ_{em}/nm[d]	Φ_F[d]	T_g/°C[e]	T_d/°C[e]	ref
76		25000	39000	1.56	41	THF	425	521	0.58	194		198
80a	50	26600	40200	1.51	67	CH_2Cl_2	368	442, 463	0.66	165	248	199
80b	50	45300	54600	1.15	94	CH_2Cl_2	380	455	0.67	139	240	199
80c	47	46000	60400	1.31	81	CH_2Cl_2	433	537	0.35	165	275	199
82a	57	23800[g]	27400[g]	1.15[g]	57	THF	484	n/a	n/a	*f*	275	207
82b	56	30400[g]	33700[g]	1.11[g]	61	THF	486	n/a	n/a	132	290	207
84b	5	68300[h]	71000[h]	1.04[h]	146	THF	392	508	0.12	145		123
84c	5	62300[h]	66000[h]	1.06[h]	150	THF	394	509	0.14	145		123
86a	7, 24	150600[h]	172700[h]	1.15[h]	334	THF	389	486	0.14	275	420	124
86b	7	161000[h]	189200[h]	1.18[h]	339	THF	395	497	0.28	245	350	124
86c	7	119000[h]	135700[h]	1.14[h]	347	THF	395	507	0.17	240	385	124
86d	8	127600[h]	144100[h]	1.13[h]	338	THF	404	525	0.06	238	305	124
86e	7	150700[h]	169800[h]	1.13[h]	341	THF	419	560	0.02	220	465	124
86f	7	161200[h]	178900[h]	1.11[h]	350	THF	439	615	0.001	230	375	124
92a	0.2	10600	12400	1.17	20	THF	520	541	0.37			186
92b	−13.3	11800	13200	1.12	17	THF	520	539	0.49			186
93a	−0.4	82500	118800	1.44	20/685	THF	520	539	0.70			186
93b	−13.8	59300	83600	1.41	17/463	THF	520	542	0.72			186

[a] Molecular weights (Da) based on GPC analysis vs PS standards unless noted otherwise; PDI = M_w/M_n. [b] Number average of repeating units based on GPC analysis. [c] Solvent used for photophysical studies. [d] Emission maxima upon excitation at λ_{max}; fluorescence quantum efficiency. [e] T_g = glass transition temperature, onset; T_d = decomposition temperature from TGA measurements, onset. [f] Not observed. [g] A small high molecular weight shoulder corresponding to about double the molecular weight of the main peak was observed. [h] Absolute molecular weights from GPC-MALLS detection.

Scheme 45

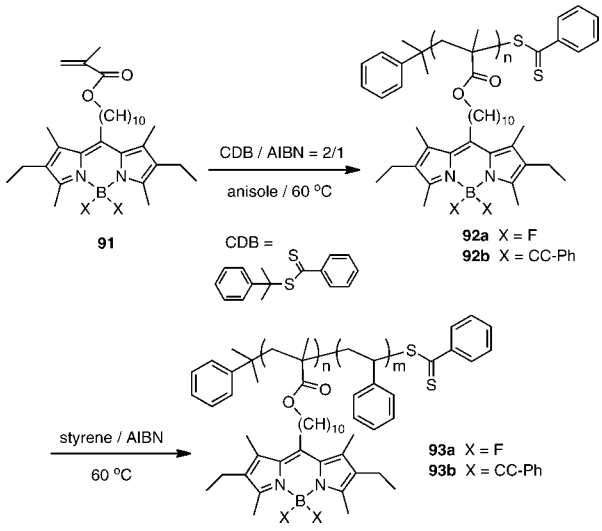

assembly of these particles was attributed to $\pi-\pi$ stacking interactions. Individual spherical particles with diameters of 143 and 571 nm, respectively, were found in the case of the block copolymers (Figure 18). In contrast, solution studies by dynamic light scattering gave much smaller diameters of 12.6 ± 1.0 nm with very uniform size distribution, suggesting that no aggregation via $\pi-\pi$ stacking interactions occurred under these conditions. In line with a decrease in interchromophore interactions for the block copolymers is that the emission quantum efficiency is enhanced for the block copolymer (e.g., 49% for **92b** vs 72% for **93b**).

4.3. Polymers with Terminal Borane Chromophores

As an alternative to the functionalization of polymer side groups with borane functionalities, controlled polymerization methods have also been developed for the preparation of telechelic polymers. In this case, the initiator contains the functional group rather than the monomer. For instance, boronic acid-terminated polymers have been examined as building blocks for supramolecular materials via Lewis acid−base interactions or reversible formation of boroxine structures.[184,202] Especially noteworthy in the context of this review is the preparation of telechelic polyesters with chromophoric end groups by Fraser and co-workers. As illustrated in Scheme 46, an emissive difluoroboron dibenzoylmethane building block[212] was functionalized with a hydroxyl group to serve as an initiator in the Sn(II)-catalyzed polymerization of D,L-lactide or caprolactone.[213,214] Using bulk polymerization, polymers **95** and **96** were obtained with low polydispersities (PDI < 1.1) when the conversion was limited to ~50%.

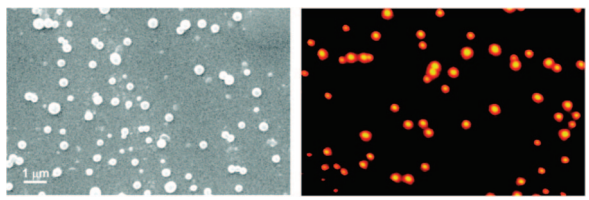

Figure 18. SEM (left) and fluorescence (right) micrograph of block copolymer **93b** deposited from THF solution on a glass plate. Adapted with permission from ref 186. Copyright 2009 American Chemical Society.

Scheme 46

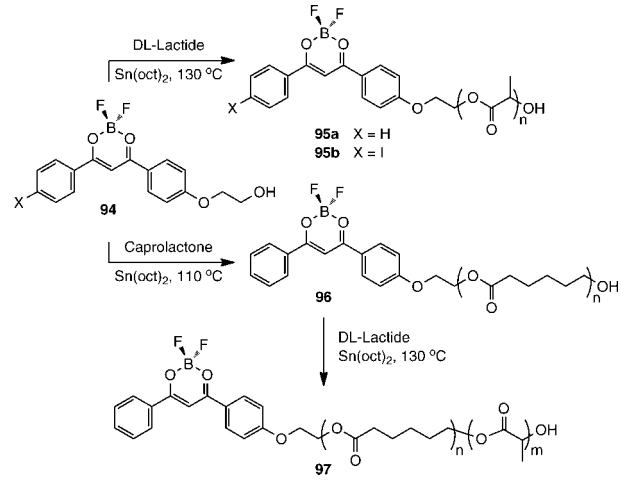

The emissive properties of these polymers turned out to be highly interesting. Under ambient conditions, polymer **95a** displayed a strong blue emission in CH_2Cl_2 solution with a quantum efficiency of 89%. Thin films in air showed a similar blue emission, but when the measurements were performed under an N_2 atmosphere, a long-lived green phosphorescence (>1 s) was observed in addition to the short-lived fluorescence (<20 ns) (Figure 19). Similar observations were made for nanoparticle suspensions in aqueous environment, which opens the door to biological imaging applications.[215]

Another interesting aspect is that the room temperature phosphorescence, which is very unusual for boron compounds, was only observed below the glass transition temperature of the polymer of $T_g = 52$ °C. This suggests that below the T_g, the rigid and ordered polymer matrix restricts movement of the boron chromophores, thereby enhancing radiative over nonradiative decay. The importance of matrix effects is clearly evident when comparing the photophysical properties of thin films of polylactide **95a** with those of polycaprolactone **96**. For the latter, phosphorescence could only be observed at temperatures of less than 0 °C ($T_g = -60$ °C).[214] For both polymers, a trend from green to blue luminescence was apparent with increasing molecular weight of the polymer used to produce thin films (Figure 20). This trend was attributed to fluorophore−fluorophore interactions that are more pronounced in low molecular weight polymer samples because of an increase in the concentration of polymer end groups.[214,216]

Block copolymers (**97**) containing both a polylactide and polycaprolactone segment were also prepared.[217] Chain

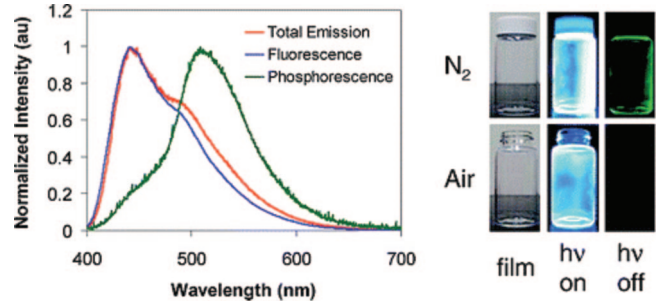

Figure 19. Emission characteristics of thin films of polymer **95a** and photographs illustrating fluorescence (hν on) and phosphorescence (hν off) response under nitrogen and air. Adapted with permission from ref 213. Copyright 2007 American Chemical Society.

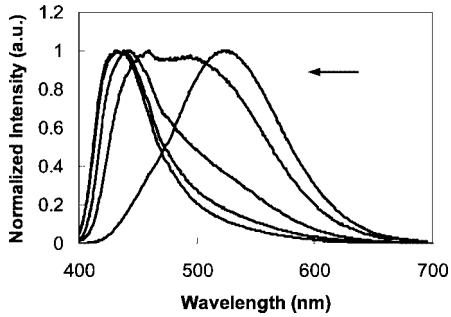

Figure 20. Fluorescence spectra of thin films of polymer **96**; increasing molecular weight from right to left: M_n = 1600, 5400, 9000, 11800, 16400 vs PS standards. Adapted with permission from ref 214. Copyright 2009 American Chemical Society.

extension of the polycaprolactone macroinitiator with D,L- or L-lactide was confirmed by GPC analysis in combination with in-line diode-array UV−vis detection used to ascertain incorporation of the dye into the resulting polymeric materials. Intriguingly, (weak) room temperature phosphorescence was restored for these materials.

Finally, a clever method for enhancing the phosphorescence relative to the fluorescence pathway in these materials was developed.[218] Attachment of iodine to the boron diketonate chromophore in **95b** (Scheme 46) facilitates intersystem crossing (ISC) because of the heavy atom effect of iodine, thereby enhancing radiative decay from the triplet state. This approach led to polymeric materials that are useful for oxygen sensing applications as further described in section 5.4.

5. Selected Applications

5.1. Optical and Electronic Device Materials

Because tricoordinate boron acts as a strong π-acceptor similar to cyano or nitro groups, it has been widely utilized in molecular donor−acceptor type compounds for nonlinear optical applications.[54,67,219] However, to date, comparatively few studies have been performed on polymeric materials. Lequan and co-workers examined the third-order nonlinear optical susceptibility of a polyurethane (**74**, Scheme 39), which features the donor−acceptor moiety $R_2N-C_6H_4-N{=}N-C_6H_4-BMes_2$ in its side chain.[196] Advantageous nonlinear optical properties were reported for thin films, which, upon poling at the glass transition temperature under an external electric field by the corona technique displayed a favorable second harmonic response. The main chain organoboron polymers **2a** and **2f** (Scheme 2), which contain vinylene-phenylene-vinylene and vinylene-fluorenylene-vinylene moieties alternating with electron deficient borane groups, were studied by Chujo via degenerate four-wave mixing, and unusually large bulk third-order susceptibilities of $\chi^{(3)} = 6.87 \times 10^{-6}$ for **2a** and 3.56×10^{-7} esu for **2f** were determined.[32]

Another attractive feature of tricoordinate organoborane moieties is their ability to accept electrons into the empty p-orbital at relatively moderate potentials. According to cyclic voltammetry studies, this is a reversible process, so long as sufficient steric bulk is introduced to preclude otherwise facile chemical decomposition pathways.[220] Chujo and co-workers studied the electrical properties of main-chain organoborane polymers.[221,222] Conductivity measurements on the tripyl-substituted organoborane polymers **3a** and **3f**

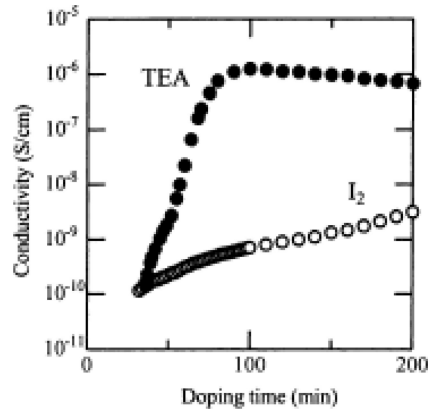

Figure 21. Electrical conductivity data of **3f** (see Scheme 2) upon doping with triethylamine (TEA) or iodine. Reprinted with permission from ref 222. Copyright 2005 Elsevier.

(Scheme 2) revealed low intrinsic conductivity of less than 10^{-10} and a sharp increase up to $\sim 10^{-6}$ S cm^{-1} upon doping with triethylamine as an electron donor (Figure 21).[221,222] In contrast, oxidative doping with iodine resulted in only a small increase in conductivity. Pulsed photoexcitation of an ITO-**3f**-Au cell clearly suggested *n*-type conductivity: the drift mobility of electrons in **3f** was about five times higher than that of holes according to transient photocurrent measurements.[222]

If indeed high electron injection rates and high electron mobilities can be realized for organoborane polymeric materials, these should be favorable characteristics for optoelectronic devices such as organic light emitting devices (OLEDs). Shirota and co-workers demonstrated in 1998 that bithiophene and terthiophene derivatives that are functionalized in the α,ω-positions with Mes_2B moieties act as effective electron conduction and emission layers in OLEDs.[146,223] Since this pioneering discovery, a number of tri- and tetracoordinate organoborane compounds have been successfully incorporated into small molecule OLEDs, serving as emitters, electron transport, and hole blocking layers.[122,224−237] An especially advantageous strategy for the preparation of high efficiency OLEDs has been the use of bipolar materials, which facilitate both hole and electron transport. Shirota successfully used the organoborane polymer **76** (Scheme 40), which features both electron-rich arylamine and electron-deficient arylborane moieties in its side chains as an emitting material in a multilayer OLED (Figure 22a).[198] Green electroluminescence was observed

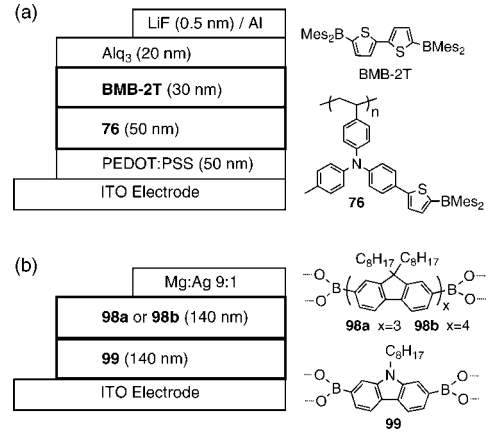

Figure 22. Device configurations for OLEDs fabricated using (a) polymer **76** and (b) boroxine networks **98a**, **98b**, and **99**.

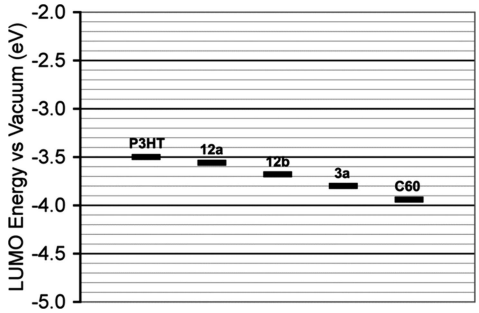

Figure 23. Comparison of the LUMO levels of boron polymers **12** (see Scheme 10) and **3a** (see Scheme 2) with those of the *p*-type polymer poly(3-hexylthiophene) (P3HT) and the *n*-type material C60.

with an emission spectrum that was very similar to the photoluminescence spectrum of a thin film.

The bipolar polymer **56** (Scheme 35) with its conjugated poly-3,6-carbazole backbone was examined by Lambert. For thin films of **56**, blue photoluminescence was observed at $\lambda_{em,max} = 461$ nm with a quantum efficiency of 15%. A single layer device was fabricated consisting of an ITO-coated glass plate, the polymer film, and an Al top contact. At an applied voltage of 8.5 V blue electroluminescence with a maximum at $\lambda = 463$ nm was observed, which is similar to the photoluminescence of the polymer film. The CIE (Commission International d'Eclairage) coordinates are (0.17, 0.21).

Ding and co-workers incorporated thermally cross-linked boroxine networks (**98a** and **98b**), which are derived from dehydration of the respective diboronic acids, as the charge transporting and emitting layer into double layer OLEDs as illustrated in Figure 22b.[238] A device with **98a** as the electron conduction layer and **99** as the hole conduction layer showed the most favorable performance. The electroluminescence spectrum matched reasonably well with the photoluminescence ($\lambda_{em} = 430$, 438 nm). The maximum luminance was 259 cd/m^2 at an electric field strength of 21 $\times$ 10^5 V cm^{-1}, and the luminance efficiency was calculated to be 0.1 cd A^{-1}. A single-layer device using only **98a** sandwiched between ITO and Mg:Ag showed comparatively very poor performance.

The ability of organoborane polymers to accept and conduct electrons is also attractive for their potential use as new materials in photovoltaic devices. So far only limited data are available regarding the evaluation of conjugated organoborane polymers in this respect. Of the organoborane polymers reported to date, **12** (Scheme 10) and **3a** (Scheme 2) are known to have low lying LUMO levels between those of the regioregular donor polymer poly(3-hexylthiophene) (P3HT) and the *n*-type material C_{60}, which is commonly utilized as an electron acceptor material in bulk heterojunction photovoltaic devices (Figure 23). Jia and co-workers performed photoluminescence quenching experiments of diboraanthracene polymers **12a** and **12b** in the presence of P3HT.[66] It is well established that C_{60} and its derivatives are able to quench the photoluminescence of *p*-type materials like P3HT because of electron transfer from the excited state of the polymer to the fullerene. Jia and co-workers found that blending of P3HT with the organoborane polymer **12b** leads to efficient emission quenching, whereas **12a** gives only a small decrease in emission intensity (Figure 24). They concluded that the relatively small energy offset of ~0.18 V between P3HT and polymer **12b** is enough for CT from P3HT to **12b** to occur. Similar results were reported by

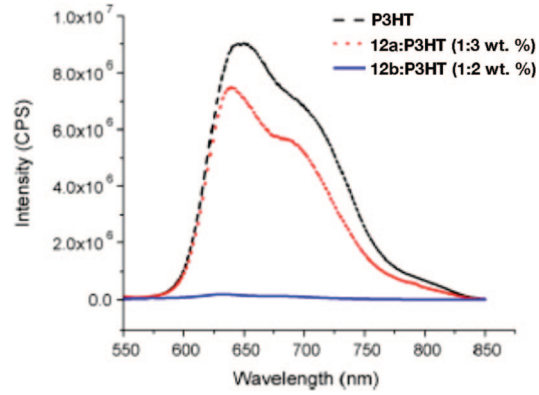

Figure 24. Photoluminescence spectra of pure rr-P3HT, a blend of **12a** and rr-P3HT and a blend of **12b** and rr-P3HT. The structures of polymers **12** are shown in Scheme 10. Reprinted with permission from ref 66. Copyright 2009 Elsevier.

Luebben and Sapp for poly(vinylenephenylenevinylene borane) **3a**.[239] Further studies will have to show whether conjugated organoborane polymers will indeed prove useful as *n*-type materials in solar cell applications.

5.2. Detection of Anions and Neutral Lewis Basic Substrates

The extension of π-conjugation via the vacant p-orbital on boron serves as the cornerstone for applications of conjugated organoborane polymers as optical sensory materials for Lewis basic substrates. As demonstrated in a seminal paper by Yamaguchi and Tamao, binding of anions (or other Lewis bases) to Lewis acidic organoborane centers that are in conjugation with an extended organic π-system leads to interruption of the conjugation pathway and hence a change in the absorption or emission characteristics of the molecule (Figure 25).[240] Most commonly observed is a hypsochromic shift of the absorption and simultaneous quenching of the luminescence (turn-off), although a number of examples of turn-on fluorescent sensing with organoboranes have also been reported in recent years.

5.2.1. Anion Recognition

The dendritic system **8a** (Scheme 6) may serve to illustrate the remarkable complexity of anion binding in multiboron systems.[240] In **8a**, the 3 peripheral borons are chemically equivalent, but distinct from the central boron atom. Upon fluoride ion titration of **8a** in THF, three different binding regimes with individual isosbestic points were identified as shown in Figure 26. Initially, the absorption band of the uncomplexed species at 524 nm decreases and a new band appears at 474 nm together with a broad shoulder around 570 nm (Figure 26a). In light of more recent reports by Müllen and co-workers[241] and Wang and co-workers[242] on conjugated organoboranes, in which two boron centers are connected through an extended organic π-system, the band at 570 nm can be attributed to charge transfer from the newly

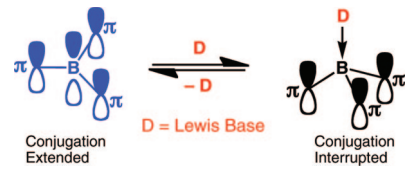

Figure 25. Concept of organoboranes as probes for anions and neutral nucleophiles.

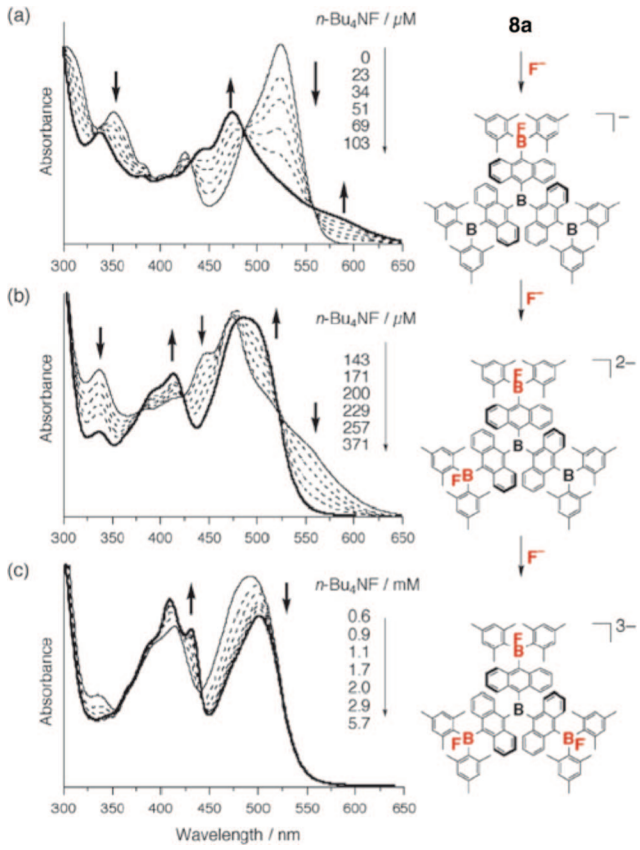

Figure 26. Spectral change of a THF solution of **8a** (4.0×10^{-5} M) upon addition of $[Bu_4N]F$. Adapted with permission from ref 240. Copyright 2001 American Chemical Society.

generated electron-rich fluoroborate moiety to the remaining uncomplexed electron-deficient organoborane sites. Upon further addition of fluoride, two additional binding regimes were observed with individual isosbestic points (Figures 26b and 26c). During these processes, the band at 570 nm completely disappears, shifting the longest wavelength absorption band to 502 nm. These changes can be interpreted as successive complexation of the three peripheral borane moieties with fluoride, while binding of fluoride to the central boron atom seems not to occur under the experimental conditions. The binding constants associated with the three different binding regimes are $K_{11} = 6.9(0.2) \times 10^4$, $K_{12} = 9.0(0.6) \times 10^2$ and $K_{13} = 2.1(0.4) \times 10^2$ M^{-1}, respectively. The decrease in the binding constant with increasing number of fluorides bound to **8a** implies a negative cooperativity effect, which is likely based on Coulombic and steric factors, and to a lesser degree through-bond interactions between the tricoordinate borane and tetracoordinate fluoroborate sites. Important to point out is that simultaneous changes in the emissive properties of these polyfunctional organoboranes can be observed, allowing for use of **8a** and related compounds as optical and fluorescent sensing materials.[12,78,243]

Similar processes as discussed for **8a** should also apply to the binding of Lewis basic substrates to organoborane polymers acting as polyfunctional Lewis acids. Chujo and co-workers first studied the effect of halide anions on the absorption and emission of the blue-luminescent poly(vinylenephenylenevinylene borane)s **2a** and **3a** (Scheme 2).[244] A decrease in intensity and concomitant hypsochromic shift of the longest wavelength absorption band is apparent upon addition of fluoride to $CHCl_3$ solutions of **2a** and **3a**, suggesting complexation of fluoride to the Lewis acidic boron

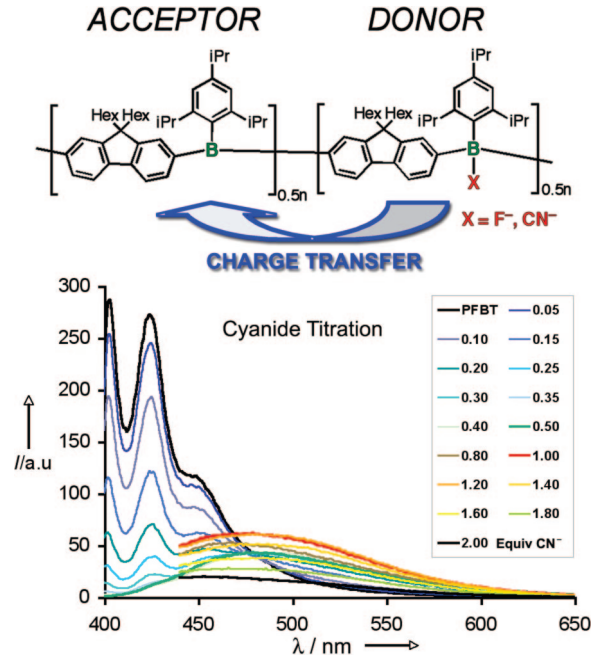

Figure 27. Titration of poly(fluorenylene borane) (**11c**, Scheme 9) with cyanide monitored by fluorescence spectroscopy. Reproduced with permission from ref 70. Copyright 2009 Wiley-VCH Verlag GmbH & Co. KGaA.

centers. Almost complete quenching of the blue fluorescence was observed upon addition of 0.5 mol equiv of fluoride ($\sim 10^{-6}$ M in $CHCl_3$), consistent with a certain degree of signal amplification in comparison to the respective monomeric organoborane species. Moreover, other halides had no effect on the absorption and emission properties, thus confirming the high selectivity for fluoride over its higher homologues.

Fluoride and cyanide binding to the related blue-violet luminescent poly(fluorenylene borane) **11c** (Scheme 9), in which electron-deficient tripylborane moieties alternate with dihexylfluorene moieties in the polymer main chain, was examined by Jäkle and co-workers.[70] As in Chujo's system, the presence of an excess of either F^- or CN^- leads to a hypsochromic shift of the absorption band and almost complete quenching of the emission. An interesting observation, however, is that after addition of $\sim$0.3−0.5 equiv of the anion source a new, very broad and red-shifted emission band at $\sim$475 nm develops, which gradually disappears again at higher ratios of anion to borane repeating units (Figure 27). This behavior was attributed to charge transfer processes in a polymer structure, in which electron-rich fluoroborate moieties coexist with electron-deficient tricoordinate organoborane groups. Such an interpretation is consistent with the observation of lower energy charge transfer emissions in conjugated diboron systems recently studied by Müllen and co-workers[241] and Wang and co-workers.[242]

Anion-induced photoluminescence quenching of the dibenzoborole-modified polyfluorene copolymer **13** (Scheme 11) was examined by Bonifácio, Scherf and co-workers.[38] They observed luminescence quenching of solutions or thin films of **13** in the presence of F^-, CN^-, I^-, whereas the sensitivity toward $H_2PO_4^-$ was lower. Quenching upon addition of F^- and CN^- was attributed to complexation of boron with these anions, in agreement with the results by Chujo and Jäkle described above. However, emission quenching is incomplete as expected for static quenching of a copolymer structure

with only 10% of the fluorenes functionalized with boron. In contrast, I^- led to almost complete quenching of the polymer emission as a result of a dynamic (collisional) mechanism with a Stern−Volmer constant of $K_{SV} = 23.2(9) \times 10^6\ M^{-1}$.

Organoborane functionalized polyolefins such as **80** (Scheme 41) can also serve as sensory materials for fluoride and cyanide.[199] DFT calculations on molecular model compounds that mimic one repeat unit of the polymer chain revealed that in the LUMO, the empty p-orbital on boron not only overlaps with the pendant bithiophene moieties, but also (to a lesser degree) with the phenyl ring of the styryl unit. Thus the strong blue (**80a**,**b**) or green (**80c**) luminescence that is observed involves both the borane pendant groups and the polystyrene backbone. Upon anion binding the conjugation pathway is interrupted leading to a hypsochromic shift in both the absorption and emission spectra. An interesting aspect is that fluoride or cyanide binding to **80c** leads to a change of the emission color from green to blue, suggesting its potential use as a ratiometric probe. Moreover, signal amplification effects were observed in the case of fluoride binding to **80b**, allowing for highly efficient detection of the anion in the low micromolar concentration range. This amplification effect, which is more commonly encountered for conjugated polymers as described above, was tentatively attributed to through-space energy migration.[199]

Colorimetric anion detection was achieved with related ferrocenylborane-substituted polystyrene (**82**, Scheme 42).[207] Polymers **82** display a characteristic dark red color in solution, which is caused by a d−d transition of the ferrocene moiety that is intensified by mixing with charge transfer from the electron-rich iron to the electron deficient borane moiety. Upon exposure to fluoride, the intensity of this absorption band dramatically decreases and the maximum shifts toward higher energy, resulting in a visual change of color from dark red to light orange. Quantitative titration studies revealed a distinct polymer effect: significantly lower binding constants were determined for the polymers in comparison to the respective molecular species. This finding was attributed to pronounced neighboring group effects in the polymer.

Finally, it should be noted that electrochemical methods have also been used to detect fluoride anions. The boronate-functionalized polypyrrole **66** (Chart 7) was studied by Fabre and co-workers,[156,160,161] who found that its electrochemical behavior was strongly modified in the presence of fluoride, whereas chloride or bromide had no effect.

5.2.2. Recognition of Amines

The presence of readily accessible, highly Lewis acidic borane groups provides an opportunity for detection of more sterically demanding neutral substrates. Jäkle and co-workers found that treatment of the blue-green fluorescent poly(bithiophene borane) **10a** (Scheme 8) with pyridine results in efficient quenching of its fluorescence.[36] On the basis of a Stern−Volmer analysis, it was concluded that at low pyridine concentration, the quenching efficiency for polymer **10a** is enhanced by a factor of ∼12 relative to a 5,5′-diborylated 2,2′-bithiophene[86] model compound.

More recently, Lee and co-workers demonstrated that conjugated polymeric materials with boron−oxygen linkages can be used to detect different aliphatic and aromatic amines.[50] Thin films of **25b** (Scheme 18), which was electropolymerized on ITO-coated glass electrodes, were briefly exposed to saturated vapor of different amines. A distinct

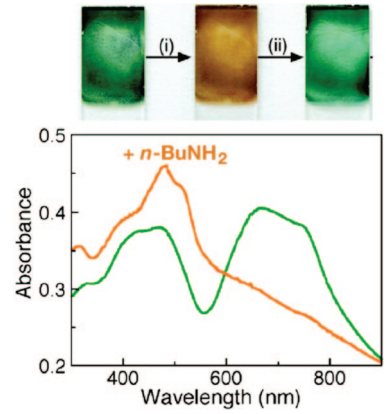

Figure 28. Reversible color change of thin films of polymer **25b** (see Scheme 18) upon exposure to *n*-$BuNH_2$ vapors. (i) *n*-$BuNH_2$ vapor. (ii) $B(C_6F_5)_3$ in CH_2Cl_2. Adapted with permission from ref 50. Copyright 2009 American Chemical Society.

change from a dark green color of the polymer films, which is the result of polaron/bipolaron electronic states in the doped oligothiophene segments, to an orange color was observed (Figure 28). This color change is believed to be the result of binding of the amine to the Lewis acidic borane sites, which effectively removes the boron empty p_z orbitals from conjugation with the quarterthiophene moieties. Similar observations were made when the polymer film was exposed to fluoride anions in THF. The process was reversed by addition of $B(C_6F_5)_3$ as a stronger Lewis acid that is able to effectively compete for binding to amines.

A conductometric sensor for n-butylamine was introduced by Freund and co-workers.[245] Exposure of poly(anilineboronic acid) (**69**, Chart 8) to ppb levels of the amine resulted in a measurable decrease in conductivity. A detection mechanism involving acid−base chemistry at the imine sites was proposed. The decrease in conductivity is irreversible, which was attributed to favorable ion pairing between borate sites and butylammonium groups. Nonetheless, a sensitive detection scheme could be realized by analyzing the differential resistance upon amine exposure.

5.3. Detection of Polyols with Boronic Acid-Functionalized Polymers

The recognition of polyols, which includes a large number of biologically active molecules such as sugars, RNA, etc., with boronic acid-functionalized polymers relies on the reversible formation of covalent boron−oxygen links, typically with formation of a dioxaborole ring and conversion to tetracoordinate boron.

The equilibrium depicted in Scheme 47 is commonly monitored by (i) a change in the solubility characteristics brought about by conversion of the neutral boronic acid sites to anionic borate moieties or by cross-linking of different polymer strands, (ii) a change in the absorption or emission color of the polymer because of changes in the electronic structure, or (iii) a change in conductivity because of conformational or electronic changes in conjugated polymers. Relevant to the discussion of optical and electro-active materials in this review are the later two options, for which a few examples are described briefly in the following.

Scheme 47

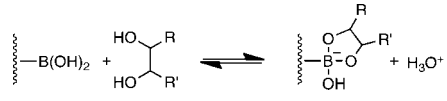

Chart 9

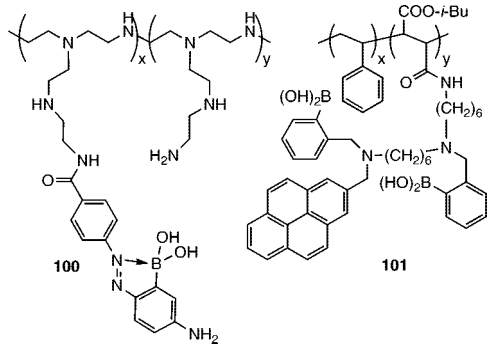

5.3.1. Change in Optical Properties

Changes in the absorption and emission characteristics have been expoited for the recognition of sugar molecules using chromophore-functionalized boronic acid polymers. Egawa and co-workers studied a polymer (**100**, Chart 9) that contains azobenzene dyes that are modified with boronic acid groups attached to poly(ethyleneimine) (MW = 60000−80000 Da).[246] Addition of glucose triggered a change in the absorption spectrum of the polymer. The binding constants for D-glucose and D-fructose in buffer solution at pH 9.0 were calculated to be 54 and 110 M^{-1}, respectively. Multilayer thin films were prepared by alternating deposition with poly(vinyl sulfate), carboxymethylcellulose, and sodium alginate, respectively. Because of its more loosely packed structure, films with carboxymethylcellulose gave the strongest response to glucose.

Fluorescence quenching of the water-soluble fluorescent polythiophene derivative **72** (Scheme 38) was exploited for highly sensitive detection of monosaccharides, lactose, ascorbic acid, and dopamine. At pH 7.4 in 0.1 M phosphate buffer, very high binding constants in the range of 3.3×10^4 to 4.6×10^5 M^{-1} were determined.[172]

In contrast, James and co-workers observed an enhancement of fluorescence upon exposure of polymer **101** (Chart 9) to glucose or fructose. In their system, binding of the sugar to the boronic acid residue leads to formation of a dative B−N bond, which prevents quenching due to photoinduced electron transfer (PET) from the amine to the pyrene moiety. The polymer with its multiple boronic acid groups and pendant pyrene fluorophores showed higher selectivity for fructose ($K = 1124$ M^{-1}) than glucose, in contrast to related molecular compounds.[247]

A change in the polymer conformation was exploited by Tao and co-workers for the detection of saccharides using an acrylamide copolymer containing spatially separated boronic acid and pyrene functional groups.[248] Saccharide binding gives rise to electrostatic effects that lead to contraction or expansion of the polymer chain, ultimately affecting the ratio of pyrene to pyrene excimer emission.

5.3.2. Change in Conductivity

Poly(anilineboronic acid) (**67**) and its copolymer with aniline (**68**) (see Chart 7) have been widely used as conductometric sensors for sugars.[158,163,169,249−251] Reversible binding of glucose, fructose, and other sugars to poly(anilineboronic acid) (**67**) in the physiological pH range was confirmed, and Freund and co-workers found that the dihedral angle O−C−C-O of the diol moieties critically influences the binding constants and thus the selectivity.[158,163]

Chart 10

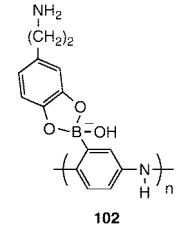

In thin films, an optimal pH of 7.4 for complexation with D-fructose and of 9.0 for complexation with D-glucose was determined based on open-circuit potential, quartz crystal microbalance, and PM-IRRAS experiments.[250]

Complexation of **67** to β-nicotinamide adenine dinucleotide (NADH) and its oxidized form NAD^+ was also confirmed by Freund and co-workers. A difference was detected between the complexation of NADH and NAD^+ according to ^{11}B NMR and open-circuit voltage measurements, which suggested that NAD^+ facilitates the formation of the pernigraniline form of the polyaniline backbone.[252]

The use of (**67**) as conductometric sensor for dopamine, a neurotransmitter in the brain that has been linked to Parkinson's decease, was first demonstrated by Fabre and co-workers.[253] The detection is based on formation of the boronate complex **102** (Chart 10). They used an interdigitated microarray electrode, which was coated with **67** by electrodeposition. In a transistor configuration, a decrease in the drain current could be related to dopamine binding at physiological pH (pH 7.4) with a detection limit in the micromolar range. Importantly, the presence of up to 10 mM ascorbic acid did not interfere with the dopamine detection. More recently, He and co-workers reported an ultrasensitive composite material, prepared from polymerization of 3-aminophenylboronic acid in the presence of carbon nanotubes that were coated with single-stranded DNA.[170,178,179] Upon modification of a gold electrode with this composite material, dopamine concentrations as low as 1 nM could be detected electrochemically at pH 7.4.

5.4. Other Detection Mechanisms

Not all optical sensing schemes involving organoborane polymers are based on analyte binding. Trogler and co-workers developed a clever approach for hydrogen peroxide detection that is based on the cleavage of boron−carbon bonds.[48] A thin film of polymer **23** (Scheme 17) was drop cast onto a substrate, which was chosen to be porous to increase the surface area for polymer-analyte interaction. Exposure to hydrogen peroxide led to a turn-on fluorescence response because of oxidative cleavage of the boronic ester groups in **23** with subsequent generation of the green-luminescent dye fluorescein (Figure 29). Using this method, detection limits of down to 3 ppm of H_2O_2 were achieved. The detection was selective for H_2O_2, and no response to organic peroxides such as di-*t*-butyl peroxide or benzoyl peroxide was registered under similar conditions.

Finally, oxygen sensing has been accomplished using polylactide with boron diketonate groups attached to one of the chain ends.[218,254] Polymer **95b** (Scheme 46) shows dual emission with simultaneous phosphorescence and fluorescence under exclusion of oxygen. However, when exposed to oxygen, the phosphorescence is quenched, retaining only the higher energy fluorescence response (Figure 30). By monitoring the intensity ratio of fluorescence ($\lambda = 450$ nm)

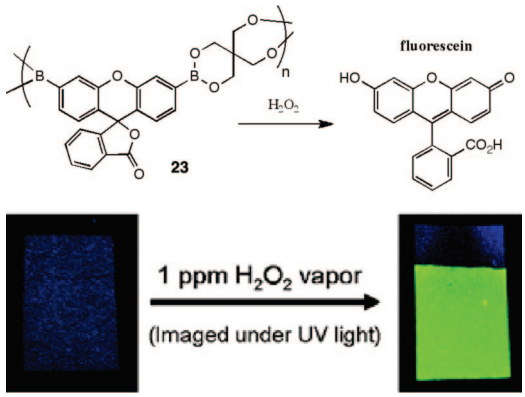

Figure 29. Color change of a thin film of polymer **23** upon exposure to H_2O_2 vapors. Reproduced with permission from ref 48. Copyright 2008 The Royal Society of Chemistry.

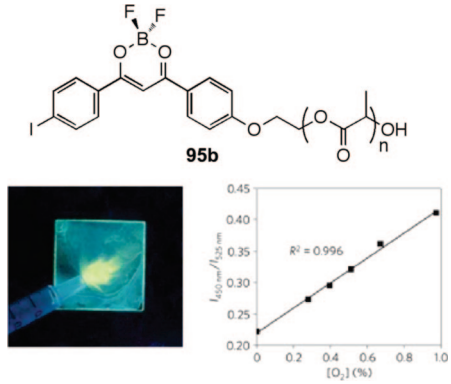

Figure 30. Effect of oxygen on the emission of a thin film of **95b** (n = 27). Left: Photograph showing yellow phosphorescence emission under a N_2 gas stream in contrast to blue green fluorescence in the presence of oxygen under ultraviolet excitation. Right: Linear relationship between oxygen level and the fluorescence/phosphorescence intensity ratio at 450 and 525 nm. Reprinted with permission from ref 218. Copyright 2009 Macmillan Publishers Ltd. (*Nature Materials*).

versus phosphorescence (λ = 525 nm), an almost linear relationship was established with increasing O_2 concentration up to 1% O_2.

Nanoparticles of this polymer (n = 95, ~98 nm diameter) were prepared by nanoprecipitation and successfully applied in ratiometric tumor hypoxia imaging.[218,254] They were used in combination with a mouse dorsal window chamber breast cancer 4T1 mammary carcinoma model. Tissue oxygen maps based on fluorescence/phosphorescence ratios during carbogen, air and brief nitrogen breathing (95%, 21%, and 0% O_2, respectively), showed excellent contrast between the microvasculature and the tumor tissue.

6. Concluding Remarks

In conclusion, the field of boron-containing organic−inorganic hybrid polymers has greatly expanded over the past decade, as a large variety of new types of organoborane polymers and related macromolecules have been reported. New methods have been established, providing for facile synthetic access, and first steps toward control over molecular weight and architecture have been taken successfully. Thus, an array of functional boron-containing materials with very desirable optical and electronic characteristics including strong absorptions in the visible region, interesting nonlinear optical behavior, intense photoluminescence, and even n-type semiconductivity have become readily available.

While most of the earlier efforts were primarily aimed at demonstrating the synthetic accessibility and establishing structure property relationships, specific applications have been explored more recently. The ability of tricoordinate boron to act as a Lewis acid site has been widely exploited for the development of sensory materials for anions, neutral nucleophiles such as toxic amines, or biologically relevant species such as saccharides or dopamine. The electron-deficient character of suitably designed triorganoborane polymers also holds significant promise for use as acceptor-type polymers in optoelectronic applications such as field effect transistors and photovoltaics. Polymers that are functionalized with boron-containing chromophores are being studied for use in organic light emitting devices (OLEDs) and even as luminescent materials for imaging in biological environments. Exciting new discoveries with boron-containing polymers in these and other new applications fields are anticipated and certain to lead to a further increase in interest in this emerging class of polymeric materials.

7. Acknowledgments

I am grateful to my current and former students for their enthusiasm and dedication and thank all of them as well as our many collaborators for their contributions to the different aspects of our research program. The research work of our group has been financially supported by the National Science Foundation (CHE-0809642), the donors of The Petroleum Research Fund, administered by the American Chemical Society, and the Rutgers University Research Council. F.J. thanks the Alfred P. Sloan Foundation for a research fellowship and the Alexander von Humboldt Foundation for a Friedrich Wilhelm Bessel Research Award.

8. References

(1) Su, J.; Li, X.-W.; Crittendon, R. C.; Robinson, G. H. *J. Am. Chem. Soc.* **1997**, *119*, 5471–5472.
(2) Kim, K.-C.; Reed, C. A.; Elliott, D. W.; Mueller, L. J.; Tham, F.; Lin, L.; Lambert, J. B. *Science* **2002**, *297*, 825–827.
(3) Sekiguchi, A.; Kinjo, R.; Ichinohe, M. *Science* **2004**, *305*, 1755–1757.
(4) Green, S. P.; Jones, C.; Stasch, A. *Science* **2007**, *318*, 1754–1757.
(5) Scheschkewitz, D.; Amii, H.; Gornitzka, H.; Schoeller, W. W.; Bourissou, D.; Bertrand, G. *Science* **2002**, *295*, 1880–1881.
(6) Bosdet, M. J. D.; Piers, W. E. *Can. J. Chem.* **2009**, *87*, 8–29.
(7) Waterman, R.; Hayes, P. G.; Tilley, T. D. *Acc. Chem. Res.* **2007**, *40*, 712–719.
(8) Segawa, Y.; Yamashita, M.; Nozaki, K. *Science* **2006**, *314*, 113–115.
(9) Welch, G. C.; Juan, R. R. S.; Masuda, J. D.; Stephan, D. W. *Science* **2006**, *314*, 1124–1126.
(10) Peng, Y.; Ellis, B. D.; Wang, X.; Fettinger, J. C.; Power, P. P. *Science* **2009**, *325*, 1668–1670.
(11) Braunschweig, H.; Herbst, T.; Rais, D.; Ghosh, S.; Kupfer, T.; Radacki, K.; Crawford, A. G.; Ward, R. M.; Marder, T. B.; Fernandez, I.; Frenking, G. *J. Am. Chem. Soc.* **2009**, *131*, 8989–8999.
(12) Hudnall, T. W.; Chiu, C.-W.; Gabbai, F. P. *Acc. Chem. Res.* **2009**, *42*, 388–397.
(13) Archer, R. D. *Inorganic and Organometallic Polymers*; Wiley-VCH: New York, 2001.
(14) Abd-El-Aziz, A. S.;, Jr.;, Jr.; Sheats, J. E.; Zeldin, M. *Macromolecules Containing Metal and Metal-Like Elements, Vol.1, A Half-Century of Metal- and Metalloid-Containing Polymers*; John Wiley & Sons: Hoboken, NJ, 2003.
(15) Mark, J. E.; Allcock, H. R.; West, R. C. *Inorganic Polymers*; Prentice Hall: Englewood Cliffs, NJ, 1992.
(16) Manners, I. *Angew. Chem., Int. Ed.* **1996**, *35*, 1602–1621.
(17) Allcock, H. R. *Chemistry and Applications of Polyphosphazenes*; Wiley-VCH: Hoboken, NJ, 2002.
(18) Brook, M. A. *Silicon in Organic, Organometallic, And Polymer Chemistry*; Wiley-VCH: New York, 2000.

(19) Manners, I. *J. Polym. Sci., Part A: Polym. Chem.* **2002**, *40*, 179–191.
(20) Gates, D. P. *Top. Curr. Chem.* **2005**, *250*, 107–126.
(21) Baumgartner, T.; Reau, R. *Chem. Rev.* **2006**, *106*, 4681–4727.
(22) Manners, I. *Angew. Chem., Int. Ed.* **2007**, *46*, 1565–1568.
(23) Neale, N. R.; Tilley, T. D. *J. Am. Chem. Soc.* **2002**, *124*, 3802–3803.
(24) Naka, K. *Polym. J.* **2008**, *40*, 1031–1041.
(25) Choffat, F.; Smith, P.; Caseri, W. *Adv. Mater.* **2008**, *20*, 2225–2229.
(26) Amadoruge, M. L.; Weinert, C. S. *Chem. Rev.* **2008**, *108*, 4253–4294.
(27) Matsumi, N.; Chujo, Y. In *Special Publication—Royal Society of Chemistry*; Royal Society of Chemistry: Cambridge, UK, 2000; Vol. 253.
(28) Jäkle, F. *J. Inorg. Organomet. Polym. Mater.* **2005**, *15*, 293–307.
(29) Jäkle, F. *Coord. Chem. Rev.* **2006**, *250*, 1107–1121.
(30) Gabel, D. In *Science of Synthesis: Houben—Weyl Methods of Molecular Transformations*; Kaufmann, D., Matteson, D. S., Eds.; Georg Thieme Verlag: Stuttgart, 2005; Vol. 6.
(31) *Macromolecules Containing Metal and Metal-Like Elements, Vol. 8: Boron-Containing Polymers*; Abd-El-Aziz, A. S., Carraher, C. E., Jr., Pittman, C. U., Jr., Zeldin, M., Eds.; John Wiley & Sons, Inc.: Hoboken, NJ, 2007.
(32) Matsumi, N.; Chujo, Y. *Polym. J.* **2008**, *40*, 77–89.
(33) Chujo, Y. *Macromol. Symp.* **1997**, *118*, 111–116.
(34) Matsumi, N.; Naka, K.; Chujo, Y. *J. Am. Chem. Soc.* **1998**, *120*, 10776–10777.
(35) Matsumi, N.; Umeyama, T.; Chujo, Y. *Polym. Bull.* **2000**, *44*, 431–436.
(36) Sundararaman, A.; Victor, M.; Varughese, R.; Jäkle, F. *J. Am. Chem. Soc.* **2005**, *127*, 13748–13749.
(37) Zhao, C.; Wakamiya, A.; Yamaguchi, S. *Macromolecules* **2007**, *40*, 3898–3900.
(38) Bonifácio, V. D. B.; Morgado, J.; Scherf, U. *J. Polym. Sci., Part A: Polym. Chem.* **2008**, *46*, 2878–2883.
(39) Reitzenstein, D.; Lambert, C. *Macromolecules* **2009**, *42*, 773–782.
(40) Matsumi, N.; Chujo, Y. *Macromolecules* **2000**, *33*, 8146–8148.
(41) Matsumoto, F.; Chujo, Y. *Macromolecules* **2003**, *36*, 5516–5519.
(42) Nagai, A.; Miyake, J.; Kokado, K.; Nagata, Y.; Chujo, Y. *J. Am. Chem. Soc.* **2008**, *130*, 15276–15278.
(43) Yamaguchi, I.; Tominaga, T.; Sato, M. *Polym. Int.* **2009**, *58*, 17–21.
(44) Chujo, Y.; Tomita, I.; Asano, T.; Saegusa, T. *Polym. J.* **1994**, *26*, 85–92.
(45) Chujo, Y.; Tomita, I.; Saegusa, T. *Macromolecules* **1994**, *27*, 6714–6717.
(46) Matsumi, N.; Naka, K.; Chujo, Y. *Polym. J.* **1998**, *30*, 833–837.
(47) Niu, W.; Smith, M. D.; Lavigne, J. J. *J. Am. Chem. Soc.* **2006**, *128*, 16466–16467.
(48) Sanchez, J. C.; Trogler, W. C. *J. Mater. Chem.* **2008**, *18*, 5134–5141.
(49) Li, H.; Jäkle, F. *Macromolecules* **2009**, *42*, 3448–3453.
(50) Liu, W.; Pink, M.; Lee, D. *J. Am. Chem. Soc.* **2009**, *131*, 8703–8707.
(51) Berenbaum, A.; Braunschweig, H.; Dirk, R.; Englert, U.; Green, J. C.; Jäkle, F.; Lough, A. J.; Manners, I. *J. Am. Chem. Soc.* **2000**, *122*, 5765–5774.
(52) Heilmann, J. B.; Scheibitz, M.; Qin, Y.; Sundararaman, A.; Jäkle, F.; Kretz, T.; Bolte, M.; Lerner, H.-W.; Holthausen, M. C.; Wagner, M. *Angew. Chem., Int. Ed.* **2006**, *45*, 920–925.
(53) Scheibitz, M.; Li, H.; Schnorr, J.; Sánchez Perucha, A.; Bolte, M.; Lerner, H.-W.; Jäkle, F.; Wagner, M. *J. Am. Chem. Soc.* **2009**, *131*, 16319–16329.
(54) Entwistle, C. D.; Marder, T. B. *Chem. Mater.* **2004**, *16*, 4574–4585.
(55) Corriu, R. J.-P.; Deforth, T.; Douglas, W. E.; Guerrero, G.; Siebert, W. S. *Chem. Commun.* **1998**, 963–964.
(56) Smith, K.; Pelter, A.; Jin, Z. *Angew. Chem., Int. Ed. Engl.* **1994**, *33*, 851–853.
(57) Pelter, A.; Smith, K.; Buss, D.; Jin, Z. *Heteroat. Chem.* **1992**, *3*, 275–277.
(58) Matsumi, N.; Naka, K.; Chujo, Y. *J. Am. Chem. Soc.* **1998**, *120*, 5112–5113.
(59) Matsumi, N.; Miyata, M.; Chujo, Y. *Macromolecules* **1999**, *32*, 4467–4469.
(60) Chujo, Y.; Sasaki, Y.; Kinomura, N.; Matsumi, N. *Polymer* **2000**, *41*, 5047–5051.
(61) Nagai, A.; Murakami, T.; Nagata, Y.; Kokado, K.; Chujo, Y. *Macromolecules* **2009**, *42*, 7217–7220.
(62) Entwistle, C. D.; Batsanov, A. S.; Howard, J. A. K.; Fox, M. A.; Marder, T. B. *Chem. Commun.* **2004**, 702–703.
(63) Matsumoto, F.; Chujo, Y. *Pure Appl. Chem.* **2009**, *81*, 433–437.
(64) Miyata, M.; Chujo, Y. *Polym. Bull.* **2003**, *51*, 9–16.
(65) Lorbach, A.; Bolte, M.; Li, H.; Lerner, H.-W.; Holthausen, M. C.; Jäkle, F.; Wagner, M. *Angew. Chem., Int. Ed.* **2009**, *48*, 4584–4588.
(66) Chai, J.; Wang, C.; Jia, L.; Pang, Y.; Graham, M.; Cheng, S. Z. D. *Synth. Met.* **2009**, *159*, 1443–1449.
(67) Yuan, Z.; Collings, J. C.; Taylor, N. J.; Marder, T. B.; Jardin, C.; Halet, J.-F. *J. Solid State Chem.* **2000**, *154*, 5–12.
(68) Miyata, M.; Matsumi, N.; Chujo, Y. *Polym. Bull.* **1999**, *42*, 505–510.
(69) Yamaguchi, S.; Akiyama, S.; Tamao, K. *J. Am. Chem. Soc.* **2000**, *122*, 6335–6336.
(70) Li, H.; Jäkle, F. *Angew. Chem., Int. Ed.* **2009**, *48*, 2313–2316.
(71) Cao, D. X.; Liu, Z. Q.; Fang, Q.; Xu, G. B.; Xue, G.; Liu, G. Q.; Yu, W. T. *J. Organomet. Chem.* **2004**, *689*, 2201–2206.
(72) Sakuda, E.; Funahashi, A.; Kitamura, N. *Inorg. Chem.* **2006**, *45*, 10670–10677.
(73) Zhao, Q.; Li, F.; Liu, S.; Yu, M.; Liu, Z.; Yi, T.; Huang, C. *Inorg. Chem.* **2008**, *47*, 9256–9264.
(74) You, Y.; Park, S. Y. *Adv. Mater.* **2008**, *20*, 3820–3826.
(75) Venkatasubbaiah, K.; Pakkirisamy, T.; Lalancette, R. A.; Jäkle, F. *Dalton Trans.* **2008**, 4507–4513.
(76) Broomsgrove, A. E. J.; Addy, D. A.; Bresner, C.; Fallis, I. A.; Thompson, A. L.; Aldridge, S. *Chem.—Eur. J.* **2008**, *14*, 7525–7529.
(77) Zhou, G.; Ho, C.-L.; Wong, W.-Y.; Wang, Q.; Ma, D.; Wang, L.; Lin, Z.; Marder, T. B.; Beeby, A. *Adv. Funct. Mater.* **2008**, *18*, 499–511.
(78) Hudson, Z. M.; Wang, S. *Acc. Chem. Res.* **2009**, *42*, 1584–1596.
(79) Braunschweig, H.; Dirk, R.; Müller, M.; Nguyen, P.; Resendes, R.; Gates, D. P.; Manners, I. *Angew. Chem., Int. Ed.* **1997**, *36*, 2338–2340.
(80) Matsumi, N.; Chujo, Y.; Lavastre, O.; Dixneuf, P. H. *Organometallics* **2001**, *20*, 2425–2427.
(81) Matsumoto, F.; Matsumi, N.; Chujo, Y. *Polym. Bull.* **2001**, *46*, 257–262.
(82) Heilmann, J. B.; Qin, Y.; Jäkle, F.; Lerner, H.-W.; Wagner, M. *Inorg. Chim. Acta* **2006**, *359*, 4802–4806.
(83) Jäkle, F.; Berenbaum, A.; Lough, A. J.; Manners, I. *Chem.—Eur. J.* **2000**, *6*, 2762–2771.
(84) Scheibitz, M.; Heilmann, J. B.; Winter, R. F.; Bolte, M.; Bats, J. W.; Wagner, M. *Dalton Trans.* **2005**, 159–170.
(85) Venkatasubbaiah, K.; Doshi, A.; Nowik, I.; Herber, R. H.; Rheingold, A. L.; Jäkle, F. *Chem.—Eur. J.* **2008**, *14*, 444–458.
(86) Sundararaman, A.; Venkatasubbaiah, K.; Victor, M.; Zakharov, L. N.; Rheingold, A. L.; Jäkle, F. *J. Am. Chem. Soc.* **2006**, *128*, 16554–16565.
(87) Brière, J.-F.; Côté, M. *J. Phys. Chem. B* **2004**, *108*, 3123–3129.
(88) Tanaka, K.; Ueda, K.; Koike, T.; Ando, M.; Yamabe, T. *Phys. Rev. B* **1985**, *32*, 4279–4281.
(89) Tanaka, K.; Yamanaka, S.; Ueda, K.; Takeda, S.; Yamabe, T. *Synth. Met.* **1987**, *20*, 333–345.
(90) Yamanaka, S.; Inoue, T.; Aoyagi, T.; Komatsu, T. *Synth. Met.* **1992**, *46*, 221–225.
(91) Salzner, U.; Lagowski, J. B.; Pickup, P. G.; Poirier, R. A. *Synth. Met.* **1998**, *96*, 177–189.
(92) Narita, Y.; Hagiri, I.; Takahashi, N.; Takeda, K. *Jpn. J. Appl. Phys.* **2004**, *43*, 4248–4258.
(93) Cao, H.; Ma, J.; Zhang, G.; Jiang, Y. *Macromolecules* **2005**, *38*, 1123–1130.
(94) Zhang, Y.; Cai, X.; Bian, Y.; Li, X.; Jiang, J. *J. Phys. Chem. C.* **2008**, *112*, 5148–5159.
(95) Gerwarth, U. W. *Z. Naturforsch.* **1977**, *32b*, 1408–1415.
(96) Wolfe, P. S.; Wagener, K. B. *Macromolecules* **1999**, *32*, 7961–7967.
(97) Mastalerz, M. *Angew. Chem., Int. Ed.* **2008**, *47*, 445–447.
(98) Fujita, N.; Shinkai, S.; James, T. D. *Chem.—Asian J.* **2008**, *3*, 1076–1091.
(99) Severin, K. *Dalton Trans.* **2009**, 5254–5264.
(100) Korich, A. L.; Iovine, P. M. *Dalton Trans.* **2010**, *39*, 1423–1431.
(101) Niu, W.; O'Sullivan, C.; Rambo, B. M.; Smith, M. D.; Lavigne, J. J. *Chem. Commun.* **2005**, 4342–4344.
(102) Niu, W.; Rambo, B.; Smith, M. D.; Lavigne, J. J. *Chem. Commun.* **2005**, 5166–5168.
(103) Matsumi, N.; Kotera, K.; Chujo, Y. *Macromolecules* **2000**, *33*, 2801–2806.
(104) Matsumi, N.; Kotera, K.; Naka, K.; Chujo, Y. *Macromolecules* **1998**, *31*, 3155–3157.
(105) Matsumi, N.; Chujo, Y. *Macromolecules* **1998**, *31*, 3802–3806.
(106) Mulvaney, J. E.; Bloomfield, J. J.; Marvel, S. S. *J. Polym. Sci.* **1962**, *62*, 59–72.
(107) Soloway, A. H. *J. Am. Chem. Soc.* **1960**, *82*, 2442–2444.
(108) Matsumoto, F.; Chujo, Y. *J. Organomet. Chem.* **2003**, *680*, 27–30.
(109) Matsumi, N.; Chujo, Y. *Polym. Bull.* **1999**, *43*, 151–155.
(110) Matsumi, N.; Umeyama, T.; Chujo, Y. *Macromolecules* **2000**, *33*, 3956–3957.
(111) Miyata, M.; Matsumi, N.; Chujo, Y. *Macromolecules* **2001**, *34*, 7331–7335.

(112) Naka, K.; Umeyama, T.; Chujo, Y. *Macromolecules* **2000**, *33*, 7467–7470.
(113) Matsumi, N.; Umeyama, T.; Chujo, Y. *Macromolecules* **2001**, *34*, 3510–3511.
(114) Matsumoto, F.; Matsumi, N.; Chujo, Y. *Polym. Bull.* **2002**, *48*, 119–125.
(115) Nagai, A.; Miyake, J.; Kokado, K.; Nagata, Y.; Chujo, Y. *Macromolecules* **2009**, *42*, 1560–1564.
(116) Jäkle, F.; Priermeier, T.; Wagner, M. *J. Chem. Soc., Chem. Commun.* **1995**, 1765–1766.
(117) Herdtweck, E.; Jäkle, F.; Opromolla, G.; Spiegler, M.; Wagner, M.; Zanello, P. *Organometallics* **1996**, *15*, 5524–5535.
(118) Ma, K.; Scheibitz, M.; Scholz, S.; Wagner, M. *J. Organomet. Chem.* **2002**, *652*, 11–19.
(119) Matsumoto, F.; Nagata, Y.; Chujo, Y. *Polym. Bull.* **2005**, *53*, 155–160.
(120) Kamaya, E.; Matsumoto, F.; Kondo, Y.; Chujo, Y.; Katagiri, M. *Nucl. Instrum. Methods Phys. Res, Sect. A* **2004**, *529*, 329–331.
(121) Matsumoto, F.; Chujo, Y. *Pure Appl. Chem.* **2006**, *78*, 1407–1411.
(122) Wu, Q.; Esteghamatian, M.; Hu, N.-X.; Popovic, Z.; Enright, G.; Tao, Y.; D'Iorio, M.; Wang, S. *Chem. Mater.* **2000**, *12*, 79–83.
(123) Qin, Y.; Pagba, C.; Piotrowiak, P.; Jäkle, F. *J. Am. Chem. Soc.* **2004**, *126*, 7015–7018.
(124) Qin, Y.; Kiburu, I.; Shah, S.; Jäkle, F. *Macromolecules* **2006**, *39*, 9041–9048.
(125) Wang, X.-Y.; Weck, M. *Macromolecules* **2005**, *38*, 7219–7224.
(126) Nagata, Y.; Chujo, Y. *Macromolecules* **2007**, *40*, 6–8.
(127) Nagata, Y.; Chujo, Y. *Macromolecules* **2008**, *41*, 2809–2813.
(128) Tokoro, Y.; Nagai, A.; Kokado, K.; Chujo, Y. *Macromolecules* **2009**, *42*, 2988–2993.
(129) Nagata, Y.; Chujo, Y. *Macromolecules* **2008**, *41*, 3488–3492.
(130) Cui, Y.; Wang, S. *J. Org. Chem.* **2006**, *71*, 6485–6496.
(131) Ulrich, G.; Ziessel, R.; Harriman, A. *Angew. Chem., Int. Ed.* **2008**, *47*, 1184–1201.
(132) Zhu, M.; Jiang, L.; Yuan, M.; Liu, X.; Ouyang, C.; Zheng, H.; Yin, X.; Zuo, Z.; Liu, H.; Li, Y. *J. Polym. Sci., Part A: Polym. Chem.* **2008**, *46*, 7401–7410.
(133) Donuru, V. R.; Vegesna, G. K.; Velayudham, S.; Green, S.; Liu, H. *Chem. Mater.* **2009**, *21*, 2130–2138.
(134) Donuru, V. R.; Vegesna, G. K.; Velayudham, S.; Meng, G.; Liu, H. *J. Polym. Sci., Part A: Polym. Chem.* **2009**, *47*, 5354–5366.
(135) Meng, G.; Velayudham, S.; Smith, A.; Luck, R.; Liu, H. *Macromolecules* **2009**, *42*, 1995–2001.
(136) Ding, L.; Ma, K.; Dürner, G.; Bolte, M.; Fabrizi de Biani, F.; Zanello, P.; Wagner, M. *J. Chem. Soc., Dalton Trans.* **2002**, 1566–1573.
(137) Dinnebier, R. E.; Ding, L.; Ma, K.; Neumann, M. A.; Tanpipat, N.; Leusen, F. J. J.; Stephens, P. W.; Wagner, M. *Organometallics* **2001**, *20*, 5642–5647.
(138) Fontani, M.; Peters, F.; Scherer, W.; Wachter, W.; Wagner, M.; Zanello, P. *Eur. J. Inorg. Chem.* **1998**, 1453–1465.
(139) Grosche, M.; Herdtweck, E.; Peters, F.; Wagner, M. *Organometallics* **1999**, *18*, 4669–4672.
(140) Dinnebier, R. E.; Wagner, M.; Peters, F.; Shankland, K.; David, W. I. F. *Z. Anorg. Allg. Chem.* **2000**, *626*, 1400–1405.
(141) Christinat, N.; Croisier, E.; Scopelliti, R.; Cascella, M.; Röthlisberger, U.; Severin, K. *Eur. J. Inorg. Chem.* **2007**, 5177–5181.
(142) Jo, T. S.; Kim, S. H.; Shin, J.; Bae, C. *J. Am. Chem. Soc.* **2009**, *131*, 1656–1657.
(143) Li, H.; Sundararaman, A.; Venkatasubbaiah, K.; Jäkle, F. *J. Am. Chem. Soc.* **2007**, *129*, 5792–5793.
(144) Elbing, M.; Bazan, G. C. *Angew. Chem., Int. Ed.* **2008**, *47*, 834–838.
(145) Wakamiya, A.; Mori, K.; Yamaguchi, S. *Angew. Chem., Int. Ed.* **2007**, *46*, 4273–4276.
(146) Noda, T.; Shirota, Y. *J. Am. Chem. Soc.* **1998**, *120*, 9714–9715.
(147) Zhao, C. H.; Wakamiya, A.; Inukai, Y.; Yamaguchi, S. *J. Am. Chem. Soc.* **2006**, *128*, 15934–15935.
(148) Morin, J.-F.; Leclerc, M.; Adès, D.; Siove, A. *Macromol. Rapid Commun.* **2005**, *26*, 761–778.
(149) Stahl, R.; Lambert, C.; Kaiser, C.; Wortmann, R.; Jakober, R. *Chem.—Eur. J.* **2006**, *12*, 2358–2370.
(150) Yamaguchi, I.; Choi, B.-J.; Koizumi, T.-A.; Kubota, K.; Yamamoto, T. *Macromolecules* **2007**, *40*, 438–443.
(151) Nagata, Y.; Otaka, H.; Chujo, Y. *Macromolecules* **2008**, *41*, 737–740.
(152) Cui, Y.; Liu, Q.-D.; Bai, D.-R.; Jia, W.-L.; Tao, Y.; Wang, S. *Inorg. Chem.* **2005**, *44*, 601–609.
(153) Li, X.-N.; Feng, J.-K.; Ren, A.-M. *Chin. J. Chem.* **2008**, *26*, 1979–1984.
(154) Qin, Y.; Kiburu, I.; Shah, S.; Jäkle, F. *Org. Lett.* **2006**, *8*, 5227–5230.
(155) Nagai, A.; Kokado, K.; Nagata, Y.; Chujo, Y. *Macromolecules* **2008**, *41*, 8295–8298.
(156) Nicolas, M.; Fabre, B.; Marchand, G.; Simonet, J. *Eur. J. Org. Chem.* **2000**, 1703–1710.
(157) Douglade, G.; Fabre, B. *Synth. Met.* **2002**, *129*, 309–314.
(158) Shoji, E.; Freund, M. S. *Langmuir* **2001**, *17*, 7183–7185.
(159) Ma, Y.; Cheung, W.; Wei, D.; Bogozi, A.; Chiu, P. L.; Wang, L.; Pontoriero, F.; Mendelsohn, R.; He, H. *ACS Nano* **2008**, *2*, 1197–1204.
(160) Nicolas, M.; Fabre, B.; Simonet, J. *Chem. Commun.* **1999**, 1881–1882.
(161) Nicolas, M.; Fabre, B.; Simonet, J. *J. Electroanal. Chem.* **2001**, *509*, 73–79.
(162) Shoji, E.; Freund, M. S. *J. Am. Chem. Soc.* **2001**, *123*, 3383–3384.
(163) Shoji, E.; Freund, M. S. *J. Am. Chem. Soc.* **2002**, *124*, 12486–12493.
(164) Pringsheim, E.; Terpetschnig, E.; Piletsky, S. A.; Wolfbeis, O. S. *Adv. Mater.* **1999**, *11*, 865–868.
(165) Deore, B. A.; Yu, I.; Freund, M. S. *J. Am. Chem. Soc.* **2004**, *126*, 52–53.
(166) Deore, B. A.; Hachey, S.; Freund, M. S. *Chem. Mater.* **2004**, *16*, 1427–1432.
(167) Yu, I.; Deore, B. A.; Recksiedler, C. L.; Corkery, T. C.; Abd-El-Aziz, A. S.; Freund, M. S. *Macromolecules* **2005**, *38*, 10022–10026.
(168) Deore, B. A.; Yu, I.; Aguiar, P. M.; Recksiedler, C.; Kroeker, S.; Freund, M. S. *Chem. Mater.* **2005**, *17*, 3803–3805.
(169) Huh, P.; Kim, S.-C.; Kim, Y.; Wang, Y.; Singh, J.; Kumar, J.; Samuelson, L. A.; Kim, B.-S.; Jo, N.-J.; Lee, J.-O. *Biomacromolecules* **2007**, *8*, 3602–3607.
(170) Cheung, W.; Chiu, P. L.; Parajuli, R. R.; Ma, Y.; Ali, S. R.; He, H. *J. Mater. Chem.* **2009**, 6465–6480.
(171) Yakuphanoglu, F.; Senkal, B. F. *Polym. Eng. Sci.* **2009**, *49*, 722–726.
(172) Xue, C.; Cai, F.; Liu, H. *Chem.—Eur. J.* **2008**, *14*, 1648–1653.
(173) Recksiedler, C. L.; Deore, B. A.; Freund, M. S. *Langmuir* **2006**, *22*, 2811–2815.
(174) Deore, B. A.; Yu, I.; Woodmass, J.; Freund, M. S. *Macromol. Chem. Phys.* **2008**, *209*, 1094–1105.
(175) Deore, B. A.; Freund, M. S. *Macromolecules* **2009**, *42*, 164–168.
(176) Ma, Y.; Ali, S. R.; Wang, L.; Chiu, P. L.; Mendelsohn, R.; He, H. *J. Am. Chem. Soc.* **2006**, *128*, 12064–12065.
(177) Ma, Y.; Ali, S. R.; Dodoo, A. S.; He, H. *J. Phys. Chem. B.* **2006**, *110*, 16359–16365.
(178) Ali, S. R.; Ma, Y.; Parajuli, R. R.; Balogun, Y.; Lai, W. Y. C.; He, H. *Anal. Chem.* **2007**, *79*, 2583–2587.
(179) Ali, S. R.; Parajuli, R. R.; Balogun, Y.; Ma, Y.; He, H. *Sensors* **2008**, *8*, 8423–8452.
(180) Ma, Y.; Chiu, P. L.; Serrano, A.; Ali, S. R.; Chen, A. M.; He, H. *J. Am. Chem. Soc.* **2008**, *130*, 7921–7928.
(181) Qin, Y.; Sukul, V.; Pagakos, D.; Cui, C.; Jäkle, F. *Macromolecules* **2005**, *38*, 8987–8990.
(182) Cambre, J. N.; Roy, D.; Gondi, S. R.; Sumerlin, B. S. *J. Am. Chem. Soc.* **2007**, *129*, 10348–10349.
(183) Roy, D.; Cambre, J. N.; Sumerlin, B. S. *Chem. Commun.* **2008**, 2477–2479.
(184) De, P.; Gondi, S. R.; Roy, D.; Sumerlin, B. S. *Macromolecules* **2009**, *42*, 5614–5621.
(185) Roy, D.; Cambre, J. N.; Sumerlin, B. S. *Chem. Commun.* **2009**, 2106–2108.
(186) Nagai, A.; Kokado, K.; Miyake, J.; Chujo, Y. *Macromolecules* **2009**, *42*, 5446–5452.
(187) Cui, C.; Bonder, E. M.; Jäkle, F. *J. Polym. Sci., Part A: Polym. Chem.* **2009**, *47*, 6612–6618.
(188) Kim, K. T.; Cornelissen, J. J. L. M.; Nolte, R. J. M.; van Hest, J. C. M. *J. Am. Chem. Soc.* **2009**, *131*, 13908–13909.
(189) Kim, K. T.; Cornelissen, J. J. L. M.; Nolte, R. J. M.; van Hest, J. C. M. *Adv. Mater.* **2009**, *21*, 2787–2791.
(190) Ramakrishnan, S.; Berluche, E.; Chung, T. C. *Macromolecules* **1990**, *23*, 378–382.
(191) Chung, T. C.; Janvikul, W. *J. Organomet. Chem.* **1999**, *581*, 176–187.
(192) Kondo, Y.; García-Cuadrado, D.; Hartwig, J. F.; Boaen, N. K.; Wagner, N. L.; Hillmyer, M. A. *J. Am. Chem. Soc.* **2002**, *124*, 1164–1165.
(193) Bae, C.; Hartwig, J. F.; Boaen Harris, N. K.; Long, R. O.; Anderson, K. S.; Hillmyer, M. A. *J. Am. Chem. Soc.* **2005**, *127*, 767–776.
(194) Ramakrishnan, S. *Macromolecules* **1991**, *24*, 3753–3759.
(195) Chung, T. C.; Rhubright, D. *J. Polym. Sci., Part A: Polym. Chem.* **1993**, *31*, 2759–2763.
(196) Branger, C.; Lequan, M.; Lequan, R. M.; Large, M.; Kajzar, F. *Chem. Phys. Lett.* **1997**, *272*, 265–270.
(197) Branger, C.; Lequan, M.; Lequan, R. M.; Large, M.; Kajzar, F.; Barzoukas, M.; Fort, A. *MCLC S&T, Sect. B: Nonlinear Opt.* **1997**, *17*, 281–303.
(198) Mutaguchi, D.; Okumoto, K.; Ohsedo, Y.; Moriwaki, K.; Shirota, Y. *Org. Electron.* **2003**, *4*, 49–59.

(199) Parab, K.; Venkatasubbaiah, K.; Jäkle, F. *J. Am. Chem. Soc.* **2006**, *128*, 12879–12885.
(200) Cui, C.; Jäkle, F. *Chem. Commun.* **2009**, 2744–2746.
(201) Qin, Y.; Cui, C.; Jäkle, F. *Macromolecules* **2008**, *41*, 2972–2974.
(202) Qin, Y.; Cui, C.; Jäkle, F. *Macromolecules* **2007**, *40*, 1413–1420.
(203) Doshi, A.; Jäkle, F. *Main Group Chem.* **2006**, *5*, 309–318.
(204) Qin, Y.; Cheng, G.; Achara, O.; Parab, K.; Jäkle, F. *Macromolecules* **2004**, *37*, 7123–7131.
(205) Qin, Y.; Cheng, G.; Sundararaman, A.; Jäkle, F. *J. Am. Chem. Soc.* **2002**, *124*, 12672–12673.
(206) Sundararaman, A.; Jäkle, F. *J. Organomet. Chem.* **2003**, *681*, 134–142.
(207) Parab, K.; Jäkle, F. *Macromolecules* **2009**, *42*, 4002–4007.
(208) Costela, A.; García-Moreno, I.; Gómez, C.; Amat-Guerri, F.; Liras, M.; Sastre, R. *Appl. Phys. B: Lasers Opt.* **2003**, *76*, 365–369.
(209) López Arbeloa, F.; Bañuelos Prieto, J.; López Arbeloa, I.; Costela, A.; García-Moreno, I.; Gómez, C.; Amat-Guerri, F.; Liras, M.; Sastre, R. *Photochem. Photobiol.* **2003**, *78*, 30–36.
(210) Álvarez, M.; Costela, A.; García-Moreno, I.; Amat-Guerri, F.; Liras, M.; Sastre, R.; López Arbeloa, F.; Bañuelos Prieto, J.; López Arbeloa, I. *Photochem. Photobiol. Sci.* **2008**, *7*, 802–813.
(211) Costela, A.; García-Moreno, I.; Pintado-Sierra, M.; Amat-Guerri, F.; Sastre, R.; Liras, M.; López Arbeloa, F.; Bañuelos Prieto, J.; López Arbeloa, L. *J. Phys. Chem. A.* **2009**, *113*, 8118–8124.
(212) Zhang, G.; Evans, R. E.; Campbell, K. A.; Fraser, C. L. *Macromolecules* **2009**, *42*, 8627–8633.
(213) Zhang, G.; Chen, J.; Payne, S. J.; Kooi, S. E.; Demas, J. N.; Fraser, C. L. *J. Am. Chem. Soc.* **2007**, *129*, 8942–8943.
(214) Zhang, G.; St. Clair, T. L.; Fraser, C. L. *Macromolecules* **2009**, *42*, 3092–3097.
(215) Pfister, A.; Zhang, G.; Zareno, J.; Horwitz, A. F.; Fraser, C. L. *ACS Nano* **2008**, *2*, 1252–1258.
(216) Zhang, G.; Kooi, S. E.; Demas, J. N.; Fraser, C. L. *Adv. Mater.* **2008**, *20*, 2099–2104.
(217) Zhang, G.; Fiore, G. L.; St. Clair, T. L.; Fraser, C. L. *Macromolecules* **2009**, *42*, 3162–3169.
(218) Zhang, G.; Palmer, G. M.; Dewhirst, M. W.; Fraser, C. L. *Nat. Mater.* **2009**, *8*, 747–751.
(219) Entwistle, C. D.; Marder, T. B. *Angew. Chem., Int. Ed.* **2002**, *41*, 2927–2931.
(220) Kaim, W.; Schulz, A. *Angew. Chem., Int. Ed. Engl.* **1984**, *23*, 615–616.
(221) Kobayashi, H.; Sato, N.; Ichikawa, Y.; Miyata, M.; Chujo, Y.; Matsuyama, T. *Synth. Met.* **2003**, *135*−*136*, 393–394.
(222) Sato, N.; Ogawa, H.; Matsumoto, F.; Chujo, Y.; Matsuyama, T. *Synth. Met.* **2005**, *154*, 113–116.
(223) Noda, T.; Ogawa, H.; Shirota, Y. *Adv. Mater.* **1999**, *11*, 283–285.
(224) Wu, Q.; Esteghamatian, M.; Hu, N.-X.; Popovic, Z.; Enright, G.; Breeze, S. R.; Wang, S. *Angew. Chem., Int. Ed.* **1999**, *38*, 985–988.
(225) Liu, S.-F.; Seward, C.; Aziz, H.; Hu, N.-X.; Popovic, Z.; Wang, S. *Organometallics* **2000**, *19*, 5709–5714.
(226) Wang, S. *Coord. Chem. Rev.* **2001**, *215*, 79–98.
(227) Kinoshita, M.; Fujii, T.; Tsuzuki, T.; Shirota, Y. *Synth. Met.* **2001**, *121*, 1571–1572.
(228) Kinoshita, M.; Kita, H.; Shirota, Y. *Adv. Funct. Mater.* **2002**, *12*, 780–786.
(229) Liu, Q.; Mudadu, M. S.; Schmider, H.; Thummel, R.; Tao, Y.; Wang, S. *Organometallics* **2002**, *21*, 4743–4749.
(230) Jia, W.-L.; Bai, D.-R.; McCormick, T.; Liu, Q.-D.; Motala, M.; Wang, R.-Y.; Seward, C.; Tao, Y.; Wang, S. *Chem.*—*Eur. J.* **2004**, *10*, 994–1006.
(231) Mazzeo, M.; Vitale, V.; Sala, F. D.; Anni, M.; Barbarella, G.; Favaretto, L.; Sotgiu, G.; Cingolani, R.; Gigli, G. *Adv. Mater.* **2005**, *17*, 34–39.
(232) Jia, W. L.; Moran, M. J.; Yuan, Y.-Y.; Lu, Z. H.; Wang, S. *J. Mater. Chem.* **2005**, *15*, 3326–3333.
(233) Jia, W. L.; Feng, X. D.; Bai, D. R.; Lu, Z. H.; Wang, S.; Vamvounis, G. *Chem. Mater.* **2005**, *17*, 164–170.
(234) Liu, Q.-D.; Mudadu, M. S.; Thummel, R.; Tao, Y.; Wang, S. *Adv. Funct. Mater.* **2005**, *15*, 143–154.
(235) Zhang, H.; Huo, C.; Zhang, J.; Zhang, P.; Tian, W.; Wang, Y. *Chem. Commun.* **2006**, 281–283.
(236) Cui, Y.; Li, F. H.; Lu, Z.-H.; Wang, S. *Dalton Trans.* **2007**, 2634–2643.
(237) Li, F.; Jia, W.; Wang, S.; Zhao, Y.; Lu, Z.-H. *J. Appl. Phys.* **2008**, *103*, 034509/1−6.
(238) Li, Y.; Ding, J.; Day, M.; Tao, Y.; Lu, J.; D'Iorio, M. *Chem. Mater.* **2003**, *15*, 4936–4943.
(239) Luebben, S.; Sapp, S. *Mater. Matters (Sigma-Aldrich)* **2007**, *2*, 11–14.
(240) Yamaguchi, S.; Akiyama, S.; Tamao, K. *J. Am. Chem. Soc.* **2001**, *123*, 11372–11375.
(241) Zhao, G.; Baumgarten, M.; Müllen, K. *J. Am. Chem. Soc.* **2008**, *130*, 12477–12484.
(242) Zhao, S.-B.; Wucher, P.; Hudson, Z. M.; McCormick, T. M.; Liu, X.-Y.; Wang, S.; Feng, X.-D.; Lu, Z.-H. *Organometallics* **2008**, *27*, 6446–6456.
(243) Yamaguchi, S.; Akiyama, S.; Tamao, K. *J. Organomet. Chem.* **2002**, *652*, 3–9.
(244) Miyata, M.; Chujo, Y. *Polym. J.* **2002**, *34*, 967–969.
(245) English, J. T.; Deore, B. A.; Freund, M. S. *Sens. Actuators, B* **2006**, *115*, 666–671.
(246) Egawa, Y.; Gotoh, R.; Seki, T.; Anzai, J.-i. *Mater. Sci. Eng., C* **2009**, *29*, 115–118.
(247) Arimori, S.; Bell, M. L.; Oh, C. S.; Chan, S.; Frimat, K. A.; James, T. D. *Chem. Commun.* **2001**, 1836–1837.
(248) Kanekiyo, Y.; Sato, H.; Tao, H. *Macromol. Rap. Commun.* **2005**, *26*, 1542–1546.
(249) Shoji, E. *Chem. Sens.* **2005**, *21*, 120–128.
(250) Deore, B. A.; Braun, M. D.; Freund, M. S. *Macromol. Chem. Phys.* **2006**, *207*, 660–664.
(251) Rajkumar, R.; Katterle, M.; Warsinke, A.; Moehwald, H.; Scheller, F. W. *Biosens. Bioelectron.* **2008**, *23*, 1195–1199.
(252) Deore, B. A.; Freund, M. S. *Chem. Mater.* **2005**, *17*, 2918–2923.
(253) Fabre, B.; Taillebois, L. *Chem. Commun.* **2003**, 2982–2983.
(254) Fraser, C. L.; Zhang, G. *Mater. Today* **2009**, *12*, 38–40.

CR100026F